

**THE AKWATIA DIAMOND FIELD, GHANA, WEST AFRICA:  
SOURCE ROCKS**

**By  
Dylan G. Canales**

Department of Earth &  
Environmental Science  
New Mexico Tech  
Socorro, NM 87801

**Submitted as partial fulfillment of the  
Requirements for the Degree of  
Master of Science in Geology  
May 14, 2005**

**Department of Earth and Environmental Science  
New Mexico Institute of Mining and Technology  
Socorro, NM**

## ABSTRACT

The Akwatia diamond field is located within the Birimian (Early Proterozoic) volcano-sedimentary rocks and has produced more than 100 million carats of diamonds. These diamonds were assumed to be alluvial owing to the lack of any diamond indicator minerals typically associated with kimberlites or lamproites. However, diamonds show no evidence of transport and are associated with metamorphosed syn-eruptive volcanoclastic mega-turbidites with a composition resembling komatiite. Akwatia is anomalous in that it is associated with arc sediments and does not occur within an Archean craton.

Diamond-bearing rocks form elongate bodies that outcrop over an 18-km<sup>2</sup> area and are intercalated with an actinolite-tremolite schist and/or volcanoclastic rocks that include turbidites, phyllites and greywackes. Small-scale mine workings in diamond-bearing rock extend to depths greater than 20 m. High diamond-grades in soils correlate with the komatiitic rock and diamond grades in these rocks are 0.93 carats per cubic yard (.71 carats per cubic meter). Clasts in the diamondiferous units are concordant with the schistosity of the nearly vertically dipping host rock, and are apparently common throughout the diamondiferous area. Field evidence suggests that these komatiitic rocks were coeval with the metasediments, indicating an age of 2185-2155 Ma for the diamond deposit. Major and trace element analysis of these rocks indicate they are petrogenetically

similar to the diamond-bearing volcanoclastic komatiites in French Guiana, and the incompatible-element rich, porphyritic komatiites and komatiitic volcanoclastic rocks described at Steep Rock and Lumby Lake Canada, Murchison Terrane Australia, and Karasjok Norway; which are named Karasjok- type komatiites.

## ACKNOWLEDGEMENTS

First I would like to thank John Munt and Neil O'Brien who are responsible for the inspiration that led me to geology. Marisa Wolfe's love and support made all of this possible. I thank Dave Norman for his help, encouragement and friendship. Ramon Capdevila assisted me with data and ideas. Henry Aphiah and Robert Nartey whose help and hospitality in Ghana are much appreciated. The value of Sammy Ndur's help in Ghana and his humor cannot be overestimated. Tom McCandless got me thinking about diamonds in komatiites. I thoroughly enjoyed my travel with Al Perry whose patient advice I will always take. Virgil Lueth has taught me more than most and encouraged me to follow my dreams. Kent Condie always listened to my hyperbolic ideas with bemused respect. Bill Chavez, one of the best teachers ever, always treated me as an equal and colluded with my humor and me. Bob Eveleth and Patty Frisch made work play. I would like to thank everyone I have worked with at Tech. A special thanks goes out to all the secretaries in the Graduate Office, Department of Earth and Environmental Sciences and the Bureau of Geology and Mineral Resources. Rob Sanders and Amber Macintosh have played a large part in my decision to stay in the Socorro area. Last, but certainly not least, I would like to thank the small-scale miners of Ghana who gave me the answers the geologist could not.



## TABLE OF CONTENTS

|                           | Page       |
|---------------------------|------------|
| <b>TITLE PAGE</b>         | <b>i</b>   |
| <b>ABSTRACT</b>           |            |
| <b>ACKNOWLEDGEMENTS</b>   | <b>ii</b>  |
| <b>TABLE OF CONTENTS</b>  | <b>iii</b> |
| <b>LIST OF TABLES</b>     | <b>IV</b>  |
| <b>LIST OF FIGURES</b>    | <b>V</b>   |
| <b>LIST OF APPENDICES</b> | <b>VI</b>  |
| <b>INTRODUCTION</b>       | <b>1</b>   |
| Diamond Source Rock       | 1          |
| Previous Work             | 2          |
| <b>GEOLOGY</b>            | <b>8</b>   |
| Regional Geology          | 8          |
| Akwatia Diamond Field     | 14         |
| Local Geology             | 14         |
| Diamonds                  | 18         |
| <b>METHODS</b>            | <b>19</b>  |

|  |           |
|--|-----------|
| <b>RESULTS</b>                           | <b>22</b> |
| <b>Field and Laboratory Observations</b> | <b>22</b> |
| <b>Diamond Distribution</b>              | <b>34</b> |
| <b>Geochemistry</b>                      | <b>39</b> |
| <i>Major Element Oxides</i>              | <b>40</b> |
| <i>Minor and Rare Earth Elements</i>     | <b>44</b> |
| <b>Weathering and Alteration</b>         | <b>50</b> |
| <i>Diamond Bearing Rocks</i>             | <b>59</b> |
| <i>Siderophile Elements</i>              | <b>59</b> |
| <i>Chalcophile Elements</i>              | <b>59</b> |
| <i>Lithophile Elements</i>               | <b>59</b> |
| <i>Rare Earth Elements</i>               | <b>60</b> |
| <i>Immobile Elements</i>                 | <b>61</b> |
| <i>Actinolite Schist</i>                 | <b>61</b> |
| <i>Siderophile Elements</i>              | <b>61</b> |
| <i>Chalcophile Elements</i>              | <b>61</b> |
| <i>Lithophile Elements</i>               | <b>62</b> |
| <i>Rare Earth Elements</i>               | <b>63</b> |
| <i>Immobile Elements</i>                 | <b>64</b> |

|   |            |
|---|------------|
| <b>DISCUSSION</b>                         | <b>65</b>  |
| Cerium Anomaly                            | 65         |
| General Conclusions Related to Weathering | 67         |
| Weathering and Protolith Identification   | 68         |
| Diamonds in Bedrock                       | 71         |
| Diamond-Bearing Rocks                     | 72         |
| Komatiite Generation and Tectonic Setting | 80         |
| Crustal Contamination                     | 82         |
| Tectonic Setting                          | 83         |
| Emplacement of Akwatia Rocks              | 86         |
| Resorption                                | 87         |
| Akwatia Compared to Dachine               | 90         |
| A Speculative Model                       | 94         |
| <b>CONCLUSIONS</b>                        | <b>96</b>  |
| <b>REFERENCES</b>                         | <b>98</b>  |
| <b>APPENDICES</b>                         | <b>102</b> |

## LIST OF TABLES

|   |    |
|---|----|
| Table 1: Geological events in the Paleoproterozoic of Ghana | 13 |
| Table 2: Rare earth elements (maximum and minimum)          | 46 |
| Table 3: Chemical index of alteration                       | 51 |
| Table 4: Geochemical losses and gains due to weathering     | 58 |

## LIST OF FIGURES

|   |    |
|---|----|
| Figure 1: Location of Ghana, West Africa                              | 3  |
| Figure 2: Geologic map of Ghana                                       | 10 |
| Figure 2a: Legend for Figure 2  | 11 |
| Figure 3: Geologic map of the Akwatia area                            | 17 |
| Figure 4: GCD prospecting map, Beduwara Hill                          | 21 |
| Figure 5: Beduwara Hill brecciated diamond bearing rock               | 26 |
| Figure 6: Sample G-12 showing preferential orientation of clasts      | 27 |
| Figure 7: Sample DM-2 showing diamond in matrix                       | 28 |
| Figure 8: Close up of DM-2 showing diamond in matrix.                 | 29 |
| Figure 9: Pelitic contact, diamond bearing rock and actinolite schist | 30 |
| Figure 10: Close up undulating pelitic contact between diamond        | 31 |
| Figure 11: Diamond bearing dyke-like body                             | 32 |
| Figure 12: Close up of contact of diamond-bearing dyke-like body      | 33 |
| Figure 13: Diamond distribution top soil                              | 35 |
| Figure 14: Diamond distribution B1 horizon                            | 36 |
| Figure 15: Diamond distribution bedrock                               | 37 |
| Figure 16: Diamond distribution (directional derivative) bedrock      | 38 |



|  |    |
|--|----|
| Figure 17: Sample location map   | 42 |
| Figure 18: Komatiitic discrimination diagram                             | 43 |
| Figure 19: Rare earth element spidergrams                                | 47 |
| Figure 20: Multi-element spidergrams                                     | 48 |
| Figure 21: Trace element tectonic discrimination diagram                 | 49 |
| Figure 22: Isocons sample G-2 and G-3                                    | 53 |
| Figure 23: Isocons Sample G-4 and G-9                                    | 54 |
| Figure 24: Isocons sample 93-16 and sample 93-33                         | 55 |
| Figure 25: Isocons sample 93-20 and 93-19                                | 56 |
| Figure 26: Isocons sample G-10 and G-5                                   | 57 |
| Figure 27: Rare earth elements spidergram comparing sample G-9/G-10      | 66 |
| Figure 28: Graph of Mg compared to immobile elements                     | 69 |
| Figure 29: Komatiitic discrimination diagram (affects of weathering)     | 70 |
| Figure 30: REE spidergram (Kimberlite, Lamproite, Akwatia)               | 75 |
| Figure 31: Ternary plot (Al/Nb/Hf)                                       | 76 |
| Figure 32: Rare earth element spidergrams (Dachine and Akwatia)          | 77 |
| Figure 33: Rare earth element spidergrams (Akwatia, world komatiites)    | 78 |
| Figure 34: Ratio plot (Gd/Yb and Al/Ti)                                  | 79 |
| Figure 35: P/T conditions komatiite generation (diamond stability field) | 81 |
| Figure 36: High field strength element bivariate plot Akwatia rocks      | 85 |
| Figure 37: Diagram conditions for resorption                             | 89 |
| Figure 38: Paleoreconstruction of Africa and South America               | 91 |
| Figure 39: World wide "anomalous" diamonds                               | 95 |

## LIST OF APPENDICES

|  |     |
|--|-----|
| Appendix 1: Akwatia samples analyzed in this study                       | 102 |
| Appendix 2: Akwatia samples analyzed by McKittrick                       | 104 |
| Appendix 3: Samples from Dachine, French Guiana<br>from Capdevila (2003) | 105 |
| Appendix 4: Sample descriptions  | 107 |
| Appendix 5: Field site descriptions                                      | 115 |
| Appendix 6: Statistical reports generated by “Surfer” for image maps     | 121 |
| Appendix 7: Results of magnetometer survey                               | 142 |

This thesis is accepted on behalf of the  
Faculty of the Institute by the following committee:

David L. Norman

Advisor.

Ken D. Linder

Vigil W. Jones

April, 26, 2005

Date

I release this document to the New Mexico Institute of Mining and Technology.

[Signature]

Student's Signature

Apr. 26, 2005

Date

## INTRODUCTION

### **Diamond Source Rocks**

The principle source of commercial grade diamonds is thought to be ultramafic kimberlites or lamproites (Janse and Sheahan, 1995). Diamondiferous kimberlites of commercial grade are mostly restricted to areas underlain by Archean cratons (Janse and Sheahan, 1995). However, the Argyle mine diamond-lamproites of north central Australia occur in an area underlain by a Proterozoic craton (Janse and Sheahan, 1995). Both kimberlites and lamproites are accompanied by pyrope garnet, chrome diopside, chrome spinel and picroilmenite (magnesian ilmenite) indicator minerals though they are smaller and less numerous in lamproites (Ross et al., 1989).

A different type of diamond source rock is described in French Guiana. Captevilla, Arndt et al. (1999) describe a diamond deposit in the Inini greenstone belt at Dachine, French Guiana hosted in rare volcanoclastic komatiite. During the early Proterozoic, Ghana and French Guiana were part of the same land mass and were in close proximity (Caen-Vachette, 1988; Gruau et al., 1985; Nomade et al., ; Onstott and Hargraves, 1981). Comparative studies of paleomagnetism, geochronology, lithology and large-scale structural features in the Guyana shield show the Eburnean orogeny of West Africa correlates with the trans-Amazonian orogeny in south America (Caen-Vachette, 1988; Gruau et al., 1985; Onstott and Hargraves, 1981).

## Previous Work

Diamonds were first discovered at Akwatia, Ghana in 1919 (fig. 1). Production at Akwatia from 1925 and 1992 was over 101 million carats (Janse and Sheahan, 1995; Nixon and Griffin, 1995) at an average grade about 2 cts/cu.yd (2.6 cts/cu.m). For the past few years production is about 1 million carats/year comprised of 80% gems and 20% industrial stones. These diamonds are principally produced from alluvium, colluvium, and residual soils over a concession area of about 104 sq.km.

Akwatia is not considered a primary diamond deposit. This is because there is little evidence for an underlying Archon (Abouchami et al., 1990; Boher et al., 1992; Taylor et al., 1992); diamond indicator minerals are wholly absent; and kimberlite is not positively identified (Junner, 1943; Kaminsky, 1996; Kesse, 1985). There are no known primary diamond deposits in Ghana. Thus the source of Akwatia diamonds is considered enigmatic.

It is suspected (Junner, 1943) that the source of the diamonds is the local metamorphosed ultramafic rocks because a strong correlation exists between the strike and diamond distribution. He speculated that the Akwatia diamonds were sourced in a distant kimberlite or metamorphic genesis, or possibly there was an extraterrestrial source. Others proposed that the diamond source was ancient stream deposits that capped the hilltops at Akwatia (Kesse, 1985), and hilltop diamond-bearing soils are still referred to today by Akwatia mine geologists as terrace deposits. But there is no supporting evidence for Akwatia diamond transport during in the Precambrian or Tertiary.



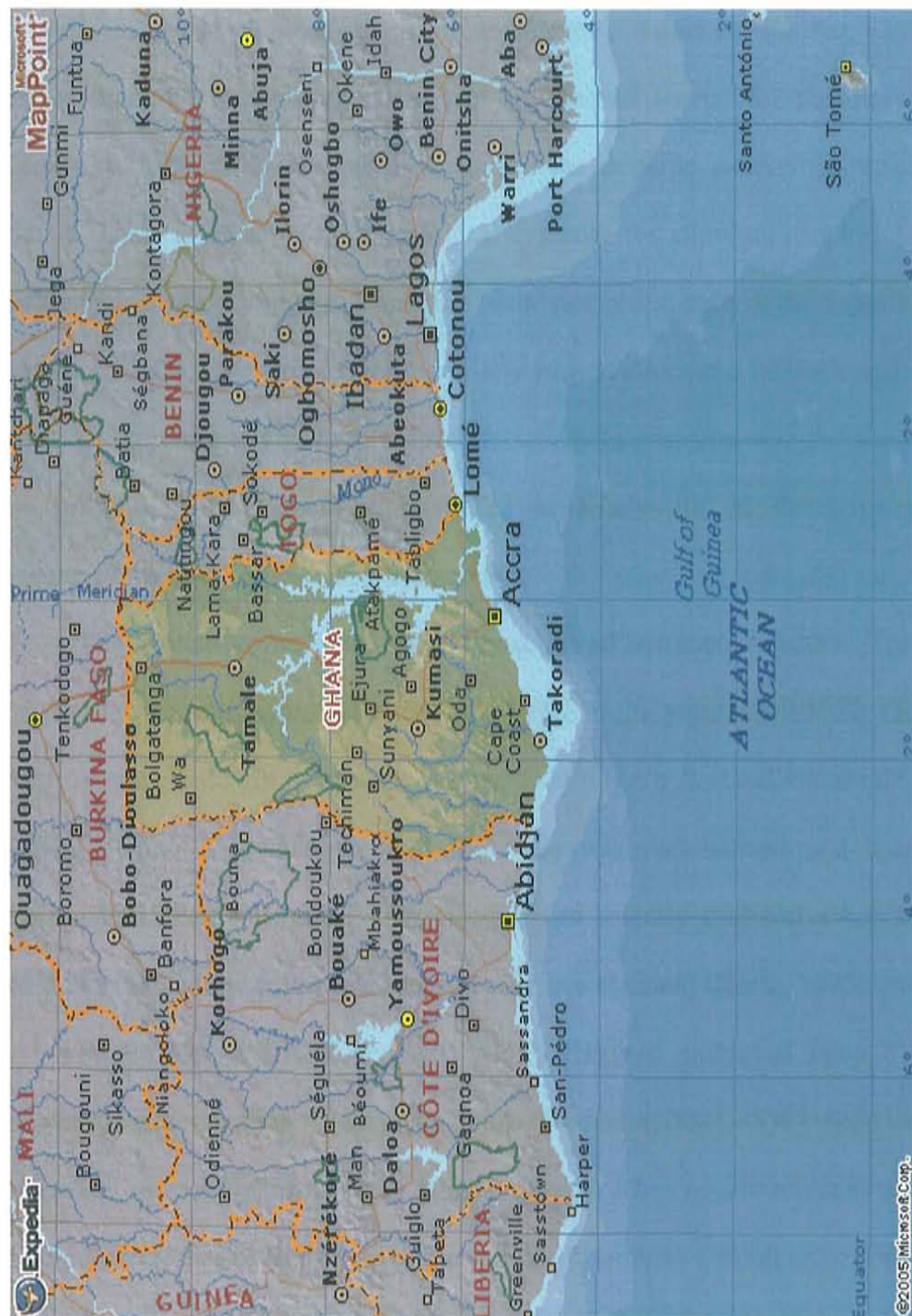


Figure 1. Location of Ghana, West Africa.

Two studies; one a report to Carlin resources (Kaminsky, 1996) obtained from Ghana Consolidate Diamonds (GCD) and a M.S. thesis by Ward (1997) both concluded Akwatia diamonds show no signs of sedimentary transport. Further, distribution of various diamond morphologies suggests a proximal source for the alluvial deposits (Kaminsky, 1996). (Kesse, 1985) also notes the extreme paucity of broken diamond crystals. There is no supporting geological evidence for alluvium capping Akwatia hills and trenching and drilling confirms that diamonds occur deep in the saprolitic bed rock (Gammon, 2003). McKitick (1996) partially mapped Akwatia bedrock and reports that diamonds are definitely hosted in bedrock, which he assumed was the actinolite schist. The protolith of this rock he identified as Kimberlite on the basis of elevated concentrations of REE (rare earth elements).

The British owned company, Consolidated African Selection Trust (CAST,) operated the Akwatia diamond mine until 1972. In the years 1969-1972, Ghana ranked fourth in the world for total diamond production with 2-4 million carats per annum (Kesse, 1985). In October 1972 the mine was nationalized and became Ghana Consolidated Diamonds (GCD). Production has steadily declined since 1974 due to exhaustion of shallow valley reserves and poor management (Kesse, 1985).

In the 1950's CAST geologist J.H.E. Haggard embarked upon a program to discover the source of the Akwatia diamonds (Gammon, 2003). Systematic sampling was undertaken in areas of exceptional alluvial grades. After negative results in these areas attention was turned to Beduwara hill, an area with extensive small-scale bedrock mining. Consolidated African Selection Trust geologists described the bedrock at Beduwara hill as "interbedded, brecciated basic schists (actinolite-tremolite schist), phyllites and



tuffaceous greywackes. (Junner, 1943) assigns these “basic schists” to the upper Birimian and the phyllites and tuffaceous greywackes to the lower Birimian. It was assumed by (Junner, 1943) and Haggart (Gammon, 2003) that if there is a primary source for the diamonds it is these “basic schists” as these rocks are apparently derived from an ultramafic protolith. Extensive trenching of the rocks on Beduwara hill revealed diamonds in the schist and the tuffaceous greywacke. Making matters more confusing, Haggard noted that it was impossible to distinguish the basic schists from the tuffaceous greywackes and it is likely that hybrids exist. Compounding the confusion, further sampling at various depths revealed diamonds penetrate into the weathered bedrock by bioturbation. It was determined that the tuffaceous greywacke was the source of diamonds on Beduwara hill carrying an average grade of .93 carats per cubic yard. Drilling at Beduwara hill to 223ft. reveals clasts of phyllite within the basic schists and no evidences the actinolite schist or its protolith intruded the sediments. This combined with the idea that the actinolite schists were distinctly younger than the sediments gave rise to a (outdated) hypothesis that the schists were derived from the sediments by “metamorphic differentiation”. CAST geologists also concluded that since the “host” rock was lower Birimian, and there were no older rocks in Ghana and that the primary source could never be found (Gammon, 2003).

In 1993 Scott McKittrick investigated the Akwatia diamond field. The area was mapped; samples of the actinolite schist (samples 93-16, 93-19, 93-20, 93-33 and Ha-2) were collected in the field. Borehole cores of the metasediments on Beduwarra Hill drilled by CAST (referred to above) were obtained from GCD (samples with the BH prefix). These bore holes were drilled in the immediate vicinity of diamond-bearing rock

sampled for this study though the author cannot confirm the presence of diamonds in these core samples. Twenty-three samples were analyzed for major and trace elements using a Rigaku XRF spectrometer and INAA gamma ray detectors at New Mexico Tech; these results are used in this research. Thin sections of representative samples were prepared for petrographic analysis.

McKitrick's analysis show that most of the "metasediments" in the area are part of, or contained within, a coarse grained clastic turbidite. Meta-sandstones consist of framework quartz 30-50%, feldspar 30-50% with An value ~30 content for plagioclase and lithic fragments 0-20%. Sorting of local meta-sandstones and conglomerates is very poor. Clasts are sub-angular to sub-rounded and sub-parallel to bedding. Beds are 1-2m and interbedded with 10 -50 cm argillaceous beds, which may contain rip-up clasts but no ripple marks. Meta-greywacks classify as feldspathic quartz wacks, generally matrix supported with clay and mica comprising 30-60% of rock volume. McKitrick (1993) concluded the metasediments contained a significant volcanic component and were derived from an island arc provenance (based on bulk composition and REE element ratios). The actinolite schists show variable degrees of contact metamorphism revealed by crystalloblastic laths of radiating, nematoblastic, tremolite-actinolite in a matrix of fine white mica, chlorite and quartz with accessory rutile, iron oxides and carbonaceous material as well as clasts of country rock (phyllite). McKitrick observed a minimally weathered outcrop revealing a concordant, undulating contact between a clast-rich brecciated rock and turbiditic metasediments showing no evidence of heating or intrusion. Observing changes in "Younging" directions over a 30 to 60 m distance with no change in strike McKitrick concluded the local strata is isoclinally folded. The

enriched REE signature of the actinolite schist led McKittrick to hypothesize the actinolite schist is a metamorphosed kimberlite and thus is the source of the diamonds. Other researchers (Gammon, 2003; Junner, 1943; McKittrick, 1996) note a significant volcanic component in the clastic sediments in the Akwatia area.

The purpose of this work is to study the occurrence and distribution of diamond source rock at Akwatia. The aerial extent of Akwatia diamond source rock was not known, nor was details of source rock chemistry and whether the source rock was conformable to or intruded into Birimian formations. Assays of Akwatia material pitting and shallow drilling that penetrated bedrock are compiled to determine the aerial extent of diamond source rock. Geophysical mapping was attempted, but not completed because of logistic and access problems. Diamond source rock at seven sites, exposed by small-scale mine workings are mapped and samples are analyzed for major and trace elements.



## **GEOLOGY**

### **Regional Geology**

Archean rocks are not found in Ghana, which lies on the West Africa Craton, however they do crop out in Liberia and Sierra Leone (Wright et al., 1985). Ghana basement rocks are the Early Proterozoic Birimian Group of volcanoclastic breccias and metavolcanics (figure 2) that are intruded by foliated and non-foliated granites, and overlain by the Tarkwain Group of alluvial sediments. North-South trending basalts and gabbros intrude all early Proterozoic rocks. The Pan-African fold belt occupies the southeastern portion of Ghana and is separated from the West African Shield by a major Northeasterly trending thrust fault system. The fold belt consists primarily of gneissic rocks of the Dahomeyan Series but includes a sequence of quartzites, schists and serpentinites of the Togo series (Wright et al., 1985). A substantial portion of the West African craton including the Birimian domain is covered by flat-lying undeformed sediments of Neoproterozoic- Paleozoic age. In Ghana these are the Voltain clastic sediments that cover much of the central and eastern regions. Along the southern coast minor amounts of Cretaceous rocks lie on the Proterozoic formations.

Kitson (1918) first used the term Birimian to describe rocks of the Birimian river valley. In 1928 Kitson published a geologic map of the Gold Coast and eastern Togo land establishing the Birimian as a stratigraphic unit. (Junner, 1943) describes Birimian

stratigraphy as a Lower Birimian comprising mostly volcanoclastic metasediments that are slates, phyllites, greywacks, and turbidites with lesser tuffs and lavas and their schistose and gneissic derivatives, and an Upper Birimian, which are greenstones, comprised of metamorphosed basic and intermediate lavas and pyroclastic rocks, hypabyssal igneous rocks and intercalated bands of phyllite and greywacke. (Feybesse and Milesi, 1994), describe, for Ivory Coast, an older volcanosedimentary and sedimentary supergroup (B1 lower Birimian) and a younger volcanic supergroup (B2 upper Birimian). Based on new mapping, (Leube et al., 1990) argue that the Ghana lower and upper Birimian were deposited contemporaneously as lateral facies equivalents.

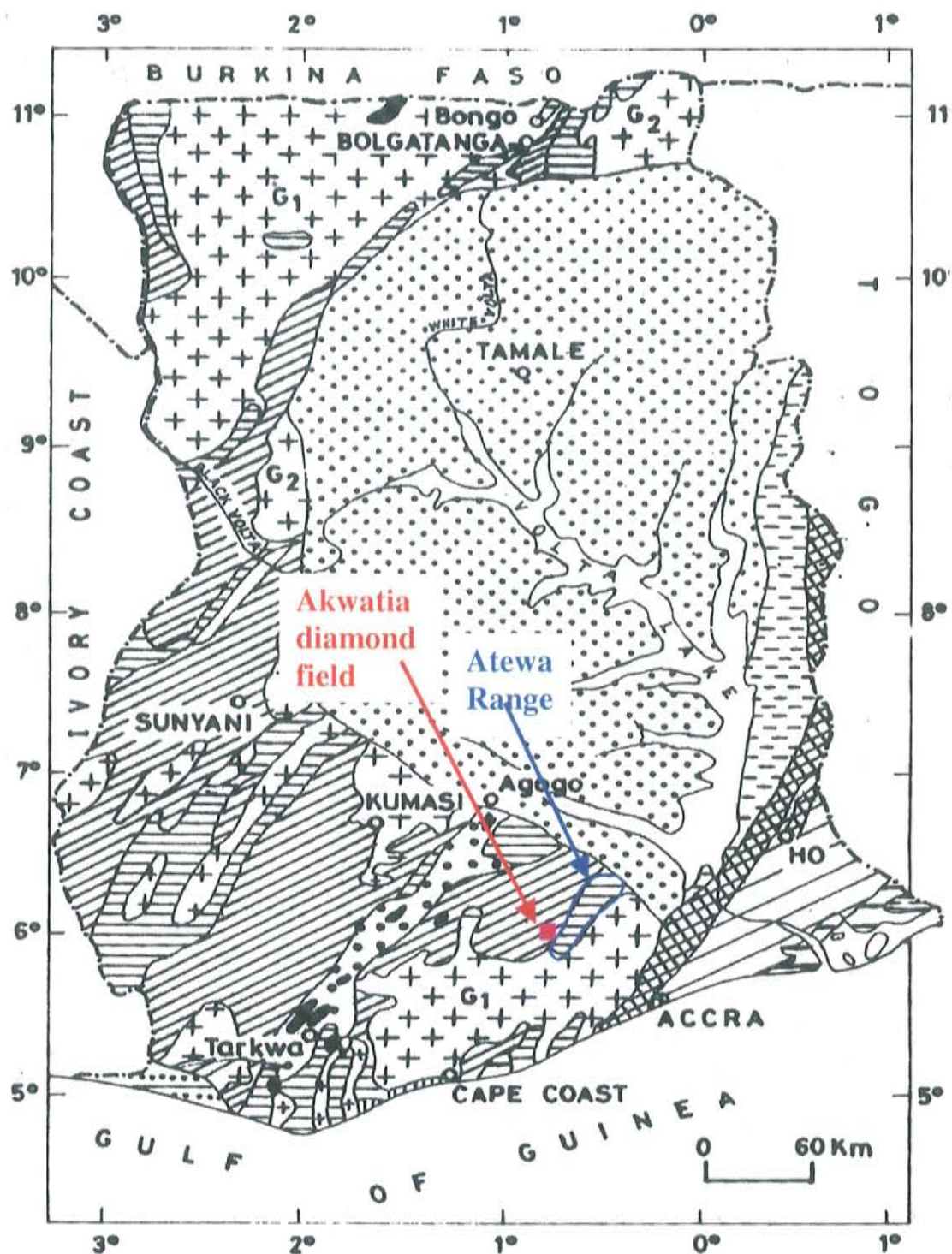


Figure 2. Geologic map of Ghana (Modified after Kesse 1985),  
legend, on the next page.




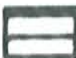









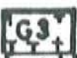

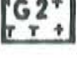



|  |   |  |
|--|---|--|
| RECENT   |    | Unconsolidated sand, clay and gravel.  |
| TERTIARY   |    | Red continental deposits mainly limonitic sand, sandy clay and gravel.   |
| APOLLONIAN FORMATION<br>(Upper Cretaceous)               |    | Alternating sands, clay and limestone.   |
| AMISIAN FORMATION<br>(Upper Jurassic - Lower Cretaceous) |    | Interbedded soft pebbly grits, conglomerates, sandstone, arkose and clay.  |
| SEKONDIAN SERIES<br>(Middle Devonian - Lower Cretaceous) |    | Sandstones and shales with conglomerates, pebble beds, grits and mudstone.   |
| ACCRAIAN SERIES<br>(Early to Middle Devonian)            |    | Alternating shales, sand stone, mudstone and pebbly grits.   |
| VOLTAIAN SYSTEM<br>(Late Proterozoic - Early Paleozoic)  |    | Quartzite, shale, mudstone, conglomerate, limestone, arkose.   |
| BUEM FORMATION<br>(Upper Precambrian)                    |    | Shale, sandstone, arkose, lava.  |
| TOGO SERIES<br>(Upper Precambrian)                       |    | Quartzite, shale, phyllite.  |
| DAHOMAYAN SYSTEM<br>(Middle - Late Precambrian)          |   | Acidic and basic gneiss, schists and migmatites.   |
| TARKWAIAN SYSTEM<br>(Middle Precambrian)                 |    | Quartzite, phyllite, grit, conglomerate  |
| GRANITOIDS<br>(Middle Precambrian)                       | <div> <div>BONGO</div> <div>DIXCOVE</div> <div>CAPE COAST</div> </div> <div>    </div> | <div> <div>Porphyritic hornblende microcline granites.</div> <div>Potash rich muscovite - biotite granite.</div> <div>Soda - rich hornblende biotite granite.</div> </div> |
| BIRIMIAN SYSTEM<br>(Middle Precambrian)                  | <div>UPPER</div> <div>LOWER</div> <div></div> <div></div>   | <div>Metamorphosed lava and pyroclastic rock.</div> <div>Phyllite, schist, tuff and greywacke.</div>   |
| BASIC INTRUSIVES   |    | Gabbro, dolerite, diabase, norite, epidiorite, serpentine etc.   |

Figure 2a. Legend for Figure 2, modified after (Kesse, 1985)

Birimian sediments and volcanics were deformed, metamorphosed and intruded by granitoids during the Eburnean orogeny ~2.1Ga. Four deformational phases are recognized, the D1- D4 (Feybesse and Milesi, 1994). The D4 event is very weak in most of Ghana. The "Cape Coast" or "basin" granitoids are, foliated and occur mostly in Birimian volcanics; "Dixcove" or "belt" granitoids are non-foliated and spatially associated with Birimian sediments. Birimian rocks and Eburnean intrusives have been shown by geochronological studies in Burkina Faso, Mali, Ghana, Côte d' Ivoire eastern Mauritania and Senegal to have been formed over a maximum period of 2.25-2.05 Ga. (Abouchami et al., 1990; Boher et al., 1992; Davis et al., 1994a; Hirdes et al., 1992; Hirdes et al., 1996; Taylor et al., 1992). "Dixcove" or "belt" granitoids are ~60 to 90 Ma. older than "Cape Coast" or "basin" granitoids (Davis et al., 1994a; Hirdes et al., 1992). Using precise U-Pb dating (+/- 2 Ma.) these authors obtain dates of 2172 Ma and 2179 Ma respectively for the Ashanti and Sefwi belt granitoids. The Kumasi and Sunyani basin granitoids in contrast have respective U-Pb (+/- 1Ma.) age of 2116 Ma. and 2088 Ma. The authors conclude that basin granitoids were intruded towards the end of deformation (late-kinematic) and belt granitoids were coeval with the belt volcanics. Single-zircon-grain dating of a Kumasi-Basin volcanoclastic wacke sample (Davis et al., 1994a) demonstrates that Birimian sediments were derived from volcanic belt terrains where rocks with crystallization ages of ~ 2185-2155 Ma dominated. Eisenlohr and Hirdes (1992) and (Oberthur et al., 1998) show that the Birimian and Tarkwaian rocks as well as the Dixcove granitoids within the volcanic belts were all deformed in a single progressive deformational event involving northwest-southeast crustal shortening and regional, lower greenschist facies metamorphism. Geological events in the Paleoproterozoic of Ghana are



summarized in the table 1 and are based on a model of progressive accretion of volcanic arcs and ocean plateaus onto an Archean continental mass in the southeast.

Table 1. Geological events in the Paleoproterozoic of Ghana.

| Age (Sm-Nd model) | Event   |
|-------------------|---|
| 2590 Ma           | Minimum age of continental crustal contribution to Winneba granitoid (areally restricted to small portion of SE Ghana).   |
| 2245 $\pm$ 4 Ma   | Age of oldest detrital zircon in Tarkwaian sediment (source unknown)  |
| 2190-2155 Ma.     | Formation of bulk of belt volcanics, volcanoclastics and associated synvolcanic belt plutons, and contemporaneous sedimentation in adjacent sedimentary basins. |
| 2135 Ma           | Latest igneous activity in volcanic belts, final stage of sedimentation in adjacent sedimentary basins.   |
| 2135—2132 Ma      | Uplift and erosion.   |
| 2132—2116 Ma      | Formation of Tarkwaian depositories and deposition of Tarkwaian. Sediments.   |
| 2100—2090 Ma      | Peak of deformation (NW—SE crustal shortening) and regional metamorphism.   |
| 2116—2088 Ma      | Emplacement of syn- to late-tectonic basin plutons.   |
| 2086—2073 Ma      | Hydrothermal alteration in basin granitoids (possibly related to gold mineralization).  |

From (Davis et al., 1994a).

There is no firm evidence that crustal rocks of Archean age underlie Birimian rocks. Isotopic evidence for the involvement of Archean or very early Proterozoic crust in Birimian volcanic and intrusives is negligible (Abouchami et al., 1990; Boher et al., 1992; Taylor et al., 1992). Two exceptions to this are located proximal to the Birimian/Archean boundary, which are the Winneba granitoid in the southeast of Ghana (Taylor et al., 1992) and granitoid plutons in south Guinea with Nd modal ages of ~2.7-2.4 Ga. (Boher et al., 1992).

## **Akwatia Diamond Field**

There are four diamondiferous areas in Ghana. Akwatia is by far the largest and the only deposit being commercially exploited on an industrial basis. The Birim diamondiferous area is ~ 40 square miles (64 km.) although the total area currently being exploited is somewhat smaller (32 km). Mining operations in the past were on residual, colluvial and alluvial deposits on small first order streams. Production today by the government owned Ghana Consolidated Diamonds (GCD) is predominately on Birim River alluvium downstream from the main Akwatia diamond field.

The Akwatia diamond field is about 80 km northwest of Accra. The area is covered by dense tropical rainforest, much of it secondary due to intensive strip mining. Elevation varies between 120-250 meters above sea level. Well-defined gravel terraces occur at several levels above the Birim River valley. The lower terrace corresponds with the annual maximum flood level of the Birim River. Terraces are covered with coarse, well-rounded, closely packed quartz gravel. A hard cap of laterized clayey quartz gravel covers the area. Intense tropical weathering extends to depths > 20m. Bedrock exposure is limited to drainage channels, strip mined areas and steep interfluvial slopes.

## **Local Geology**

The Akwatia diamond field lies within the Birimian supergroup. (Junner, 1943) noted the composition of Birimian rocks in the diamond field is intermediate between the upper Birimian greenstones of the Atewa range to the east and typical lower Birimian to the west (see figure 2). Interbedded tuffaceous greywacks, phyllites and schists after impure argillaceous rocks predominate. Tuffs, basic and ultrabasic rocks are common but

subordinate. (Junner, 1943) mapped a large elongate unit of predominantly basic, ultrabasic and pyroclastic rocks (figure 3). The majority of these rocks are represented by an actinolite-tremolite schist.

Birimian rocks are intruded by granite, basalt and cut by veining. The Cape Coast granite batholith intrudes Birimian rocks in the southern part of the diamond field. The batholith is dated by the U-Pb method at 2090(+/- 1) Ma. (Davis et al., 1994a), which partially constrains the age of the diamond field rocks. The batholith has a contact metamorphic aureole that overprints the D1-D3 events. Proximal to the batholith, basic igneous rocks are converted to hornblende schists, gneisses and amphibolites, and pelitic rocks are converted to biotite gneisses and schists. Garnet and kyanite occur in the metapelites near the granite contact; staurolite is common to 1.5 km from the contact. Rare basalt dikes cross-cut both strike and dip of the Birimian strata, show well-defined chill margins and are only slightly metamorphosed (Junner, 1943). Concordant and discordant quartz veins are abundant in the Birimian rocks, and are related to local silica, chlorite, carbonate, sericite, tourmaline and pyrite alteration.

Structural relationships in the diamond field are obscured by vegetation metamorphism and laterization. The strike of the Birimian rocks in the diamond field is predominantly NE-SW with some local variation especially near the granite contact where strikes tend to conform to the contact. Dips are between 90-70 degrees; dips less than 60 degrees are rare. The metasediments in the area are chiefly coarse-grained clastic turbidites including wackes with subordinate conglomerates and interbedded argillites (McKittrick, 1996). Distinct marker beds are absent making correlation between beds difficult or impossible. Normally graded bedding is common. Local changes in



“Younging” direction noted by (Junner, 1943), (McKittrick 1996) and CAST geologists (Gammon, 2003) confirm the presents of isoclinal folding. Clear evidence for faulting is absent but is suspected (Junner, 1943).

No classical diamond indicator minerals are reported in the Akwatia diamond field. Mineralogical analysis of washing and concentrate samples from the Akwatia diamond field by (Kaminsky, 1996) show the heavy fraction consists of non-magnesian ilmenite, staurolite and rutile. All samples contain sizable amounts of magnetite, hematite, limonite and aggregates of iron hydroxides, hematite and sericite. Almandine garnet, amphibole, tourmaline, kyanite, zircon, apatite, sphene and blue spinel are present in moderate amounts.



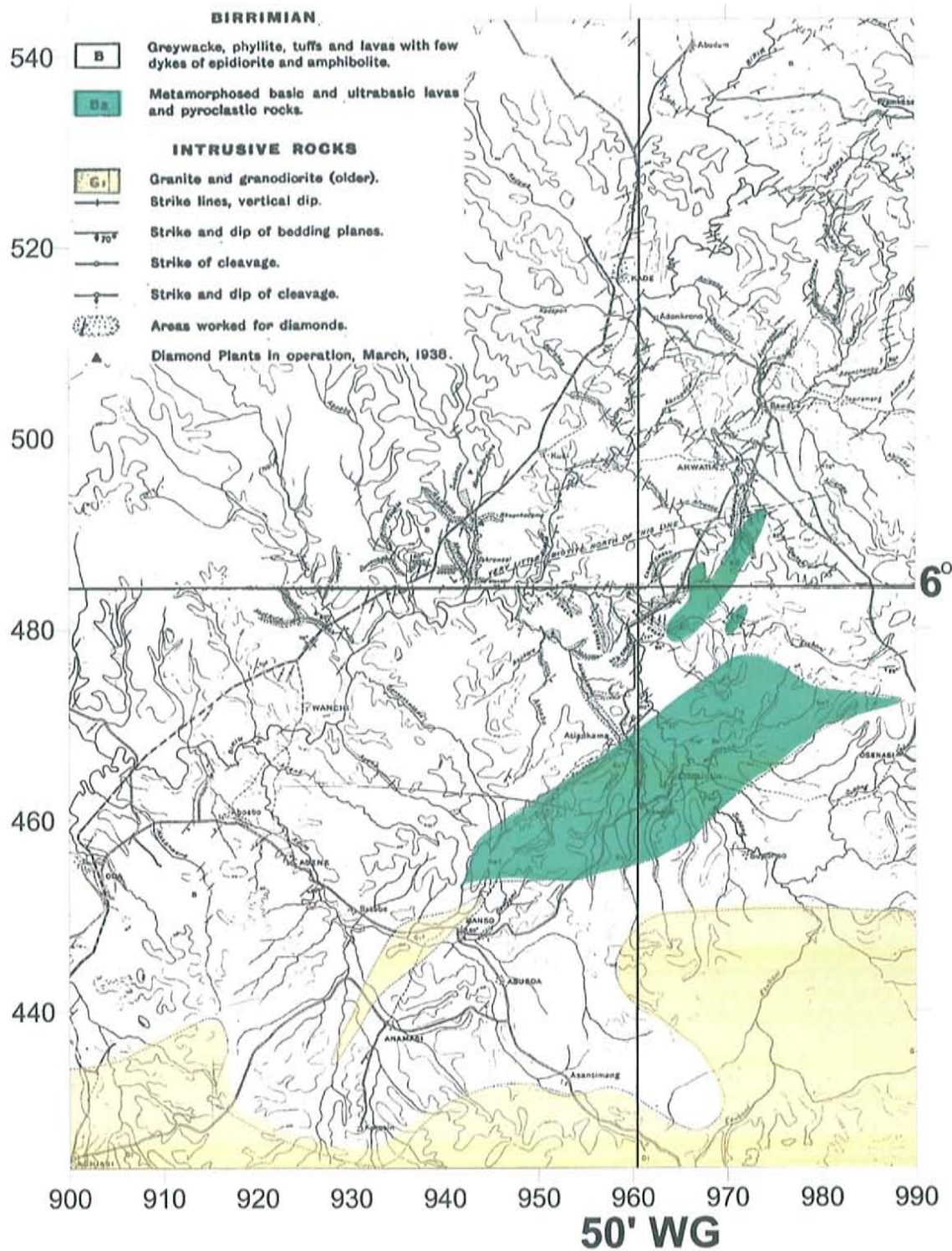


Figure 3. Geologic map of the Akwatia area. One map unit equals 1000 feet; crossed black lines are 6 degrees longitude 50 minutes latitude west of Greenwich. Modified after Junner (1943).

## Diamonds

Akwatia diamonds tend to be small, but of high quality. The average size of the diamonds is .5-4mm in diameter (75-83 %) and the average weight is ~ 8.84 mg. There are few diamonds smaller than .5 mm, and apparently no micro diamonds. The weights of individual crystals varies from .5 mg to 157.8 mg. Dodecahedroids (also called rounded dodecahedron or tetrahexahedroids) are the predominate morphology making up approximately 45% of diamonds followed by octahedrons at ~18%, cubes are rare (Gammon, 2003). The majority of Akwatia diamonds are colorless. Less numerous colored stones are smoky brown and gray. Green stones are occasionally found; yellow and red stones are rare. Diamond inclusions are exclusively of peridotitic affinity (Kaminsky, 1996; Meyer and Boyd, 1972; Ward, 1998).

## METHODS

Seven locations where small-scale miners exploit the diamondiferous bedrock were visited; at site the miners were interviewed, samples were taken, the site photographed and the orientation, width, contact rocks, strike of the diamond horizon and GPS coordinates recorded. Approximately 100 samples were transported to NM Tech. Twelve rock samples (G1-12) were analyzed for major and minor elements by ALS Chemex by means of ICP-MS and ICP-AES instruments. Sample Dm-2 was similarly analyzed by Activation laboratories. Heterogeneous lithologies (breccias) were channel sampled to obtain average compositions. Samples weighing ~ 1kg. were pulverized and then homogenized in a plastic container by turning and shaking to avoid gravitational settling of heavy minerals. Sixty grams of the resulting material (per sample) was submitted for analysis. One duplicate set was submitted (samples G-11 and G-12) for quality assurance. Photos of rock samples were taken with a digital camera attached to a binocular microscope at New Mexico Tech.

Diamond grade maps were prepared by compiling analyses on maps (figure 4) obtained from the GCD. These were digitized using a digitizing tablet and Microsoft Excel. The data is in the form of exploration pits (short number columns) and drill sites (long number columns) spaced about 200 ft (61m) apart, diamond grades are in cts/yd<sup>3</sup>. Pit sizes are about 1 by 2 yards in plan view; the A1, the B1 soil horizon, coluvium or alluvium soils, and saprolitic bedrock, and in some cases B2 soil horizon were assayed.



Where hard bedrock was encountered maps indicate bedrock, and no assay was done. A second form of sampling uses twenty-two inch (56 cm) diameter drill holes that are assayed every foot. Data from 13,000 exploration sites includes: if they are pit or drill sites; if the material is "terrace" (residual soils) then the label is "T"; if the material is "valley" (colluvial and first-order-stream alluvial material) then the label is "V", or waste (mine tailings) then the label is "W" or "WF"; and the thickness assayed. Compiled pit assays are named A, B1, B2, and bedrock. Drill hole analyses were compiled using the first 1-foot interval A, the second foot B1, the third foot interval B2, and the bottom most assay "bedrock".

These data are used to generate "surfer" (surface mapping software) maps. Over 13,000 assay points were digitized with over 30,000 sample grades.

Several inconclusive magnetometer surveys were conducted using a Geometrics proton precession magnetometer. Details and results are in Appendix B.





## RESULTS

### Field and Laboratory Observations

Akwatia lithologies are complex intercalated mix of volcano-sedimentary facies from fine-grained pelitic schists to mega-turbidites and ultramafic schists. As mentioned above CAST geologists are unable to definitively differentiate these lithologies. For the purposes of diamond exploration and this study Akwatia rocks may be divided into four lithological units on the basis of texture or in the case of the actinolite schist geochemistry. See appendix A for detailed sample and field site descriptions.

The most common is phyllite-designated b1 on Junner's map (figure 3). Properly this rock is fine-grained pelitic schist, but Junner's rock name will be used here. When fresh this rock is hard, brittle, dark silver-grey and rings when struck with a hammer. It contains euhedral pyrite crystals mostly cubic and quartz veins both concordant and discordant with the poor slaty cleavage. The phyllite weathers to a light gray and becomes more silvery in appearance, produces a dull thud when struck with a hammer, breaks or parts along the slaty cleavage and the pyrite oxidizes leaving behind casts. There is no evidence the phyllite contains diamonds. Interlayered with the phyllites are sub-aqueous-volcano-sedimentary lithologies (commonly turbiditic).

Less common is actinolite, tremolite, chlorite talc schist that may contain varying amounts of rutile, biotite, muscovite iron oxides and carbonaceous matter. When fresh

the actinolite schist is greenish-gray has well developed schistosity, is extremely fine grained, is soft like talc but compact, dense, impermeable and produces a dull thud when struck with a hammer (even when unweathered). When weathered it becomes powdery and mostly uniform gray but may be stained with iron oxides giving it a yellowish or brownish color. The small-scale miners never exploit this rock for diamonds and the presence of diamonds is exceptional.

The third lithology is breccia, which is the diamond-bearing rock (figures 5-8). This rock has a brecciated texture, is very poorly sorted and commonly contains sharp, angular clasts (up to at least 18 cm) of the other metasedimentary lithologies and the actinolite schist and is always matrix supported. It is only known as weathered where it is has colors of red, yellow, white, and brown a (see Appendix 4 and 5 for detailed descriptions of each sample and field site). In outcrop the rock consists of ferruginised clays, variable amounts of re-crystallized granoblastic quartz, carbonaceous material and minor rutile. It is highly porous, permeable, and friable and is highly weathered to at least 30m. Clasts are mostly fragments of country rock, in many bedding is seen. The clasts are preferentially aligned and are concordant with the overall nearly vertical bedding and schistosity of the surrounding rock. The rock exhibits poor though distinct schistosity. The fourth rock type is the finer grained metasediments including high Mg samples analyzed by (McKittrick, 1996), finer grained turbidites, and sediments of uncertain origin.

Deep, trenches with minimal slumping at Beduwara Hill expose diamond bearing rock and allow observation of rock texture and clast orientation, severe weathering, slumping and disturbances by small-scale mining activities at many of the locations



visited obscures these features. Clasts size varies from location to location (> 16cm to 1cm) a brecciated texture is observed at all locations visited.

The exposed diamond bearing body at Beduwara Hill is 1600 meters long 500 meters wide and has been trenched to 15 meters. The strike of the body is NE-SW, the dip of the bedding and schistosity is 80-90 degrees. The exposed area of the diamond bearing body at sample location Dm-2 is 400 meters long 20 meters wide and has been trenched to 10 meters; the strike and dip of bedding and schistosity are the same as Beduwara Hill. The other sample locations are areas of approximately half a square kilometer, where diamond bearing rock is exposed by discontinuous pitting and trenching through the laterite cap, estimates of the size of diamond bearing bodies at these locations is speculative at best. The strike and dip of these diamond-bearing rocks is NE-SW with vertical dips (see Appendix 5 for more details).

The breccia units exist as long, narrow dike-like structures within the actinolite schist or phyllite. These dike-like structures are most certainly bedding upturned by isoclinal folding. The breccia unit is usually in contact with the actinolite schist less commonly with the phyllite. The trend of these dike-like structures is always concordant with the overall schistosity and strike of the local rocks. The contact between schist and the volcanoclastic breccia unit commonly is composed of a thin shaly or pelitic layer of material that appears to be weathered phyllite suggesting an unconformity (figures 10 and 11). Laterite and saprolite are well developed throughout the area. The laterite forms a tough cap above both units. The diamond grades are relatively high in the laterite and the small-scale miners do occasionally crush the laterite to obtain the diamonds. All units are cross cut by mesothermal quartz veins both concordantly and discordantly.



Small-scale miners exploit the volcanoclastic unit for diamonds. Figures 11 and 12 show the upper part of an approximately 30 meter deep trench dug into the diamondiferous rock. There were about a hundred small-scale miners working this trench when the photo was taken. The material is removed with hand tools, placed into grain sacks and carried to the nearest water where it is classified using a homemade screen with about 1 cm holes, and then washed to remove clay in a 55gal. drums. The material is then placed in a screen box (standard windows screen) and is jigged to concentrate the heavies while the lighter material is thrown off. The diamonds are then hand picked from this final material, which is composed mostly of quartz and laterite concretions. The small-scale miners report that twenty standard grain sacks will yield 0-7 carats.



Figure 5. Beduware Hill brecciated diamond bearing rock showing preferential, concordant alignment of clasts. The rock now consist mostly of clays and quartz, location of samples G-3 and G-12 (see sample location map figure 17).



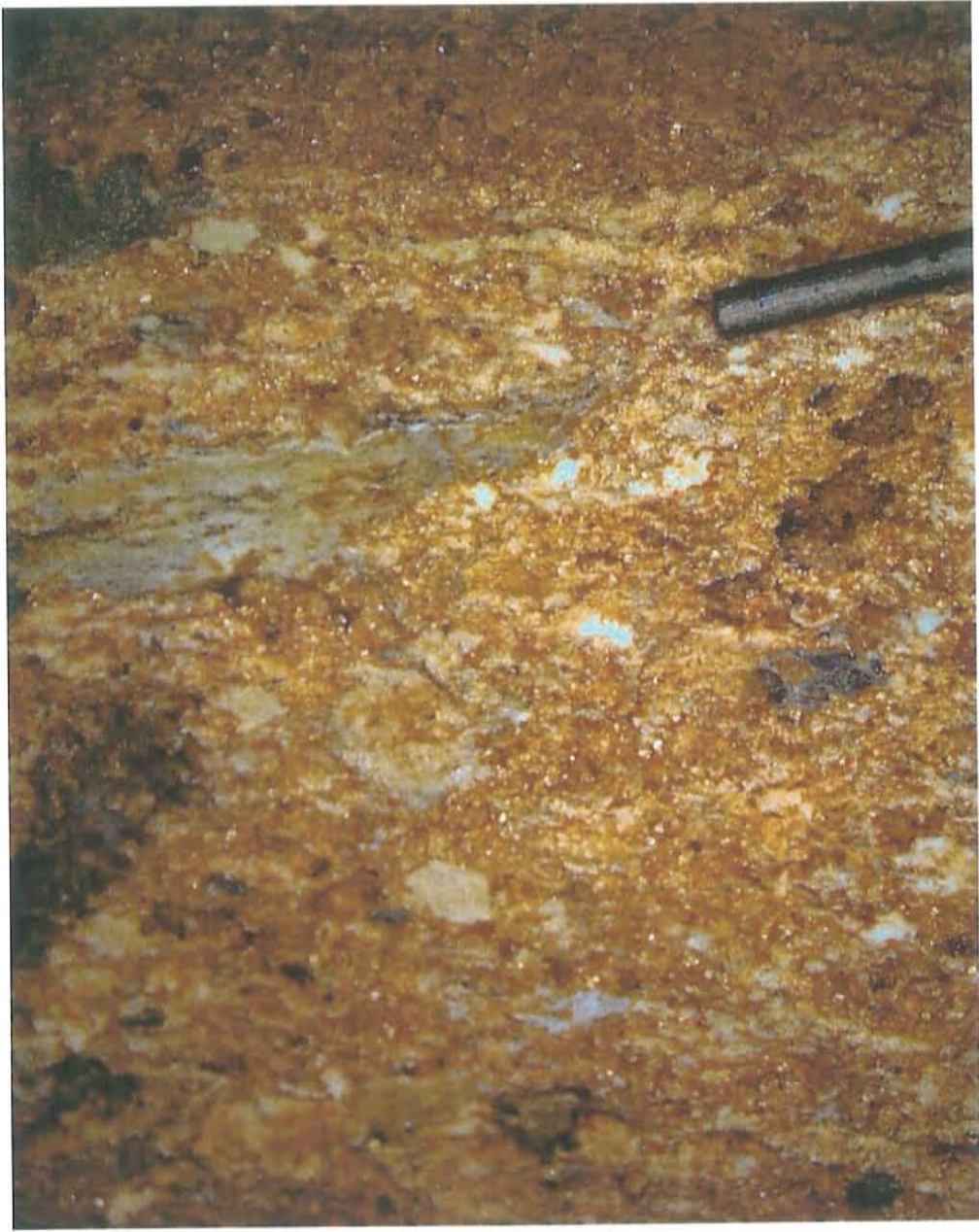


Figure 6. Binocular microscope picture of sample G-12 showing preferential orientation of clasts (.7mm pencil lead for scale).



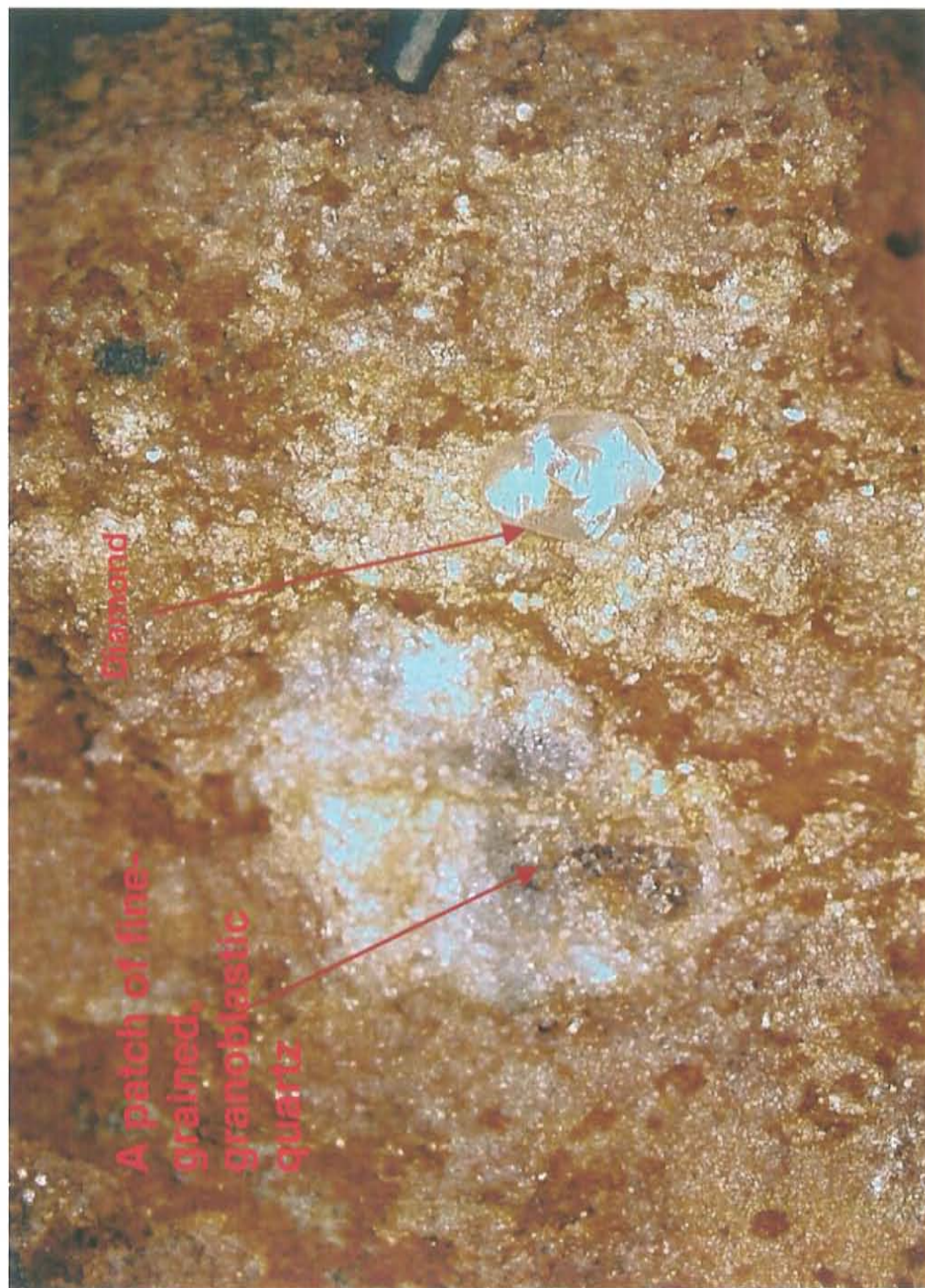


Figure 7. Binocular microscope picture of sample from same location as DM-2 (see sample location map figure 17) showing diamond in matrix (.7mm pencil lead for scale).





Figure 8. Binocular microscope picture of sample from same location as DM-2 showing diamond in matrix (.7mm pencil lead for scale).

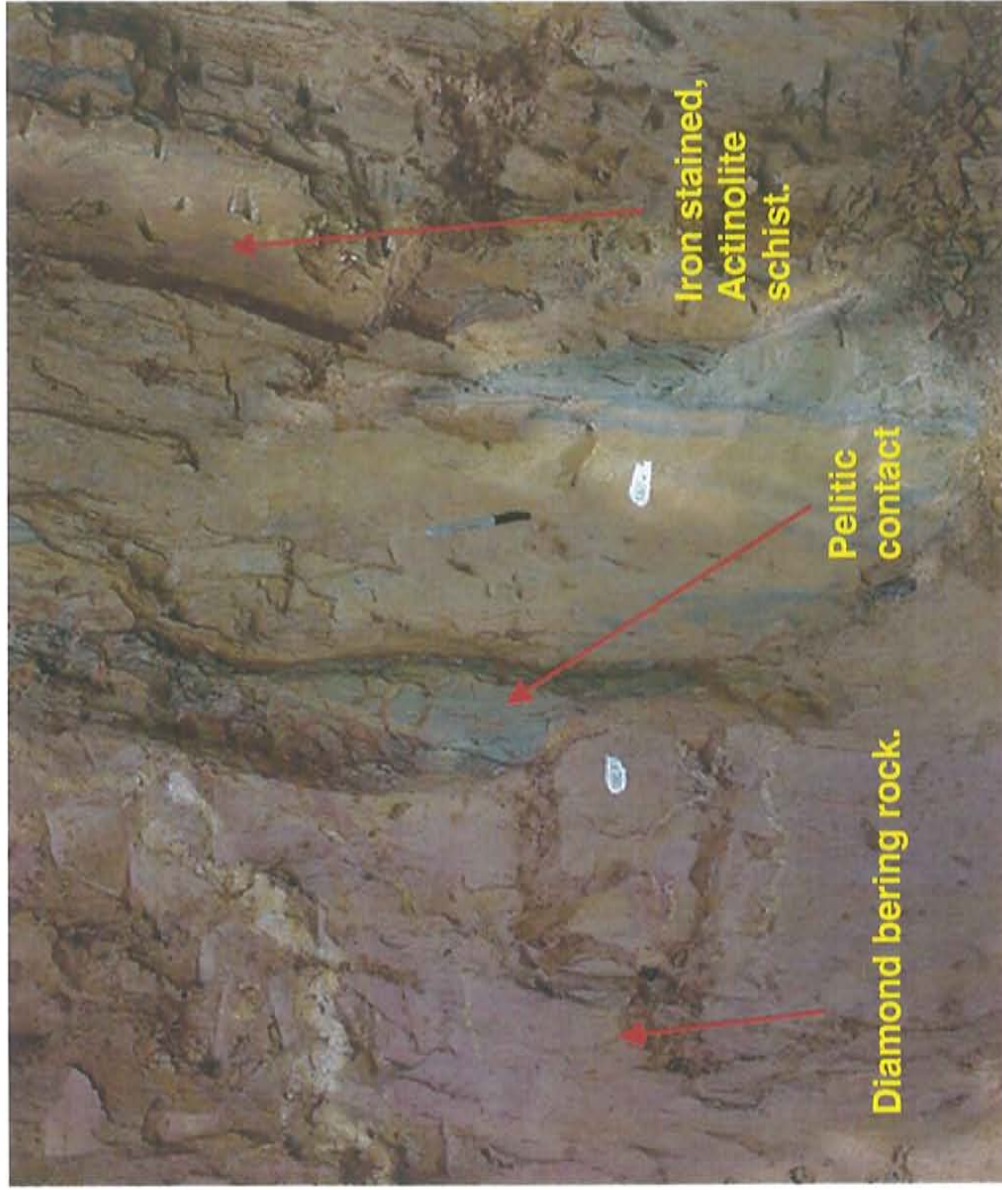


Figure 9. Pelitic contact between diamond bearing clastic rock and actinolite schist (marker pen for scale) at location of samples G-5 and G-6 (see sample location map figure 17).



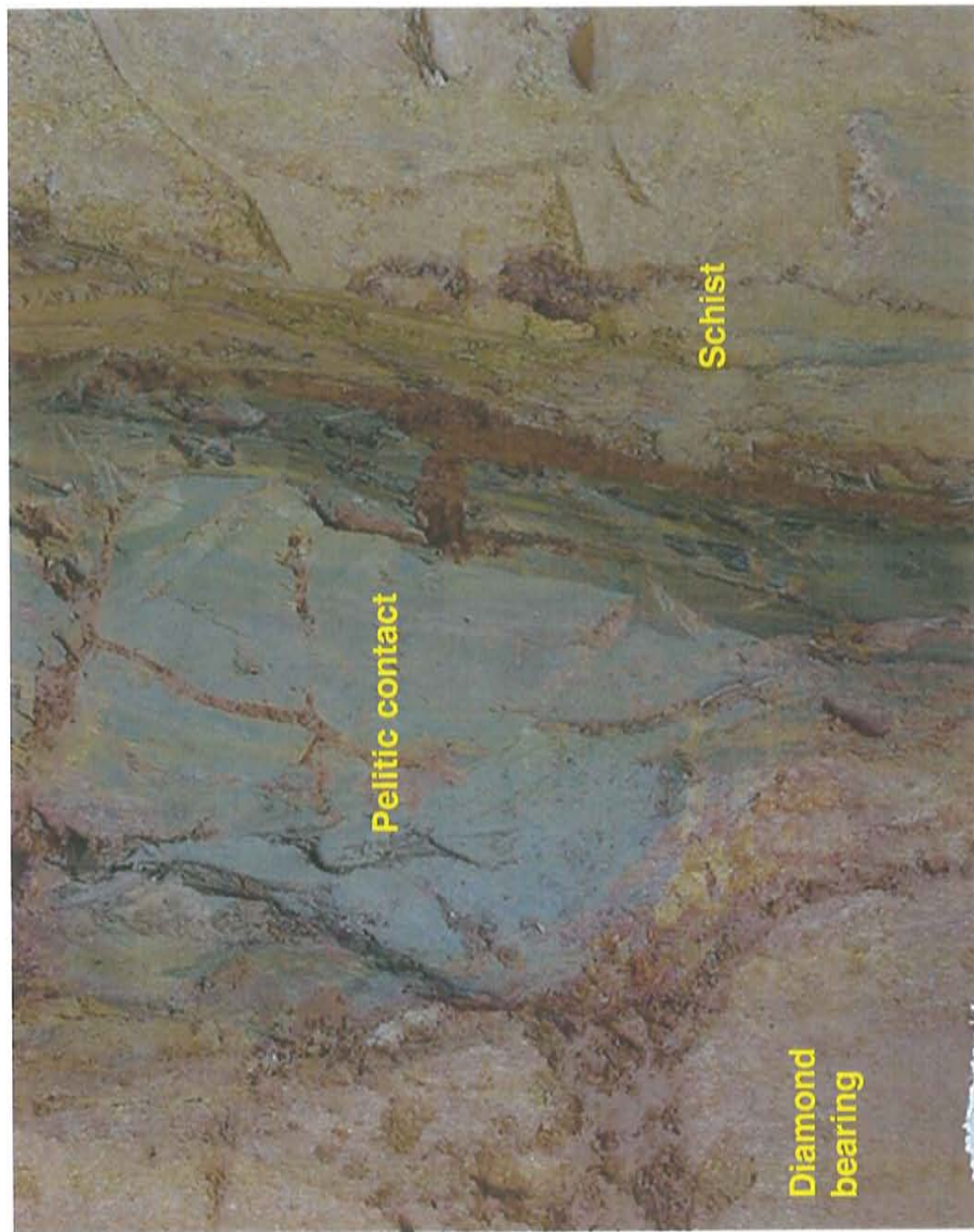


Figure 10. Close up of undulating pelitic contact between diamond bearing rock and actinolite schist.



Figure 11. Large diamond bearing dike-like body, location of sample G-2.  
On sample location map (figure 17)





Figure 12. Large diamond bearing dike-like body (close up of above contact), note the brecciated texture.

## **Diamond Distribution**

Detailed diamond distribution maps obtained from GCD are digitized. The data are used to generate "Surfer" maps. Statistical reports are provided in the appendix for each grid used to make the maps. All grids use the Natural Neighbor gridding method. All maps are in Ghana national datum and latitude/longitude west of Greenwich.

Image maps are generated of topsoil, the B1 horizon and bedrock or lowest level diamond grades in carats per cubic yard (figures 13, 14 and 15). Figure 16 is an image map produced by calculating the first derivative of number strings in the natural neighbor grid in a NW-SE direction. In other words this map shows how fast diamond grades are changing along lines perpendicular to the dominant strike of the underlying lithology.

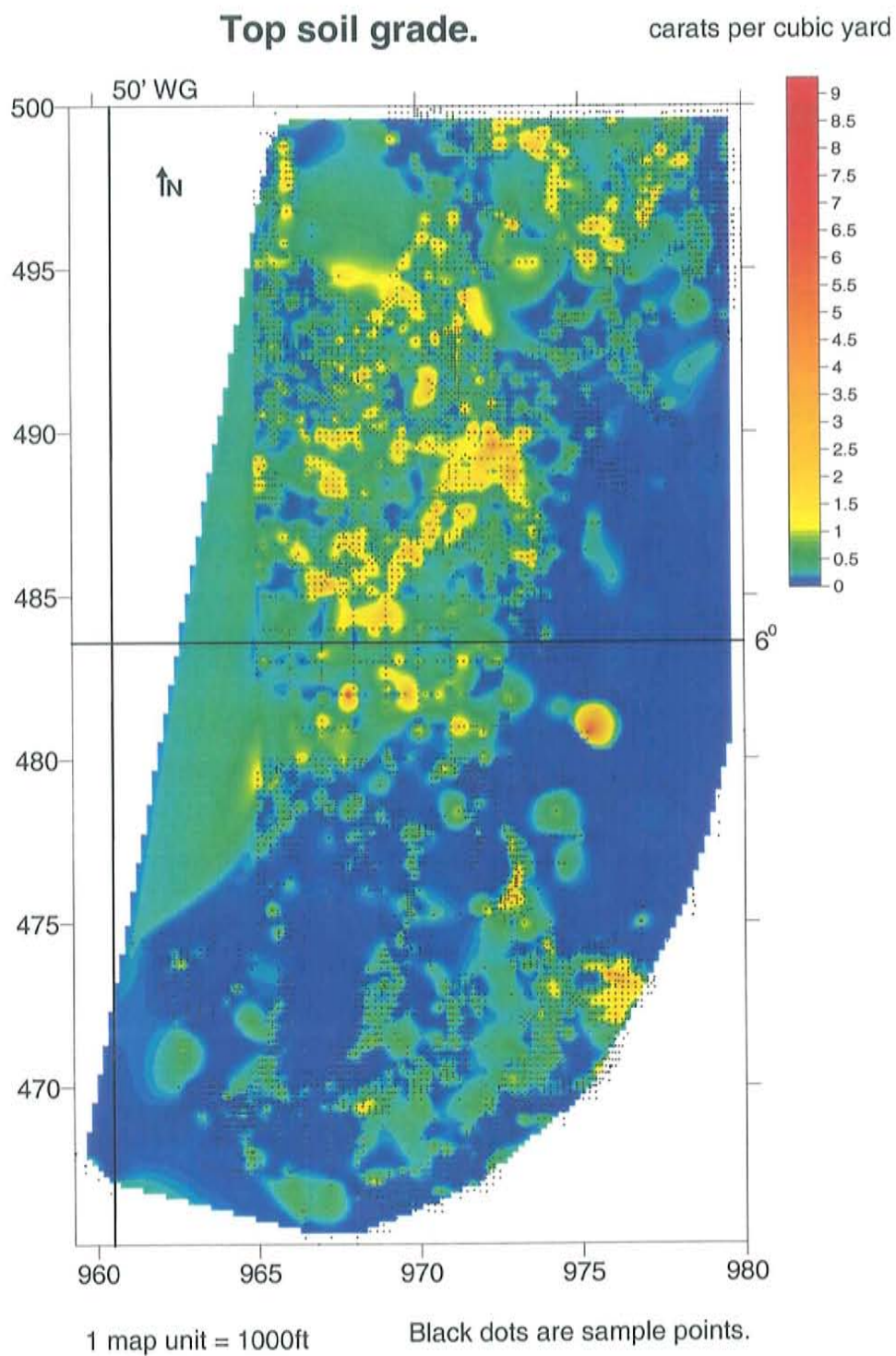


Figure 13. Image map of topsoil grade in carats per cubic yard (natural neighbor gridding method see appendix for statistics). The crossed lines are latitude/longitude 6 degrees and 50 minutes west of Greenwich.



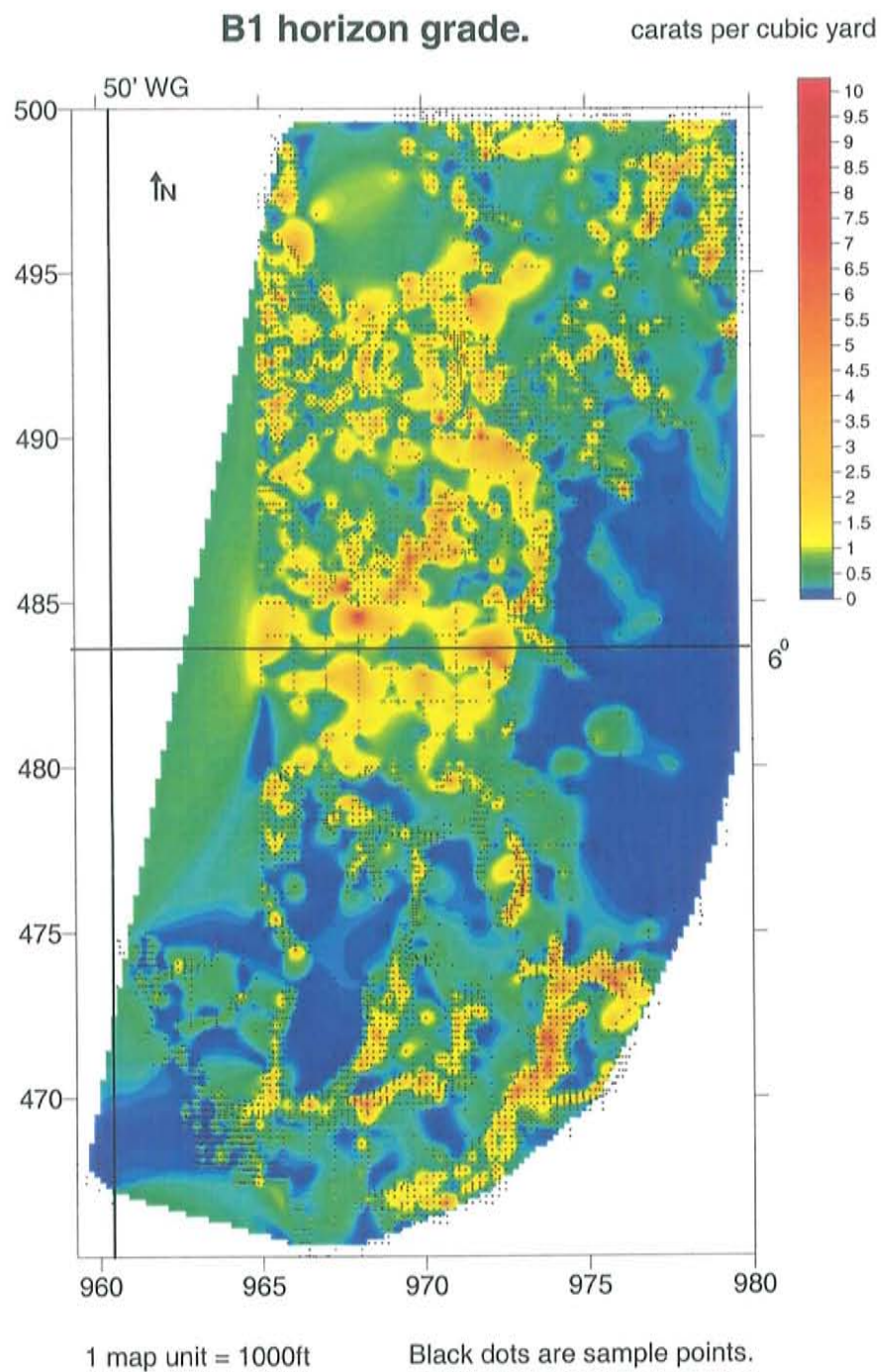


Figure 14. Image map of B1 grade in carats per cubic yard (natural neighbor gridding method see appendix for statistics). The crossed lines are latitude/longitude- 6 degrees and 50 minutes west of Greenwich.



# **Bedrock or bottom level grade.**      carats per cubic yard

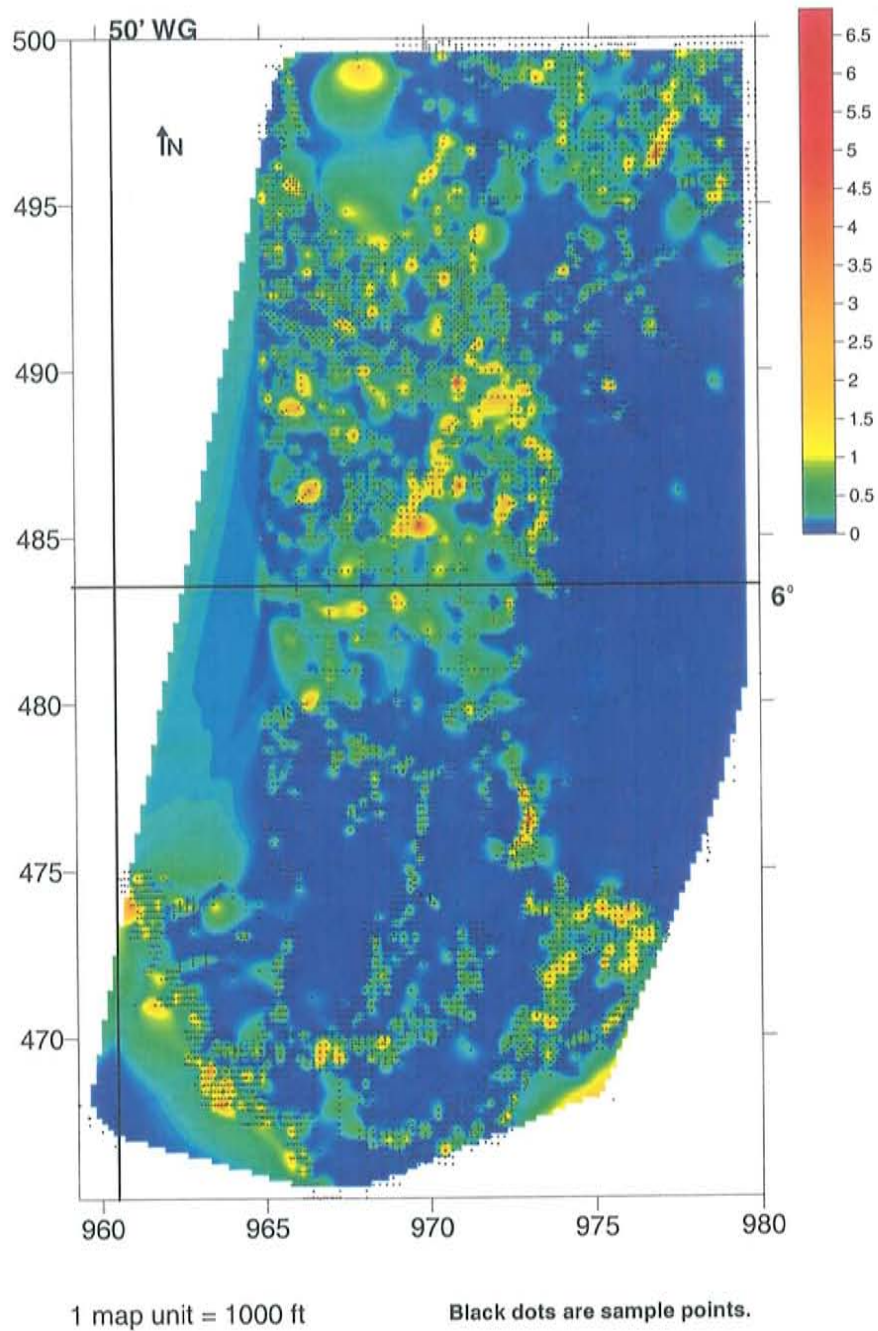


Figure 15. Image map of bedrock grade in carats per cubic yard (natural neighbor gridding method see appendix for statistics). The crossed lines are latitude/longitude- 6 degrees and 50 minutes west of Greenwich.

## NW-SE Directional derivative (first derivative)

Bedrock or bottom level grade.

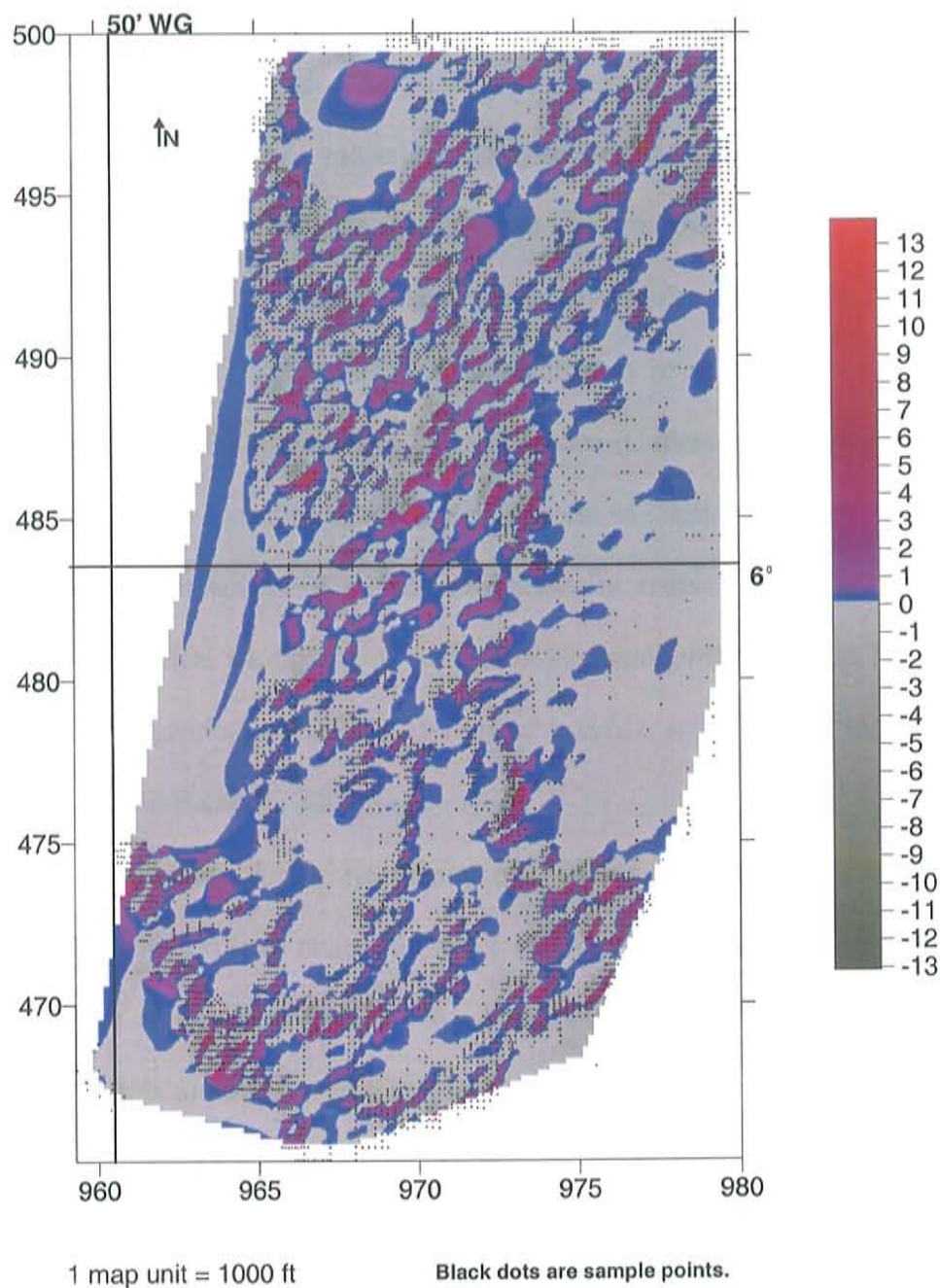


Figure 16. Image map of directional derivative in carats per cubic yard (natural neighbor gridding method see appendix B for statistics). The crossed lines are latitude/longitude- 6 degrees and 50 minutes west of Greenwich.



## Geochemistry

All Akwatia rocks are part of the Birimian supergroup (Junner, 1943; Kesse, 1985) which consist mostly of volcanic rocks or sediments derived from volcanic rocks. The diamond bearing rocks of Akwatia are likely volcanoclastic, although weathering has destroyed direct evidence of this. The presence of diamonds lacking signs of sedimentary transport is further evidence of volcanic origin. The extreme weathering of the diamond-bearing rocks makes it difficult to quantify the original major, mobile-element composition of the protolith. However since the major constituents of these rocks are now clays the original rare earth element (REE) signature may be retained. Clays are shown to faithfully retain the REE signature of the provenance (Cullers et al., 1987). Further the most important factor contributing to the REE content of clastic sediments is provenance (Fleet, 1984; McLennan et al., 1989). Additionally recent studies of geochemical behavior under tropical weathering of the Brama-Mazaruni greenstone belt in the Guiana Shield show that generally the REE patterns of bedrock are preserved in the saprolite horizon (Voicu and Bardoux, 2002).

Severe alteration due to weathering of diamond bearing rocks require that the mobility of constituents both major and minor be enumerated. This will be addressed at the end of this section. **For initial discussion, begin bulk chemistry is treated as though the rock is unaltered and a volcanic protolith or provenance is assumed.**

Samples G-2, G-3, G-4, G-9 and G-12 were gathered from locations known to be producing diamonds (figure 17). At each of these locations samples were gathered from the deepest part of the trenches to obtain the least weathered samples. Sample Dm-2 is from the same trench as the sample with a diamond *in situ*. There is no question that

samples G-2, 3, 4, 9, 12 and Dm-2 host diamonds, see appendix A. Samples G5 and G10 (G11 is a duplicate) are the actinolite-tremolite schist. Samples obtained and analyzed by (McKittrick, 1996) : 93-17, 93-19, 93-20, 93-33 and Ha-2 are actinolite schist, samples BH-170, BH-197, Bh-226, BH- 243 are fine-grained, high-Mg, metasediments (see figure 17 for locations).

### *Major Element Oxides*

Mobile oxides (Mg, Na and Ca) show the most variation between the rock suites while Ti shows the least. Aluminum oxide concentrations in diamond bearing rocks vary from 13.1-to 20.6 weight percent (wt.%), between 8.05 to 14.35 wt. % in the actinolite schist and 8.85 wt. % to 15.8 wt. % in the fine-grained, high-Mg metasediments. Titanium oxide concentrations in diamond bearing rocks vary from 1.05 to .66-wt. %, between 0.45 to 0.58 wt. % in the actinolite schist and 0.40 wt. % to 0.50 wt. % in the fine-grained, high-Mg metasediments. Total iron oxide ( $\text{Fe}_2\text{O}_3$ ) concentrations in diamond bearing rocks vary from 20.3 to 6.61 wt. %, between 11.63 to 7.63 wt. % in the actinolite schist and 7.01 wt. % to 8.05 wt. % in the fine-grained, high-Mg metasediments. Magnesium oxide concentrations in diamond bearing rocks vary from 0.04-to 6.68-wt. %, between 16 to 20.64 wt. % in the actinolite schist and 10.81 wt. % to 21.2 wt. % in the fine-grained, high-Mg metasediments.

In figure 18 Akwatia rocks are plotted on a cation discrimination diagram (Jensen, 1976) which can be used successfully (for protolith identification) with metamorphosed volcanic rocks as the elements are selected for their variability within subalkaline rocks-varying in inverse proportion to each other and for their stability under low grades of metamorphism (Rollinson, 1993). The less weathered, high-Mg samples (which include



the actinolite schist and high Mg, fine-grain metasediments from Beduwara Hill) plot in the komatiite field and severely weathered diamond-bearing rocks plot across the tholeitic and calc-alkalic fields. Extreme weathering of the diamond bearing rock has likely modified the true position of the protolith on this plot, as will be discussed later.

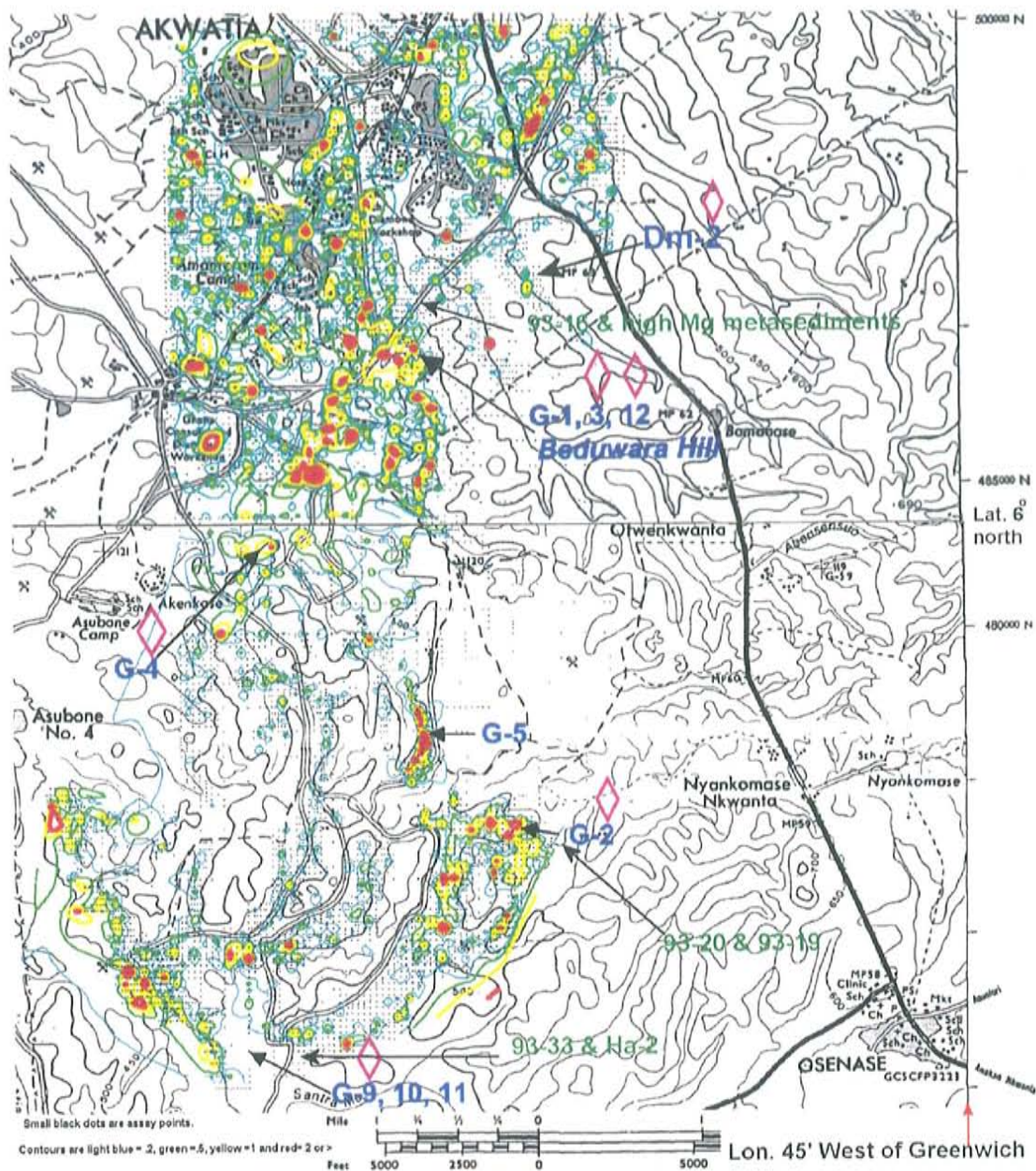


Figure. 17. Composite map. Contours are bedrock grades in carats per cubic yard. Light blue=.2, green=.5, yellow=1 and red=2 or >. Dark blue numbers are locations of trenches in diamondiferous rock and sample locations, pink diamonds are diamondiferous samples. Green numbers are samples from (McKittick, 1996). Right horizontal axis is 45 minutes West of Greenwich; the middle Latitude is 6 degrees north.

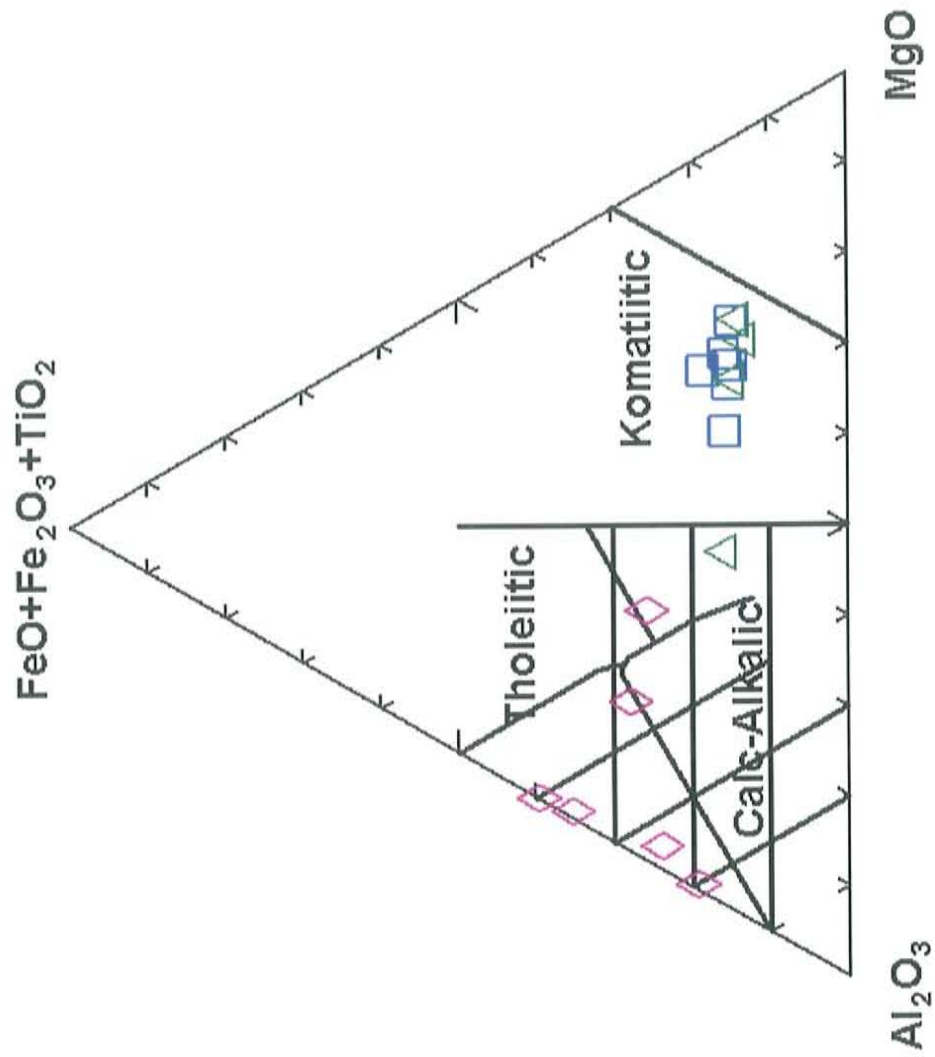


Figure 18. Discrimination diagram for volcanic rocks, open blue squares are actinolite schist, open pink diamonds are diamondiferous rocks, open green triangles are high Mg metasediments (McKittrick, 1996). The form of the diagram is from (Jensen, 1976).



### *Minor Elements and Rare Earth Elements*

Diamond bearing rocks and the high, Mg metasediments have comparable REE concentrations. Zirconium is elevated in the diamond bearing rock and REE are elevated in the actinolite schist. Zirconium content varies from 91.6 ppm to 165.5 ppm in diamond bearing rocks, 60.27 ppm to 82.28 ppm in the actinolite schist and 79.28 ppm to 57.33 ppm in the high- Mg metasediments. Thorium content varies from 3 ppm to 5 ppm in diamond bearing rocks, 2 ppm to 6 ppm in the actinolite schist and 2.5 ppm to 5.4 ppm in the high- Mg metasediments. Niobium content varies from 4 ppm to 8 ppm in diamond bearing rocks, 2.2 ppm to 5.3 ppm in the actinolite schist and 2.8 ppm to 4.4 ppm in the high- Mg metasediments. Hafnium content varies from 3 ppm to 5 ppm in diamond bearing rocks, 2 ppm to 3 ppm in the actinolite schist and 1 ppm to 2 ppm in the high-Mg metasediments.

Rare earth elements in the diamond bearing rocks and the high-Mg metasediments are only moderately variable with cerium having the most variability. Concentrations of rare earth elements in the actinolite schist are elevated relative to the other lithologies and vary considerably. Minimum and maximum REE concentrations are summarized in Table 2. (Tantalum data is near or below the detection limit).

Chondrite normalized REE diagrams are generated for diamond-bearing rocks and the actinolite schist (figures 19 A-F) to investigate the genesis of the samples and possibly unravel the petrologic processes involved at Akwatia. There are significant differences between diamond-bearing rocks and the actinolite schist REE analyses when plotted normalized to chondrite. The actinolite schist is highly enriched in REE especially in light rare earth elements (LREE) and plot with a negative slope. The diamond-bearing

rock analyses have lower concentrations of the REE and do not show the same degree of enrichment in LREE common to the schist analyses. The diamond bearing rocks exhibit a positive cerium anomaly while several of the actinolite schist samples exhibit a negative cerium anomaly. A slight negative europium anomaly is evident in all actinolite schist samples, while less evident and more variable in diamond bearing samples G-3, G-4 and Dm-2. The high Mg metasediments closely resemble the diamond bearing rocks without the cerium or europium anomaly.

Primitive mantle normalized, multi-element diagrams are plotted to depict and compare rock chemistry (Figure 20 A-C). Mobile element data scatter widely in both the actinolite schist and the diamondiferous rocks. Much of the immobile element data for the actinolite schist also scatter. Prominent negative Rb, K, Sr, Th, Nb, Pb, P, Zr and Ti anomalies are evident in the actinolite schist. Positive Cs, Th, Pb and Zr anomalies and a negative Sr anomaly are evident in the diamond bearing rock. Immobile element data for the diamondiferous rocks are more coherent than mobile elements across the suite. When average compositions of the actinolite schist and the diamondiferous rocks are plotted together concentrations of the elements Ba, Th, Nb, Pb, P, Zr and Ti agree between the two.

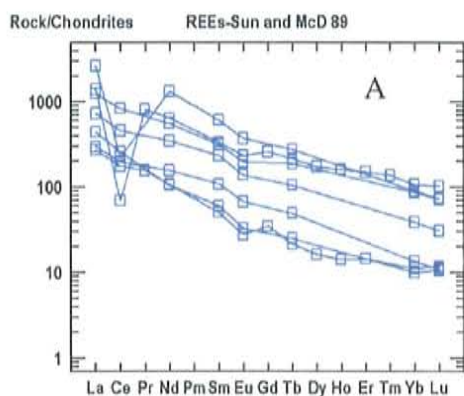
Data from Akwatia rock samples are plotted on a Th-Zr-Nb discrimination diagram (Wood, 1980; Wood et al., 1979) to reveal possible tectonic setting of protoliths. All Akwatia rocks fall in a relatively tight group in the arc basalt field. (Figure 21).

Table 2. Rare earth elements

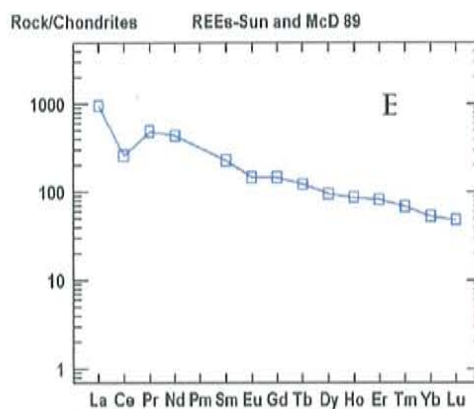
| Sample  | Element |       |      |       |      |      |      |      |     |       |      |     |      |      |
|---------|---------|-------|------|-------|------|------|------|------|-----|-------|------|-----|------|------|
| sample  | La      | Ce    | Pr   | Nd    | Sm   | Eu   | Gd   | Tb   | Lu  | Y     | Dy   | Ho  | Er   | Yb   |
| g-2     | 7.4     | 26.7  | 2.5  | 10.6  | 3.3  | 1.0  | 2.9  | 0.6  | 0.4 | 17.0  | 3.6  | 0.7 | 2.3  | 2.3  |
| g-3     | 8.8     | 22.7  | 2.2  | 8.1   | 2.3  | 1.0  | 3.3  | 0.7  | 0.4 | 27.9  | 4.8  | 1.0 | 2.9  | 2.9  |
| g-4     | 3.4     | 10.3  | 1.2  | 4.8   | 1.7  | 0.4  | 1.7  | 0.3  | 0.2 | 12.4  | 2.2  | 0.5 | 1.3  | 1.2  |
| g-9     | 6.6     | 39.4  | 2.0  | 8.0   | 1.8  | 0.6  | 1.9  | 0.3  | 0.2 | 8.6   | 1.9  | 0.4 | 1.3  | 1.4  |
| g-12    | 7.8     | 21.5  | 2.1  | 7.6   | 1.9  | 0.7  | 2.3  | 0.4  | 0.3 | 16.6  | 2.6  | 0.6 | 1.8  | 1.9  |
| DM2     | 5.2     | 13.9  | 1.3  | 5.4   | 1.5  | 0.6  | 1.5  | 0.3  | 0.2 | 9.0   | 1.6  | 0.3 | 1.1  | 1.1  |
| Minimum | 3.4     | 10.3  | 1.2  | 4.8   | 1.5  | 0.4  | 1.5  | 0.3  | 0.2 | 8.6   | 1.6  | 0.3 | 1.1  | 1.1  |
| Maximum | 8.8     | 39.4  | 2.2  | 8.1   | 2.3  | 1.0  | 3.3  | 0.7  | 0.4 | 27.9  | 4.8  | 1.0 | 2.9  | 2.9  |
| 93-33   | 626.5   | 138.1 | nd   | 614.5 | 92.9 | 21.5 | nd   | 10.3 | 1.9 | 319.5 | nd   | nd  | nd   | 15.4 |
| 93-20   | 296.6   | 514.0 | nd   | 262.0 | 47.8 | 11.4 | nd   | 7.1  | 1.8 | 96.5  | nd   | nd  | nd   | 14.6 |
| 93-19   | 105.6   | 158.0 | nd   | 49.3  | 9.2  | 1.9  | nd   | 0.9  | 0.3 | 126.2 | nd   | nd  | nd   | 1.7  |
| 93-16   | 70.8    | 121.4 | nd   | 73.3  | 16.6 | 3.9  | nd   | 1.9  | 0.3 | 32.8  | nd   | nd  | nd   | 2.3  |
| ha-2    | 173.3   | 281.4 | nd   | 163.0 | 35.8 | 8.1  | nd   | 4.0  | 0.8 | 86.5  | nd   | nd  | nd   | 6.6  |
| g-5     | 64.9    | 108.0 | 14.8 | 50.4  | 7.7  | 1.6  | 7.1  | 0.8  | 0.3 | 22.3  | 4.1  | 0.8 | 2.4  | 1.9  |
| g-10    | 332.0   | 42.7  | 77.7 | 299.0 | 51.6 | 13.6 | 53.1 | 8.0  | 2.6 | 286.0 | 44.3 | 9.1 | 24.8 | 18.1 |
| Minimum | 64.9    | 42.7  | 14.8 | 49.3  | 7.7  | 1.6  | 7.1  | 0.8  | 0.3 | 22.3  | 4.1  | 0.8 | 2.4  | 1.7  |
| Maximum | 626.5   | 514.0 | 77.7 | 614.5 | 92.9 | 21.5 | 53.1 | 10.3 | 2.6 | 319.5 | 44.3 | 9.1 | 24.8 | 18.1 |
| BH-170  | 9.6     | 21.5  | nd   | 10.3  | 2.7  | 0.9  | nd   | 0.4  | 0.2 | 12.9  | nd   | nd  | nd   | 1.4  |
| BH-197  | 8.1     | 17.9  | nd   | 8.5   | 2.2  | 0.7  | nd   | 0.3  | 0.2 | 9.7   | nd   | nd  | nd   | 1.1  |
| BH-226  | 7.7     | 16.0  | nd   | 7.5   | 2.2  | 0.6  | nd   | 0.3  | 0.2 | 9.7   | nd   | nd  | nd   | 1.0  |
| BH-243  | 12.7    | 27.2  | nd   | 12.6  | 2.3  | 0.5  | nd   | 0.2  | 0.2 | 3.5   | nd   | nd  | nd   | 0.7  |
| Minimum | 7.7     | 16.0  | nd   | 7.5   | 2.2  | 0.5  | nd   | 0.2  | 0.2 | 3.5   | nd   | nd  | nd   | 0.7  |
| maximum | 12.7    | 27.2  | nd   | 12.6  | 2.7  | 0.9  | nd   | 0.4  | 0.2 | 12.9  | nd   | nd  | nd   | 1.4  |

See appendix A for comprehensive analysis.

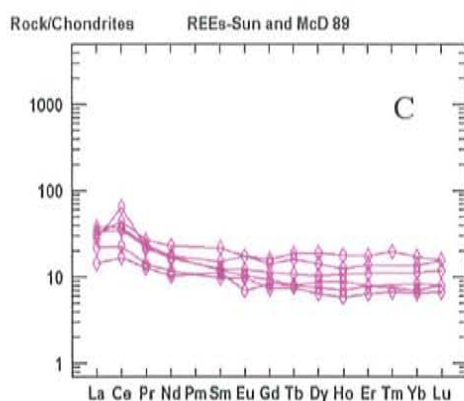




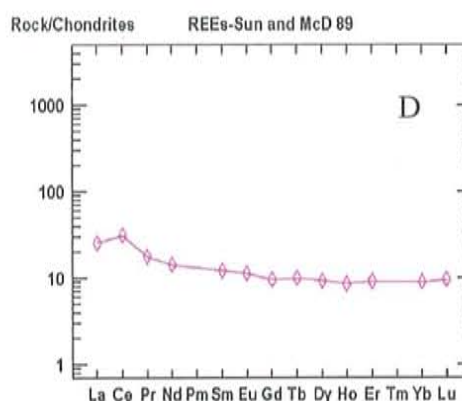
Actinolite schist (all samples)



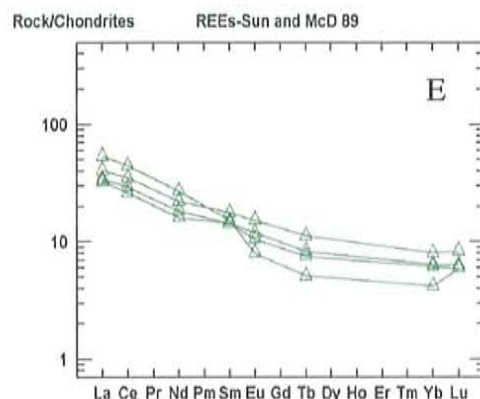
Actinolite schist (average)



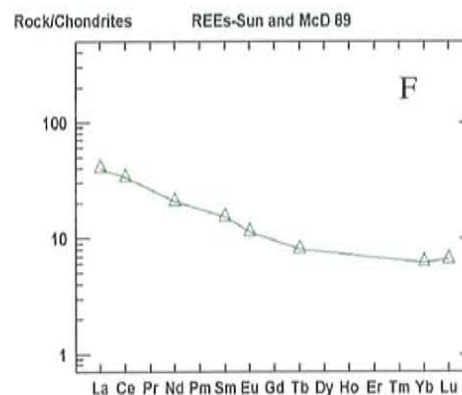
Diamondiferous rock (all samples)



Diamondiferous rocks (average)

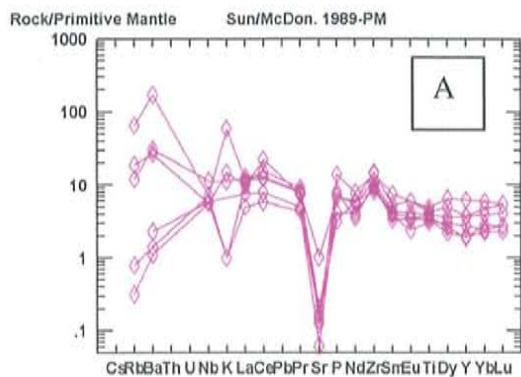


High Mg metasediments (all samples)

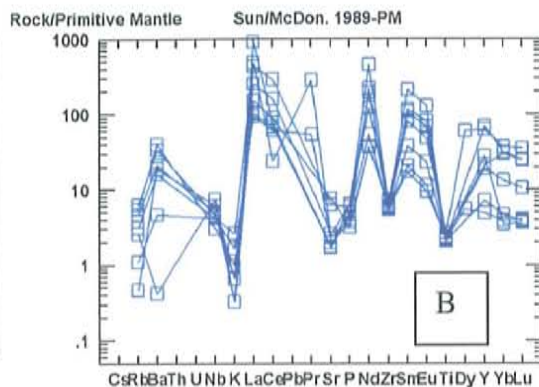


High Mg metasediments (average)

Figure 19. A. Actinolite schist (all samples).  
 B. Average actinolite schist  
 C. Diamond bearing rock (all samples).  
 D. Average diamond bearing rock.  
 E. High Mg metasediments (all samples) from (McKittrick, 1996).  
 F. High Mg metasediments (average) from (McKittrick, 1996).  
 All graphs are normalized to chondrite, normalizing values from (Sun and McDonough, 1989).



Diamondiferous rock (all samples)



Actinolite schist (all samples)

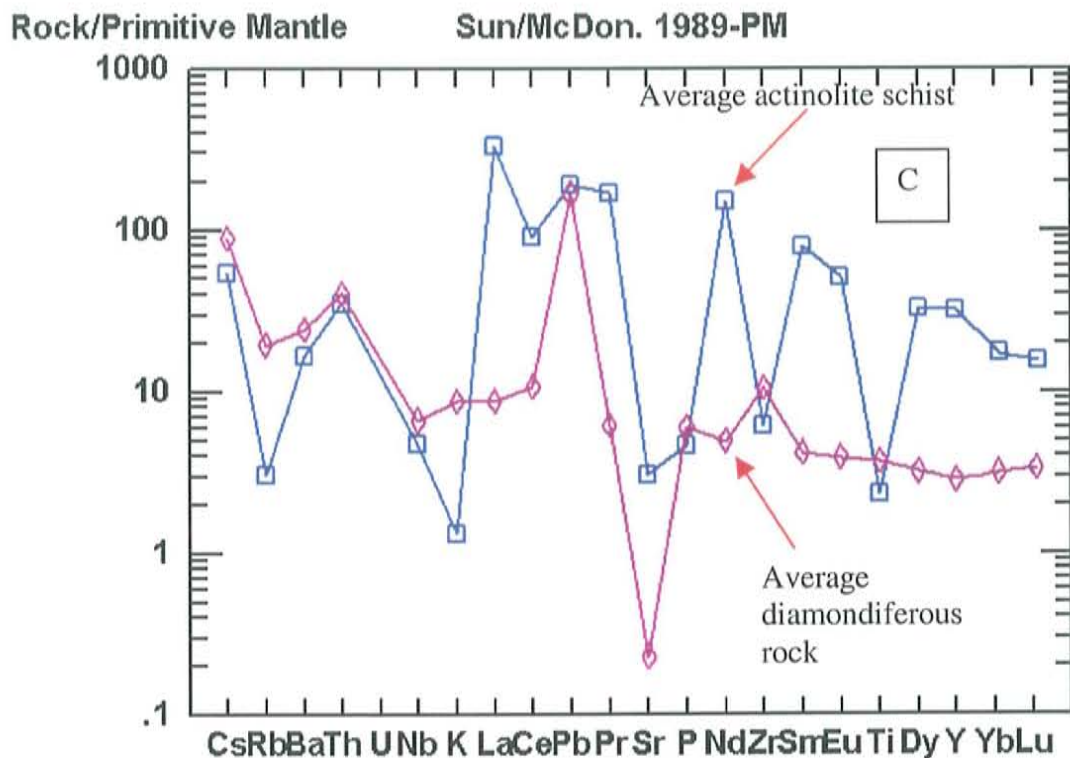


Figure 20. Primitive mantle normalized multi-element diagrams.

- A. Diamond bearing rocks all samples (open pink diamonds).
- B. Actinolite schist all samples (open blue squares).
- C. Average actinolite schist and average diamond bearing samples. Normalizing values and form from (Sun and McDonough, 1989).

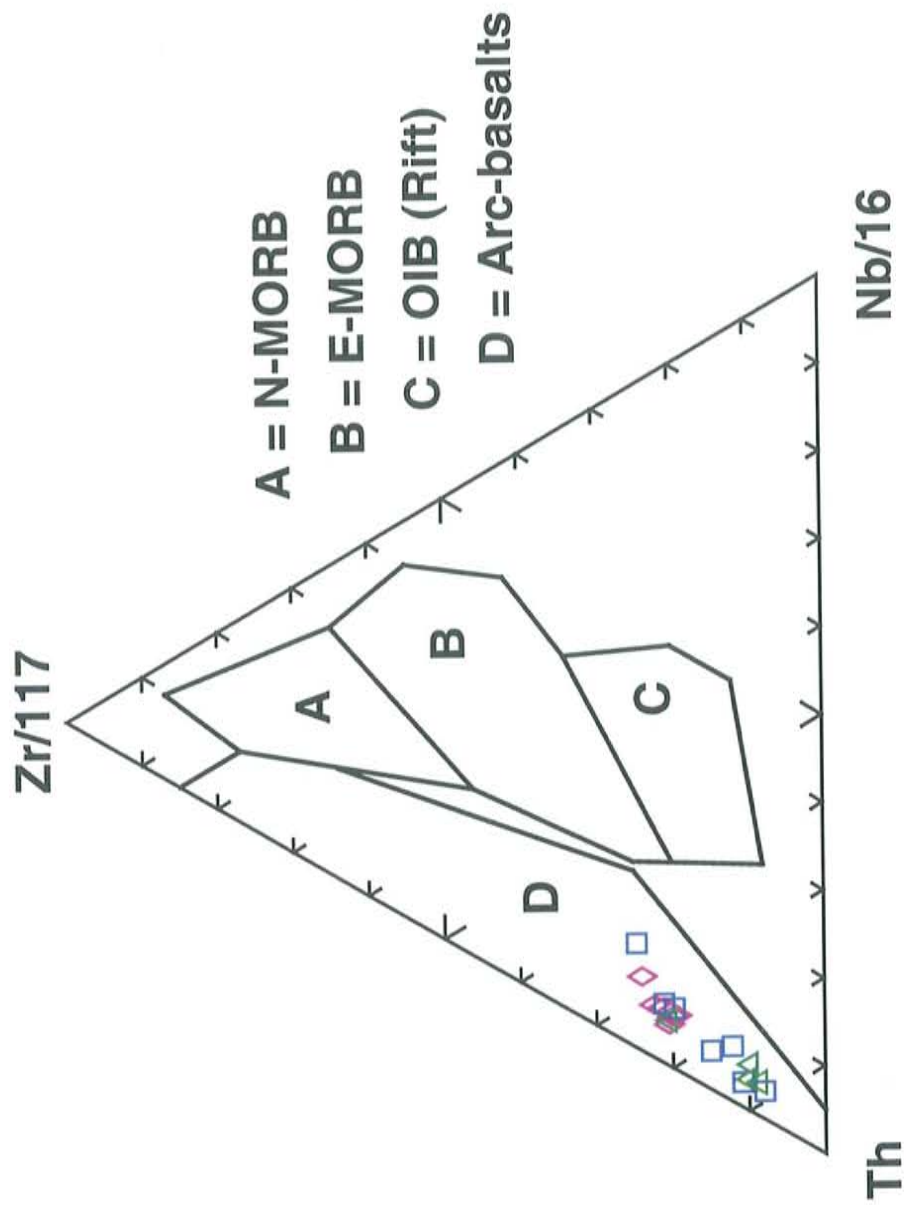


Figure 21. Tectonic discrimination diagram for basalts, open blue squares are actinolite schist, open pink diamonds are diamondiferous rocks, open green triangles are high Mg metasediments from (McKittrick, 1996), the form of the diagram is from (Wood, 1980; Wood et al., 1979).



### *Weathering and Alteration*

Deep tropical weathering and moderate metasomatism are persistent throughout the diamond field area, complicating protolith identification. Recent geochemical studies (Voicu and Bardoux, 2002) in the Barama-Mazaruni greenstone belt at Omai gold mine located in the Guiana Shield, Guyana, South America illuminate the geochemical behavior of major and minor components during intense tropical weathering. Their study uses the chemical index of alteration (CIA) to evaluate the degree of weathering of each sample. The CIA is calculated using the equation:  $CIA = [Al_2O_3 / (Al_2O_3 + CaO + Na_2O + K_2O)] * 100$  where oxides are in molecular proportions (Fedo et al., 1995; Nesbitt and Young, 1982). The CIA evaluates the degree of mineralogical weathering, which is the ratio of the transformation of a primary mineral into its equivalent alteration mineral. A sample with a CIA = 100 indicates complete transformation of a primary mineral into its equivalent weathered product and by extension, complete weathering of the parent rock. The CIA has the advantage of being an indicator of the degree of weathering independent of the depth of sampling.

Chemical index of alteration values are calculated for the diamond bearing rocks and the actinolite schist using the equation:  $CIA = [Al_2O_3 / (Al_2O_3 + CaO + Na_2O + K_2O)] * 100$  where oxides are in molecular proportions (Fedo et al., 1995; Nesbitt and Young, 1982) results are summarized in table 3.

Table 3. CIA

| sample | CIA<br>(% weathered) |
|--------|----------------------|
| g-5    | 79.34                |
| g-10   | 59.42                |
| 93-33  | 48.13                |
| 93-20  | 45.30                |
| 93-19  | 56.71                |
| 93-16  | 96.03                |
| ha-2   | 46.14                |
| g-2    | 99.84                |
| g-3    | 98.19                |
| g-4    | 99.32                |
| g-9    | 96.49                |
| g-12   | 89.69                |

Isocons and are generated to qualify the effect of weathering on the diamond bearing rocks and the actinolite schist (figures 22-26). "Isocon" plots are generated by graphically comparing the constituents of the least weathered sample against the rest of the samples in a given suit of rocks, in effect "normalizing" the suite of rocks to its least weathered member. Concentrations are relative and have been manipulated mathematically in the same way across the suite to make them fit within the space of the graph. Relative concentrations for major elements are in wt. % of oxides and trace elements are in ppm The CIA is used to determine relative weathering. The least weathered sample (the sample with the lowest CIA) G-12 is selected for comparison to the rest of the diamondiferous suite. Sample G-12 is plotted on the x-axis for the

diamondiferous suite. Sample Ha-2 and 93-20 are the least weathered of the actinolite schist suite. Sample Ha-2 is selected over 93-20, as 93-20 is an outlier with respect to Mg concentration. Sample Ha-2 is plotted on the x-axis for the actinolite schist suite. The 45-degree line is the line of constant mass and the blue line is the line of constant aluminum. The line of constant mass defines where constituents will fall on the graph when there has been no change in concentration between samples. When a constituent falls below the line of constant mass it has been depleted relative to the least weathered sample (in this case the x axis) and if it falls above the line it has been enriched. The line of constant aluminum passes through the origin and Al, and assumes total aluminum has remained the same regardless of the loss or gain of other constituents(Grant, 1986). Table 4 is a summery of relative losses or gains for each constituent in each sample.



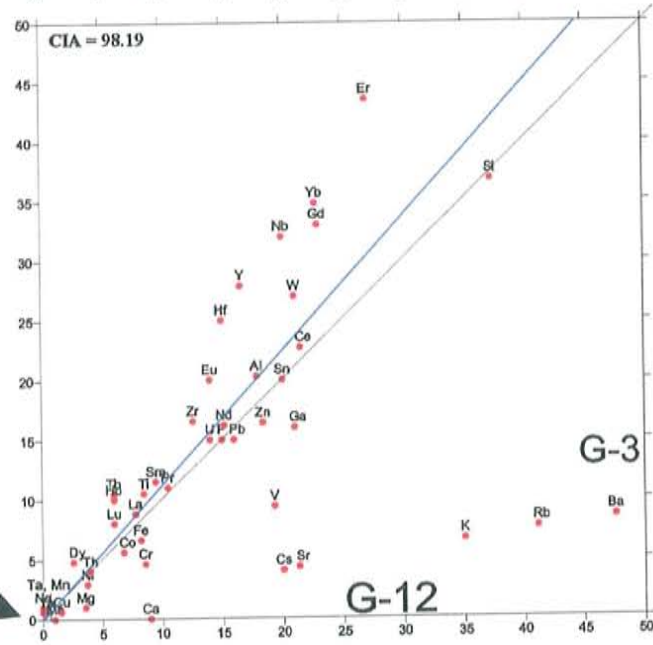
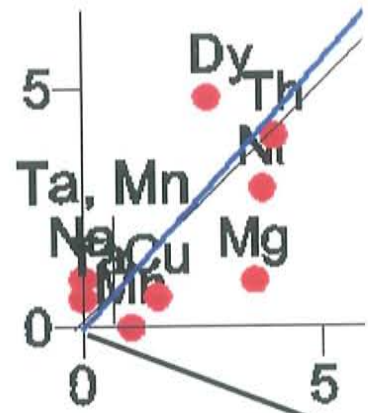
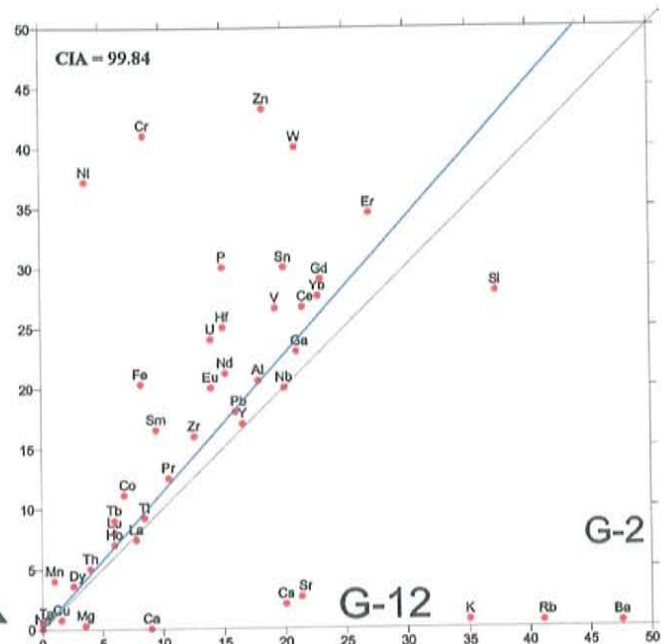
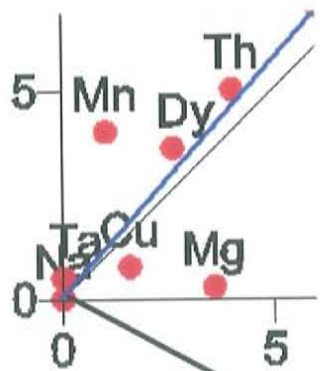


Figure 22. Isocons for diamondiferous rocks (samples G-2 and G-3). The diagonal line is line of constant mass, the blue line is the line of constant aluminum and CIA is chemical index of alteration (see text).

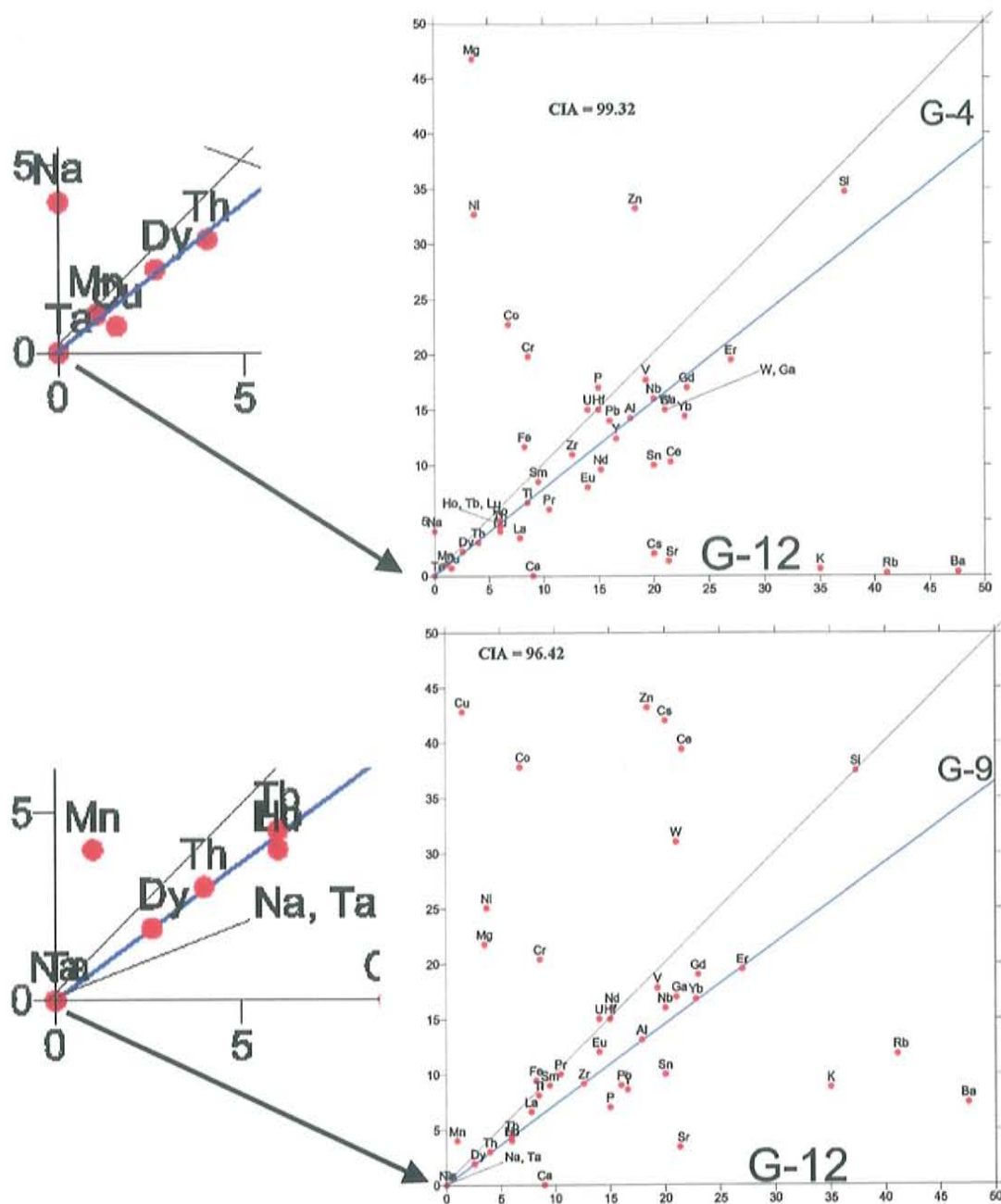


Figure 23. Isocons for diamondiferous rocks (samples G-4 and G-9). The diagonal line is line of constant mass, the blue line is the line of constant aluminum and CIA is chemical index of alteration (see text).

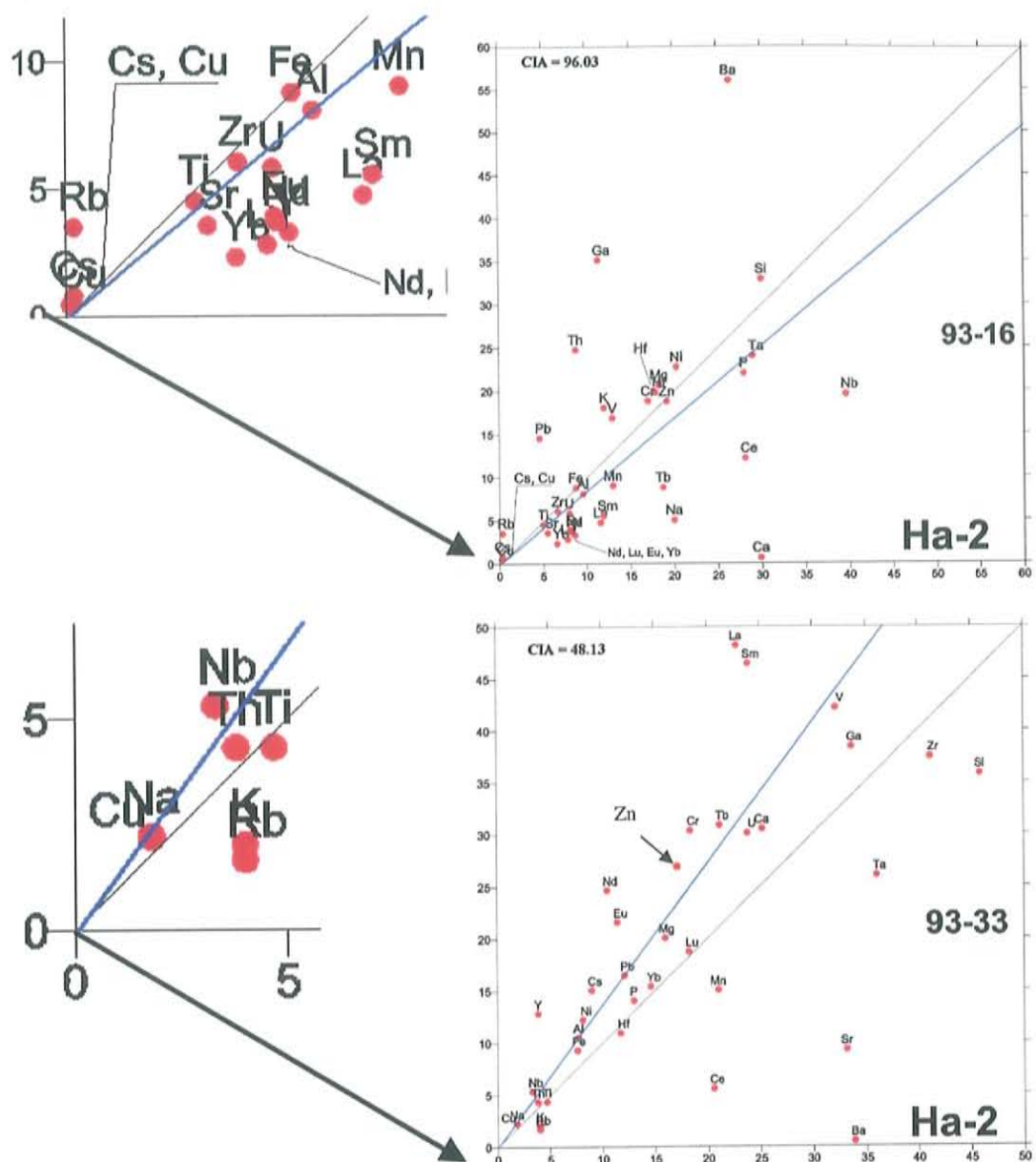
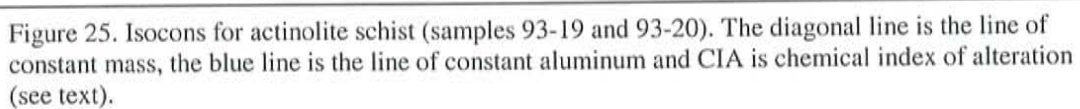


Figure 24. Isocons for actinolite schist (samples 93-16 and 93-33). The diagonal line is the line of constant mass, the blue line is the line of constant aluminum and CIA is chemical index of alteration (see text).





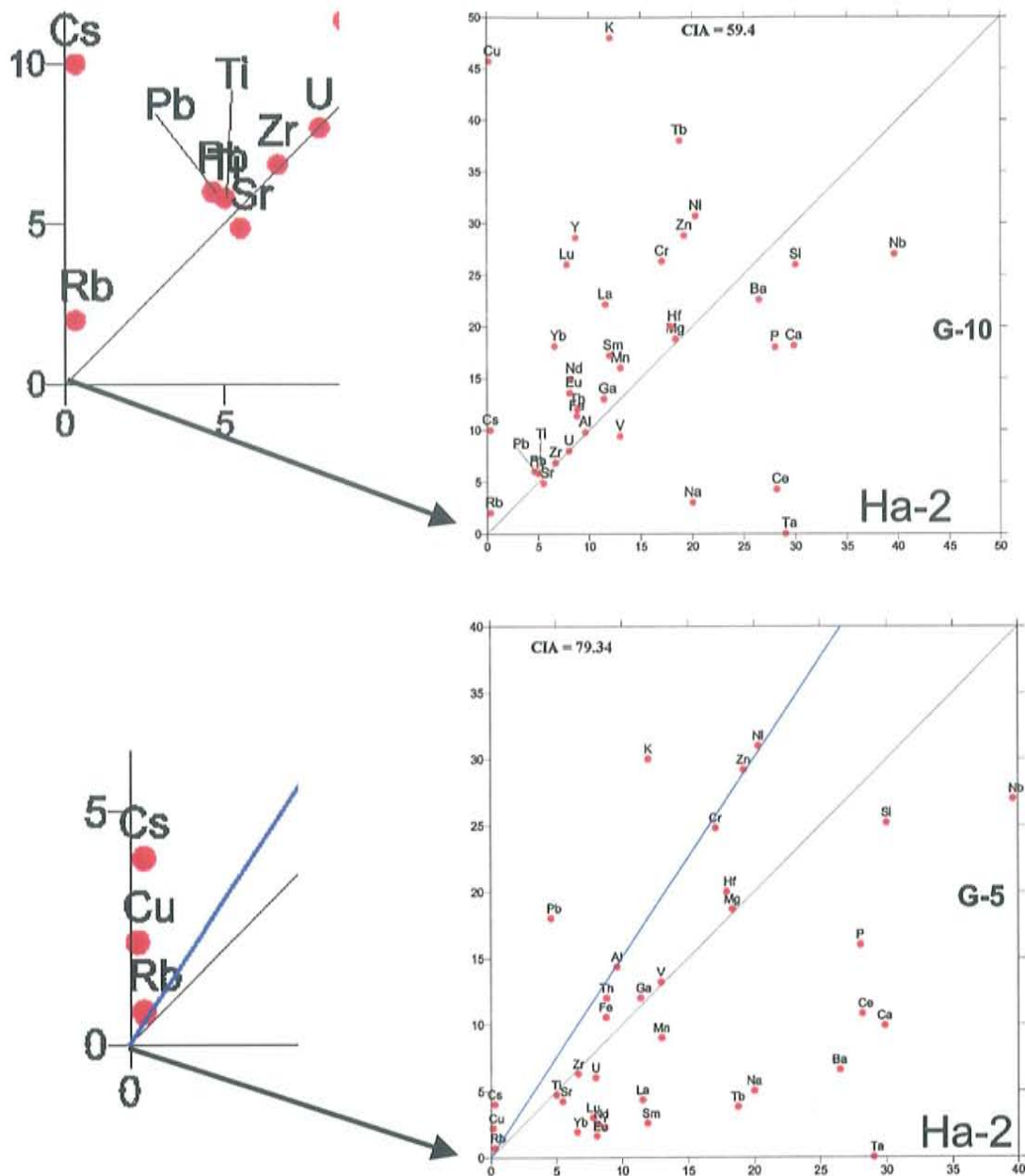


Figure 26. Isocons for actinolite schist (samples G-5 and G-10). The diagonal line is the line of constant mass and the blue line is the line of constant aluminum. CIA is chemical index of alteration (see text).

Table 4. Summary of relative losses (-) or gains (+) as compared to x (red). Numbers are the same as used in isocons (normalized).

| #  | g-2   | g-3   | g-4   | g-9   | g-12 (x) | g-5   | g-10  | 93-33 | 93-20 | 93-19 | 93-16 | ha-2 (x) |
|----|-------|-------|-------|-------|----------|-------|-------|-------|-------|-------|-------|----------|
| Si | -9.4  | -0.5  | -2.6  | 0.1   | 37.3     | -4.8  | -4.0  | -3.2  | 4.4   | -3.2  | 2.9   | 30.0     |
| Al | 5.4   | 4.8   | -7.3  | -9.6  | 35.8     | 4.8   | 0.2   | 0.9   | -1.9  | 2.3   | -1.6  | 9.6      |
| Fe | 12.1  | -1.6  | 3.4   | 1.2   | 8.3      | 1.8   | 2.6   | 0.5   | -1.1  | 1.3   | 0.0   | 8.8      |
| Ca | -9.0  | -9.0  | -9.0  | -9.0  | 9.0      | -20.0 | -11.7 | 0.6   | -4.7  | -5.4  | -29.3 | 29.9     |
| Mg | -3.3  | -2.6  | 43.2  | 18.2  | 3.6      | 0.3   | 0.4   | 1.7   | -2.4  | 1.9   | 2.3   | 18.4     |
| Na | 0.0   | 1.0   | 4.0   | 0.0   | 0.0      | -15.0 | -17.0 | -9.0  | -11.0 | -11.0 | -15.0 | 20.0     |
| K  | -34.4 | -28.4 | -34.4 | -26.2 | 35.0     | 18.0  | 36.0  | -6.0  | 0.0   | -6.0  | 6.0   | 12.0     |
| Ti | 2.5   | 7.0   | -6.7  | -1.4  | 29.8     | -0.3  | 0.8   | -0.2  | 0.2   | -0.4  | -0.5  | 5.0      |
| Mn | 3.0   | -1.0  | 0.0   | 3.0   | 1.0      | -4.0  | 3.0   | 2.0   | 8.0   | 3.0   | -4.0  | 13.0     |
| P  | 15.0  | 0.0   | 2.0   | -8.0  | 15.0     | -12.0 | -10.0 | 0.0   | -2.0  | -14.0 | -6.0  | 28.0     |
| U  | 10.0  | 1.0   | 1.0   | 1.0   | 14.0     | -2.0  | 0.0   | 22.1  | 15.8  | -1.0  | -2.2  | 8.0      |
| V  | 11.0  | -14.9 | -2.4  | -2.3  | 29.0     | 0.2   | -3.6  | -0.3  | -3.3  | -0.3  | 3.8   | 13.0     |
| W  | 19.0  | 6.0   | -6.0  | 10.0  | 21.0     | n.a.  | n.a.  | n.a.  | n.a.  | n.a.  | n.a.  | n.a.     |
| Y  | 0.4   | 11.3  | -4.2  | -8.0  | 16.6     | -6.4  | 20.0  | 23.3  | 1.0   | 4.0   | -5.4  | 8.7      |
| Yb | 4.8   | 12.0  | -8.4  | -6.0  | 22.8     | -4.7  | 11.5  | 8.8   | 8.0   | -4.9  | -4.3  | 6.6      |
| Zn | 24.8  | -2.0  | 14.8  | 24.8  | 18.4     | 10.0  | 9.6   | 7.1   | -0.9  | 1.1   | -0.5  | 19.2     |
| Zr | 3.4   | 4.0   | -1.7  | -3.4  | 12.6     | -0.4  | 0.2   | 0.8   | 1.6   | -0.3  | -0.6  | 6.7      |
| La | -0.4  | 1.0   | -4.4  | -1.2  | 7.8      | -7.2  | 10.6  | 30.2  | 8.2   | -4.5  | -6.8  | 11.6     |
| Lu | 2.0   | 2.0   | -2.0  | -2.0  | 6.0      | -4.8  | 18.2  | 10.9  | 10.4  | -5.1  | -5.0  | 7.8      |
| Nb | 0.0   | 18.0  | -6.0  | -6.0  | 30.0     | -12.6 | -12.6 | 8.1   | -9.9  | -7.9  | -20.1 | 39.6     |
| Nd | 6.0   | 1.0   | -5.6  | 0.8   | 15.2     | -5.6  | 6.8   | 22.6  | 5.0   | -5.7  | -4.5  | 8.2      |
| Ni | 33.4  | -0.9  | 28.9  | 21.3  | 3.8      | 10.7  | 10.4  | 4.0   | -4.0  | 8.6   | 2.4   | 20.3     |
| Pb | 2.0   | -1.0  | -2.0  | -7.0  | 16.0     | 13.4  | 1.4   | 11.8  | 7.5   | 22.6  | 9.9   | 4.6      |
| Pr | 2.0   | 0.5   | -4.5  | -0.5  | 10.5     | n.a.  | n.a.  | n.a.  | n.a.  | n.a.  | n.a.  | n.a.     |
| Rb | -40.6 | -33.5 | -40.9 | -29.3 | 41.1     | 0.4   | 1.7   | 1.4   | 3.7   | 2.7   | 3.2   | 0.3      |
| Sm | 7.0   | 2.0   | -1.0  | -0.5  | 9.5      | -9.4  | 5.3   | 19.0  | 4.0   | -8.9  | -6.4  | 11.9     |
| Sn | 10.0  | 0.0   | -10.0 | -10.0 | 20.0     | n.a.  | n.a.  | n.a.  | n.a.  | n.a.  | n.a.  | n.a.     |
| Sr | -18.7 | -17.0 | -20.0 | -17.9 | 21.3     | -1.3  | -0.6  | -1.8  | 7.8   | 10.5  | -2.0  | 5.5      |
| Ta | 0.5   | 0.6   | 0.0   | 0.0   | 0.0      | -29.0 | -29.0 | -3.0  | 7.0   | -14.0 | -5.0  | 29.0     |
| Tb | 3.0   | 4.5   | -1.5  | -1.5  | 6.0      | -15.0 | 19.2  | 30.1  | 14.7  | -14.3 | -10.0 | 18.8     |
| Th | 1.0   | 0.0   | -1.0  | -1.0  | 4.0      | 3.2   | 3.2   | 17.0  | 13.9  | 27.7  | 15.9  | 8.8      |
| Ba | -47.2 | -39.1 | -47.3 | -40.2 | 47.6     | -19.9 | -3.9  | -25.9 | 20.9  | 2.9   | 29.5  | 26.5     |
| Ce | 6.2   | 1.4   | -13.4 | 21.5  | 25.8     | -17.3 | -23.9 | -14.3 | 23.3  | -12.3 | -16.0 | 28.1     |
| Co | 4.3   | -1.2  | 15.9  | 31.0  | 6.8      | n.a.  | n.a.  | n.a.  | n.a.  | n.a.  | n.a.  | n.a.     |
| Cr | 32.4  | -4.0  | 11.2  | 11.8  | 8.6      | 7.7   | 9.2   | -0.4  | -7.0  | -8.9  | 1.7   | 17.1     |
| Cs | -18.0 | -16.0 | -18.0 | 22.0  | 20.0     | 3.7   | 9.7   | 2.7   | 1.5   | 1.7   | 0.5   | 0.3      |
| Cu | -0.8  | -0.9  | -0.9  | 41.2  | 1.6      | 2.0   | 45.5  | 0.4   | 0.8   | 1.5   | 0.3   | 0.2      |
| Dy | 1.0   | 2.2   | -0.4  | -0.7  | 2.6      | n.a.  | n.a.  | n.a.  | n.a.  | n.a.  | n.a.  | n.a.     |
| Er | 8.3   | 18.2  | -8.3  | -8.3  | 29.7     | n.a.  | n.a.  | n.a.  | n.a.  | n.a.  | n.a.  | n.a.     |
| Eu | 6.0   | 6.0   | -6.0  | -2.0  | 14.0     | -6.5  | 5.5   | 13.5  | 3.4   | -6.2  | -4.2  | 8.1      |
| Ga | 4.0   | -10.0 | -12.0 | -8.0  | 42.0     | 0.6   | 1.6   | 27.0  | 22.2  | 27.6  | 23.7  | 11.4     |
| Gd | 9.0   | 15.0  | -9.0  | -6.0  | 34.5     | n.a.  | n.a.  | n.a.  | n.a.  | n.a.  | n.a.  | n.a.     |
| Hf | 19.0  | 19.0  | 0.0   | 0.0   | 28.5     | 2.1   | 2.1   | 3.9   | 5.5   | 0.5   | 1.9   | 17.9     |
| Ho | 1.0   | 4.0   | -1.0  | -2.0  | 6.0      | n.a.  | n.a.  | n.a.  | n.a.  | n.a.  | n.a.  | n.a.     |

X= least weathered sample based on chemical index of alteration (CIA)



## *Diamond-Bearing Rocks*

### *Siderophile Elements*

In general, siderophile elements tend to accumulate in the more weathered samples consistent with the residual nature of these elements. Isocons for Samples G-2 and G-3 have similar distributions of elements and both have an Al line above the constant mass line. Sample G-2 has a higher CIA than G-3. Iron and Ni show moderate enrichment in sample G-2, Co and P show slight enrichment in sample G-2, while Fe, Ni, Co and P remain essentially unchanged in sample G-3. Samples G-4 and G-9 both have an Al line below the constant mass line and sample G-4 has a higher CIA than G-9. Iron is slightly enriched in sample G-4 and unchanged in sample G-9. Cobalt is moderately enriched in sample G-4 and slightly more enriched in sample G-9. Phosphorous is slightly enriched in sample G-4 and slightly depleted in sample G-9. Nickle is moderately enriched in sample G-4 and slightly less enriched in sample G-9.

### *Chalcophile Elements*

Copper and Zn are moderately variable while Pb and Ga show minor variability. Lead has remained virtually unchanged in all four samples though it is slightly enriched in the more weathered samples (G-2 and G-4). Copper is unchanged in samples G-2, 3 and 4, though strongly enriched in sample G-9. Zinc shows moderate enrichment in samples G-2, 4 and 9, with slight depletion in sample G-3. Gallium is slightly depleted in samples G-3, 4 and 9 while showing minor enrichment in sample G-2.

### *Lithophile Elements* (REE will be addressed separately)

Lithophile elements in this suite behave predictably; mobile elements are leached while immobile elements are not. The elements Na, Mg, Ca, Sr, K, Rb and Ba are all

strongly depleted in all four samples, though less so in the rocks with the lower CIA (G-3 and G-9) consistent with the moderate mobility of these cations (Rose et al., 1979). The concentrations of the immobile elements Ti and Zr are virtually unchanged and closely follow the aluminum line suggesting the hypothesis of constant aluminum is valid for this suite. Cesium is also strongly depleted in G-2, 3 and 4. Cesium is strongly enriched in sample G-9, this may be due to biogenic activity as it is the only sample gathered from a currently forested area, cesium is strongly adsorbed by plants (Palmer et al., 2002). Chromium shows moderate enrichment in samples G-4 and G-9, strong enrichment in sample G-2, with slight depletion in sample G-3. Vanadium is slightly depleted G-4 and G-9, moderately depleted in sample G-3 and slightly enriched in sample G-2. Uranium is slightly enriched in all samples. Manganese is slightly enriched in samples G-2 and G-9 and unchanged in G-4 and G-3. Silica is virtually unchanged in samples G-3, G-4 and G-9, while showing slight depletion in sample G-2. Tungsten is moderately enriched in samples G-2, G-3 and G-9, but shows slight depletion in sample G-4. Hafnium is slightly enriched in samples G-2 and G-3 but is unchanged in samples G-4 and G-9. Niobium, Th and Y concentrations are mostly un-changed. Though Th and Y show slight enrichment in sample G-3.

#### *Rare Earth Elements*

Rare earth element concentrations in diamond-bearing rocks are stable across the suite with minor exceptions; Yb and Gd are slightly enriched in sample G-3 but remain strongly coupled in all four samples, Er is also moderately enriched in sample G-3 and less so in sample G-2. Cerium shows the most variability and is likely related to the general cerium anomaly, which will be addressed at the end of this section. When the line

of constant Al diverges from the line of constant mass REE follow the Al line, reinforcing the validity of the constant Al hypothesis for this suite.

#### *Immobile Elements*

In general constituents of diamond bearing rocks behave as expected for rocks subject to extreme tropical weathering with mobile elements being leached, residual elements accumulating and immobile elements remaining constant. The isocons demonstrate the elements Al, Fe, Ga, Ti, Zr, Mn, Hf, Nb Th, Y and REE's are qualitatively immobile in the diamond bearing rocks.

#### *Actinolite Schist*

##### *Siderophile Elements*

Siderophile elements are relatively unchanged across the suite. Iron has remained unchanged in all six samples, while P and Ni have remained essentially unchanged in samples 93-16, 93-33 and 93-20. Phosphorous has been moderately depleted in samples G-5, G-10 and 93-19 while being slightly depleted in sample 93-20.

##### *Chalcophile Elements*

Chalcophile elements show moderate variability across the suite. Copper has remained virtually unchanged in samples 93-16, 93-33, 93-20, 93-16 and G-5 but is strongly enriched in sample G-10. Zinc has remained essentially unchanged in samples 93-16, 93-19 and 93-20 while being slightly enriched in samples 93-33, G-5 and G-10. Gallium is slightly enriched in samples G-5, G-10 and 93-33, moderately enriched in sample 93-20 and 93-16, and strongly enriched in sample 93-19.



*Lithophile Elements* (REE will be addressed separately)

Calcium and Na behave predictably across the suite, being preferentially depleted in the more weathered samples while other lithophile elements show mixed behavior. Strontium is moderately enriched in samples 93-20 and 93-19, unchanged in samples G-5, G-10 and 93-16 and strongly depleted in sample 93-33. Rubidium is slightly enriched in samples 93-20, 93-19, 93-16 and sample G-10, slightly depleted in sample 93-33 and unchanged in sample g-5. Barium concentration shows no relationship to degree of weathering as it is strongly enriched in samples 93-20 and 93-16, strongly depleted in samples 93-33 and G-5 and slightly depleted in samples G-10 and 93-19. Potassium concentrations also show no connection to degree of weathering, being strongly enriched in sample G-10, moderately enriched in sample G-5 and 93-16, slightly depleted in sample 93-33, moderately depleted in sample 93-19 and unchanged in sample 93-20. Silica is slightly depleted in samples 93-33, G-10, G-5 and 93-19 and slightly enriched in sample 93-20 and 93-16. Immobile elements Ti and Zr are virtually unchanged across the suite and closely follow the line of constant mass suggesting the hypothesis of constant Al is not valid for this suite though Al is largely unchanged across the suite but is slightly enriched in sample G-5. Manganese is slightly depleted in samples 93-16, G-5, moderately depleted in sample 93-33, slightly enriched in sample 93-19 and G-10 and moderately enriched in sample 93-20. Magnesium is virtually unchanged being only slightly enriched in samples 93-16, 93-19 and 93-33. Chromium is moderately enriched in samples G-5 and G-10, slightly enriched in samples 93-16 and 93-33 and moderately depleted in samples 93-19 and 93-20. Vanadium is virtually unchanged in samples 93-19

and G-5, slightly depleted in samples 93-20 and G-10 and slightly enriched in samples 93-16 and 93-33. Hafnium is unchanged across the suite except in sample 93-20 where it is slightly enriched. Thallium is strongly enriched in sample 93-19, moderately enriched in samples 93-20 and 93-16, slightly enriched in samples G-10 and G-5 and unchanged in sample 93-33. Niobium is moderately depleted in samples G-10, G-5, 93-16, 93-19, 93-20 and virtually unchanged in sample 93-33. Yttrium is slightly enriched in samples 93-20, 93-19 and 93-33, moderately enriched in sample G-10 and slightly depleted in samples 93-16 and G-5.

#### *Rare earth Elements*

Rare earth elements show extreme variability in the actinolite schist. Lanthanum is moderately enriched in sample G-10, moderately depleted in sample G-5, slightly depleted in samples 93-16 and 93-19, slightly enriched in sample 93-20 and strongly enriched in sample 93-33. Cerium is moderately depleted in samples 93-16, 93-33, 93-19 and G-5, strongly depleted in sample G-10 and strongly enriched in sample 93-20. Neodymium is slightly depleted in samples 93-19, 93-16 and G-5 and slightly enriched in samples G-10, 93-33 and sample 93-20. Samarium is slightly enriched in samples G-10 and 93-20, moderately enriched in samples G-5 and 93-19, strongly enriched in sample 93-33 and slightly depleted in sample 93-16. Europium is slightly depleted in samples 93-16 and 93-33, moderately depleted in samples 93-19 and G-5 and slightly enriched in samples G-10 and 93-20. Terbium is moderately enriched in samples G-10 and 93-20, slightly enriched in 93-33, moderately depleted in sample 93-16 and strongly depleted in samples G-5 and 93-19. Ytterbium moderately enriched in sample G-10, slightly enriched in sample 93-20, moderately depleted in samples G-5 and 93-19, slightly depleted in

sample 93-16 and unchanged in sample 93-33. Lutetium is moderately enriched in samples G-10 and 93-20, moderately depleted in samples G-5 and 93-19, slightly depleted in sample 93-16 and unchanged in sample 93-33. The enrichment and/or depletion of REE seem to bear no relationship to degree of weathering and do not follow the line of constant Al, further evidence that the hypothesis of constant Al is not valid for this suite.

#### *Immobile Elements*

Element variability (with the exception of Ca and Na) in the actinolite schist does not correlate with degree of weathering and is likely therefore to be a product of metasomatism. Isocons for the actinolite schist demonstrate the elements Ti, Al, Mg, Fe, Zr, Hf and Y (cautiously) are qualitatively immobile in the actinolite schist. Niobium concentrations though moderately depleted in most samples are consistent.



## DISCUSSION

### Cerium Anomaly

Cerium possesses two oxidation states 3+ and when conditions are very oxidizing 4+ (Krauskopf and Bird, 1995). Positive Ce anomalies in all the highly weathered diamond bearing rock and negative Ce anomalies in the less-weathered actinolite schist suggest anomalies are related to weathering. Geochemical studies at Omai, Guyana (Voicu and Bardoux, 2002) suggests however that the cerium anomaly observed there is related to permeability. Positive cerium anomalies are observed in the permeable, inter-pillow spaces in basaltic andesites while negative Ce anomalies are observed in the less permeable inner pillow parts.

This may also be the case at Akwatia as weathered diamond bearing rock is highly permeable while the actinolite schist has low permeability; furthermore the brecciated nature of the diamondiferous rock suggests that the un-weathered protolith of the diamondiferous rock was also highly permeable. Figure 27 shows a chondrite normalized REE spidergram of a sample of actinolite schist and a sample of diamondiferous rock, which were in direct contact when collected. It appears Ce was mobilized out of the actinolite schist and into the diamondiferous rock as suggested by (Voicu and Bardoux, 2002).

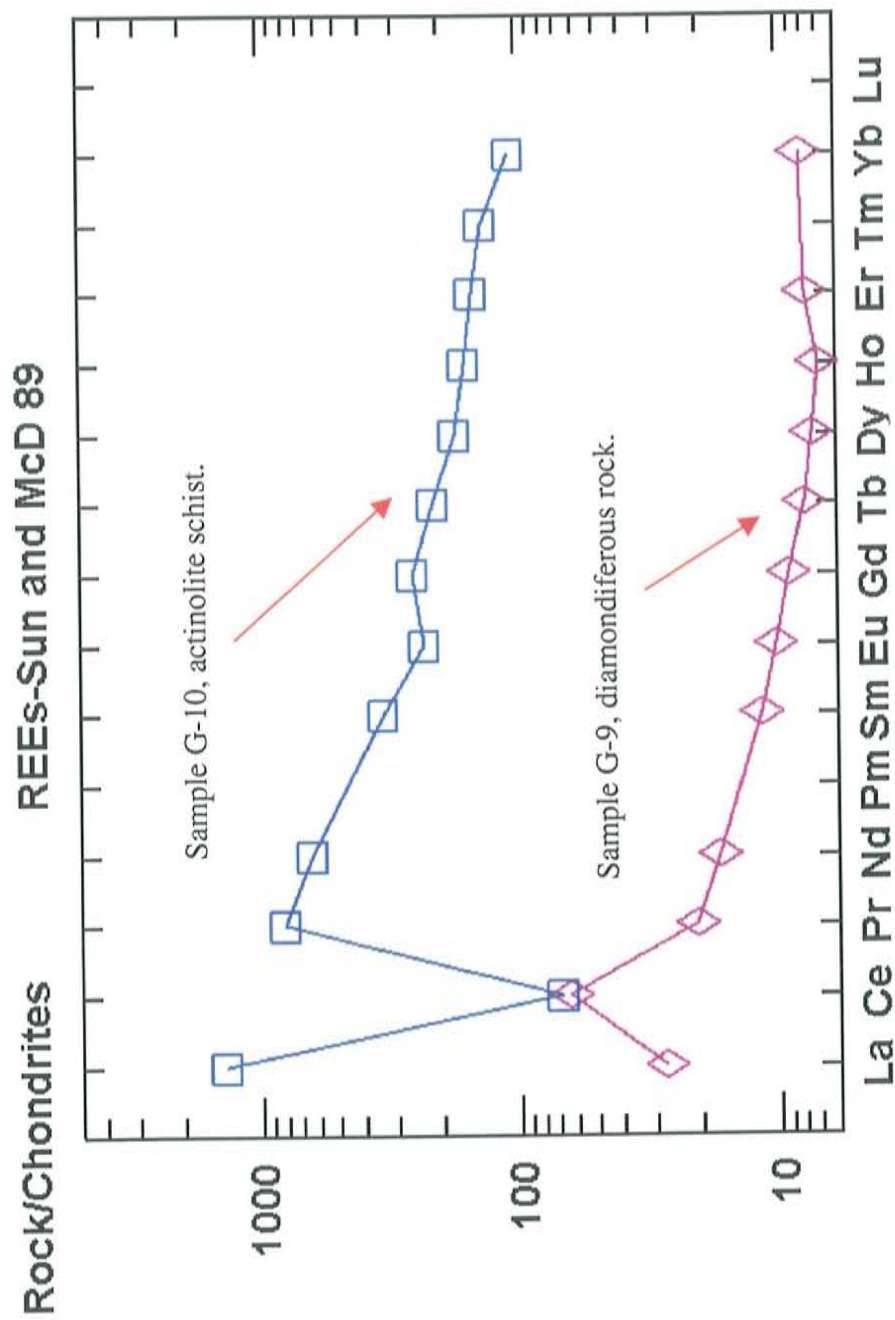


Figure 27. Chondrite normalized REE diagram of adjacent samples G-9 and G-10, showing contrasting cerium anomalies. Open blue squares are actinolite schist and open diamonds are diamondiferous rocks. Normalizing values from (Sun and McDonough, 1989).

## General Conclusions Related to Weathering

In general terms the weathering of diamond bearing rocks at Akwatia is consistent with observations by Voicu and Bardoux at the Omai gold mine located in the Guiana Shield, Guyana, South America. The results of their study indicate, generally REE patterns of the bedrock are preserved in the saprolith horizon. The chemical signatures of some oxides are preserved;  $\text{SiO}_2$  is generally not affected by weathering, though local hydrothermal silicification is frequently observed in bedrock. The oxides  $\text{Na}_2\text{O}$ ,  $\text{CaO}$  and  $\text{MgO}$  all show extreme leaching at CIA values over 65. Potassium oxides show leaching in mafic volcanics and sedimentary rocks.  $\text{Fe}_2\text{O}_3$  concentrations are highly variable though there is a gradual accumulation towards the upper part of the saprolith where water table variations are less. Aluminum oxide shows a positive correlation with the CIA in all rock types due to its retention in secondary mineral phases.  $\text{TiO}_2$  is generally immobile in mafic volcanics, though it shows gradual enrichment in weathered felsic volcanics and sedimentary rocks. Trace elements have variable behavior patterns during weathering. Some elements (Nb, Hf, Ta and partially Y) are largely un-affected by weathering. The elements V, W, Ga and Sc show moderate to strong enrichment, while Sr and Mo are leached. Other elements (Cs, Ba, U, Th, Ni, Cu, Zn, Pb, Te) have a mixed behavior. In general rubidium is completely leached during extreme weathering (Voicu and Bardoux, 2002).



## Weathering and Protolith Identification

Returning to the komatiite/ tholeiite discrimination diagram (Jensen, 1976) now modified in figure 28. Isocons demonstrate the constituents (with the exception of Mg in the diamondiferous rocks) used for this diagram are immobile. The weathered diamondiferous rocks have a very low Mg content, however when Mg is plotted against immobile, Ti, Al and Zr (figure 28), a continuous negative correlation exists between the weathered diamondiferous rocks, the schists and the un-weathered high Mg metasediments suggesting the low Mg content of the diamond bearing rocks is a result of weathering. The (modified) komatiite/ tholeiite diagram (figure 29) places the actinolite schist and most of the un-weathered metasediments associated with the diamond-bearing rocks squarely in the komatiite field. The diamond-bearing rocks fall along the weathering trend expected for a severely weathered komatiite as MgO is more mobile than Ti Al or Fe oxides and Fe is more mobile than Al.

Returning to figure 21, the tectonic discrimination diagram (Wood, 1980; Wood et al., 1979) isocons demonstrate constituents for this diagram are immobile in the diamond bearing rock. Zirconium is immobile in the actinolite schist and the shape of the arc-basalt field allows a great deal of variation in the Zr/Th ratio. The fairly tight grouping of the actinolite schist with the un-weathered, high-Mg metasediments and the diamond-bearing rock suggest this diagram may also be valid for the actinolite schist, indicating arc tectonic setting for Akwatia rocks.

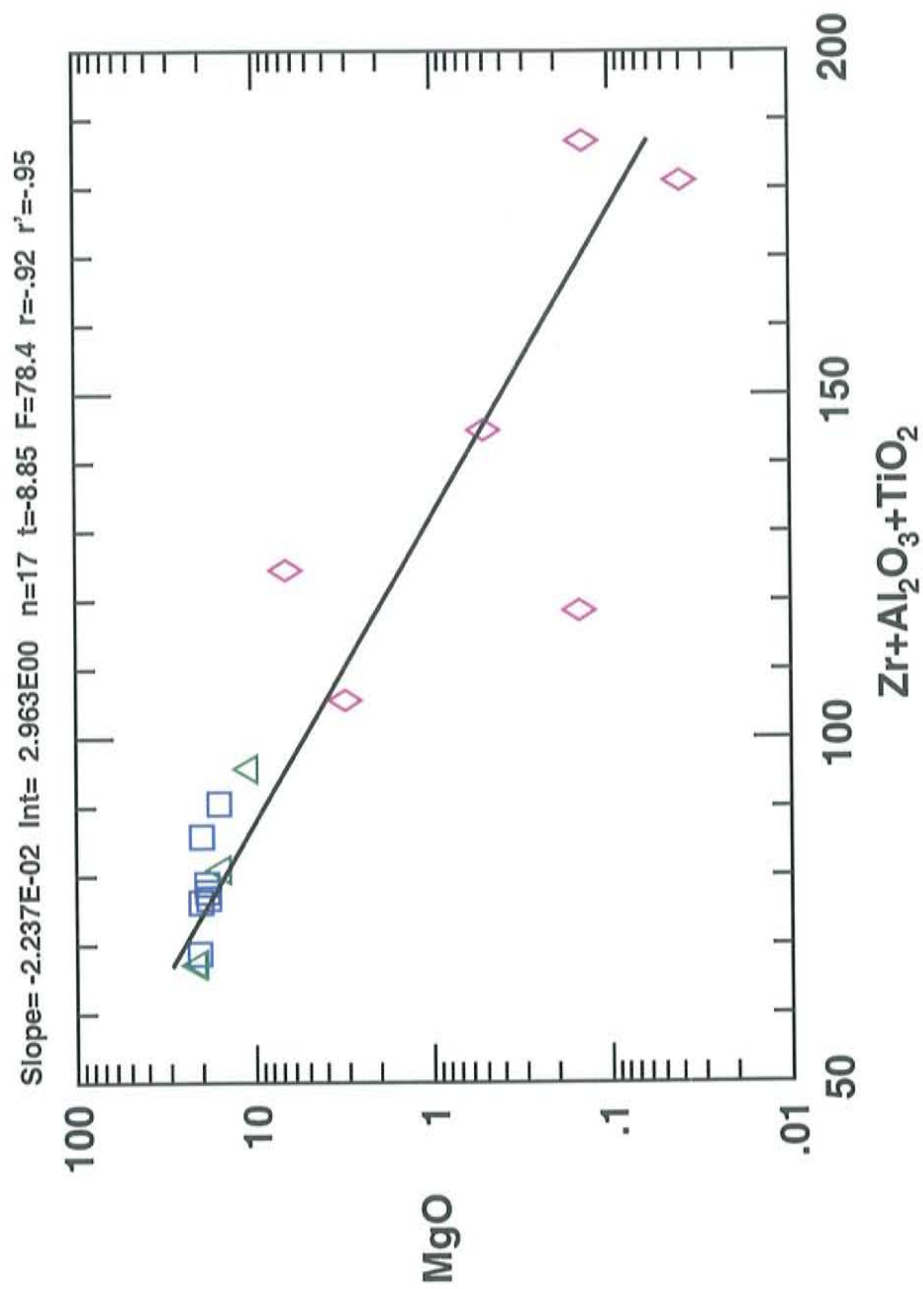


Figure 28. Graph showing a continuous, negative correlation between MgO, Zr and oxides of Al and Ti in Akwatia rocks. Open blue squares are schist, open pink diamonds are diamondiferous rocks, and open green triangles are high Mg metasediments from (McKittrick, 1996).

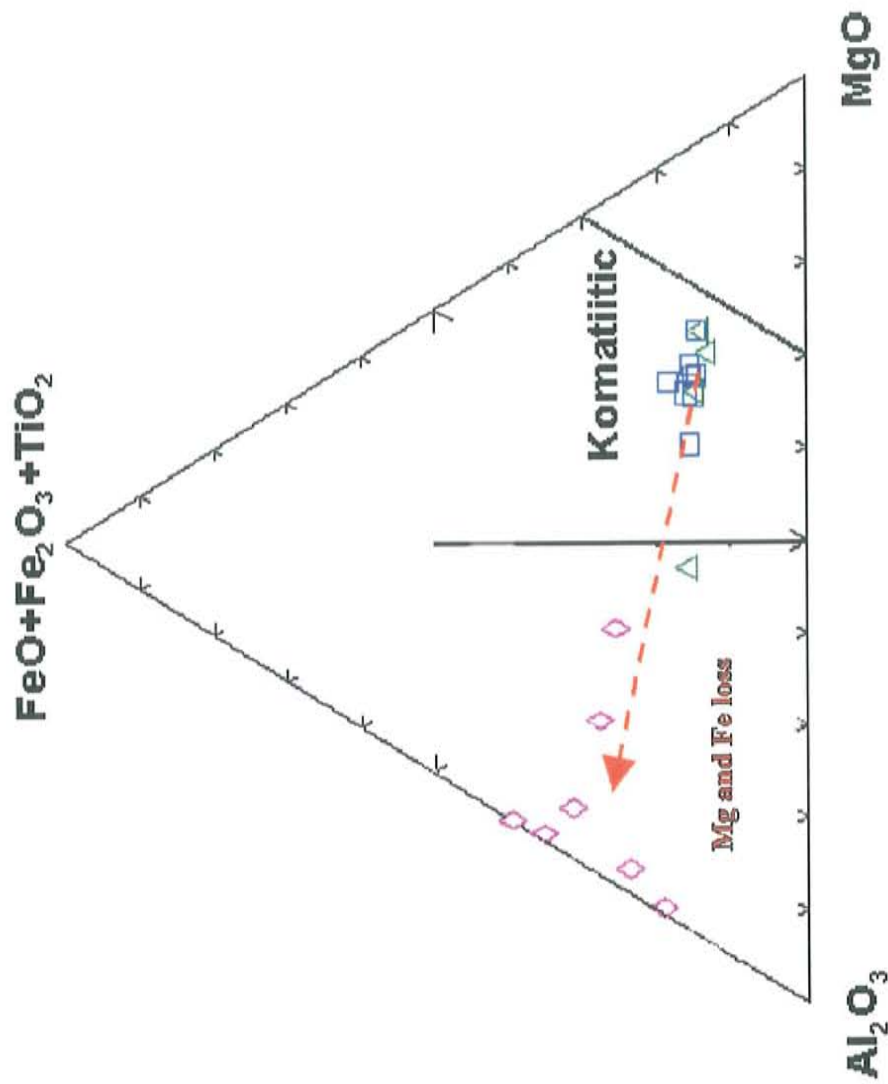


Figure 29. Komatiite discrimination diagram showing how diamond bearing rocks fall along weathering trend (Mg and Fe loss) for a komatiite. Open blue squares are actinolite schist, open pink diamonds are diamondiferous rocks, open green triangles are high Mg metasediments (McKittrick, 1996). The form of the diagram is modified from (Jensen, 1976).



## Diamonds in Bedrock

There is compelling evidence that the Akwatia alluvial-diamond source is local bedrock. Small-scale miners have won diamonds from the local bedrock for some time. Diamonds in residual soils, colluvium, and alluvium indicate a local diamond source. Variations in topsoil grades are closely mirrored in bedrock or bottom grades (Figures 13-16). Diamond grades in the soils and the B1 horizon are greater than underlying bedrock, as expected, because during tropical soil formation more than 50% of the rock-forming constituents are removed. Residual diamonds are concentrated in bands or pods that commonly occur on topographical highs (fig. 17) rather than in depressions as would be expected for a strictly alluvial deposit. Grade variations in alluvial deposits are closely related to surface contours (Ross et al., 1989). (Junner, 1943) provides evidence that the paleosurface (probably Tertiary) of the Akwatia area was a broad peneplain. This surface would be more likely to disperse diamonds rather than concentrating them.

It is unlikely that the high diamond grades (.93 carats/cu.yd.= ~ 1.2 carat/ ton) in the diamond bearing breccias are a result of sedimentary concentration. Diamonds do not have an extreme density, hence are not commonly concentrated by moving water. Residual diamonds show no evidence of transport and clasts in diamond-bearing rocks can be extremely coarse (16 cm) and angular (see figure 5) indicative of volcanoclastic megaturbidites or syn-eruptive volcanoclastic deposits from shallow submarine explosive activity (McPhie et al., 1993). CAST geologists note that diamond grades are highest in the coarser beds of metasediments (Gammon, 2003). The high grade alone is enough to distinguish Akwatia as a primary diamond deposit. In comparison the average grade for the life of a mine in the Kimberley area was 1 carat per ton with mined grades as low

as.04 carats per ton at Ottos Kopje and .56 carats per ton at Bultfontien (Ross et al., 1989).

Arguments for bedrock diamonds from infiltration are weak. No traditional source rock is known to exist in Ghana. Areas of high diamond grade distal from the Birim River show no indication of alluvial cover. CAST geologists demonstrate diamonds have a certain tendency to penetrate into the bedrock but this effect according to their work terminates at 30ft., at this depth diamond grade either stabilizes (in the source rock) or falls to nil in the "penetrated" rock (Gammon, 2003). Preferential orientation of clasts and schistosity as well as original rock textures have been preserved in deep pits making it unlikely that diamonds penetrate deeply into the rock as a result of slumping or bioturbation.

### **Diamond-Bearing Rocks**

Evidence suggests the diamond-bearing rock is a volcanoclastic breccia that is more likely to be derived from a protolith of komatiitic affinity than either kimberlite or lamproite. The actinolite-tremolite schist is known to host diamonds (Gammon, 2003; Junner, 1943), however the small scale miners never exploit the schist for diamonds. (Kaminsky, 1996) identified diamond bearing rocks and also noted a fragmental texture. I have identified five localities (other than Beduwara Hill) where the bedrock is diamondiferous (figure 17) and all these rocks display a brecciated texture.

The presence of pristine diamonds bearing peridotitic inclusions in the metasediments demonstrates the protolith must have come from a minimum depth of 150 km and thus must be ultramafic in composition. The only known diamond-bearing rocks

with diamond grades comparable to Akwatia are kimberlites, lamproites or volcanoclastic komatiites. The protolith of the actinolite schist is clearly ultramafic and the enriched REE signature resembles kimberlite or lamproite. However it contains little or no diamonds, indicator minerals are completely absent and key immobile elements Ti, P, Nb and Zr are well below the kimberlite norm. The Akwatia diamondiferous rocks differ substantially from kimberlite and lamproite, both in REE and in other immobile constituents (figures 30 and 31). A ternary plot of immobile components ( $x = \text{Al}_2\text{O}_3/5$ ,  $y = \text{Nb}$  and  $z = \text{Hf}$ ), (chosen because of their immobility at Akwatia, based on the isocon analysis for this work and the work of (Voicu and Bardoux, 2002) in the Guiana Shield) demonstrate that Akwatia diamondiferous rocks plot near diamondiferous volcanoclastic komatiites from Dachine rather than average kimberlite or lamproite (figure 31). Diamond indicator minerals magnesian ilmenite, chrome diopside and perovskite are absent and there is little evidence for an underlying Archon. Akwatia diamondiferous rocks also differ from lamproites in that mineral inclusions in the diamonds are wholly of peridotitic affinity (Kaminsky, 1996; Nixon, 1987; Ward, 1998) this also excludes the possibility that the diamonds are of metamorphic origin. Chondrite normalized REE diagrams of the diamond-bearing rocks show good correlation with worldwide komatiites (figure 32) and a strong correlation with diamondiferous volcanoclastic komatiites from Dachine French Guyana (figure 33).



The Dachine komattites are part of a petrogenetically related group of incompatible-element rich, porphyritic komatiites and komatiitic volcanoclastic rocks, which include rocks from Steep Rock-Lumby Lake Canada, Murchison Terrane Australia and Karasjok Norway; collectively called Karasjok- type komatiites (Barley et al., 2000). Figure 33 is an  $\text{Al}_2\text{O}_3/\text{TiO}_2$  vs.  $\text{Gd}_\text{N}/\text{Yb}_\text{N}$  ratio plot comparing Akwatia rocks to other komatiites mentioned in this work, Akwatia diamondiferous rocks have chondritic or near chondritic ratios of  $\text{Al}_2\text{O}_3/\text{TiO}_2$  and  $\text{Gd}_\text{N}/\text{Yb}_\text{N}$ .

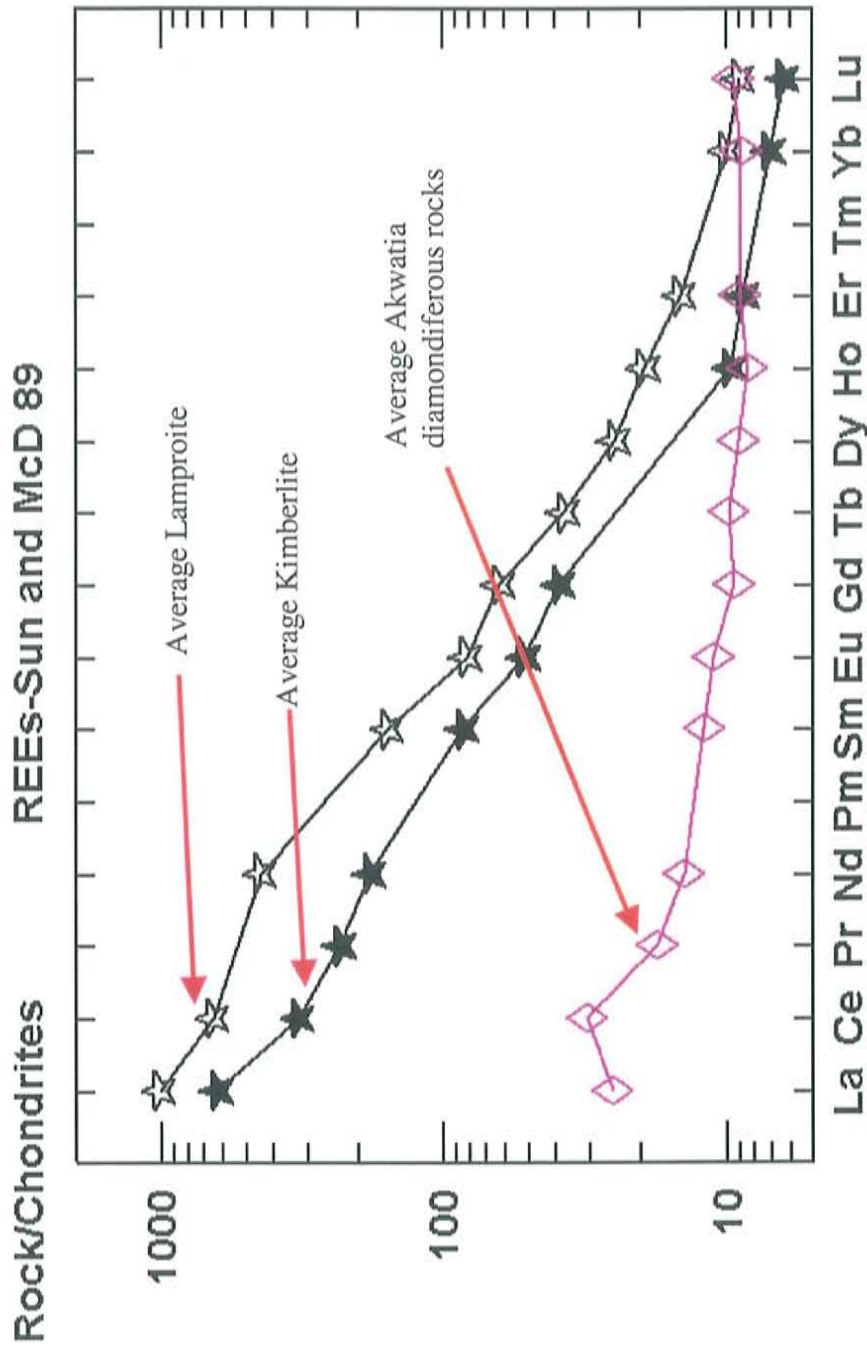


Figure 30. Chondrite normalized REE diagram comparing Akwatia diamondiferous rocks (open pink diamonds) to kimberlite (filled black stars) and lamproite (open black stars). Normalizing values from (Sun and McDonough, 1989) Data for average Kimberlite and lamproite from Mitchell in (Ross et al., 1989).

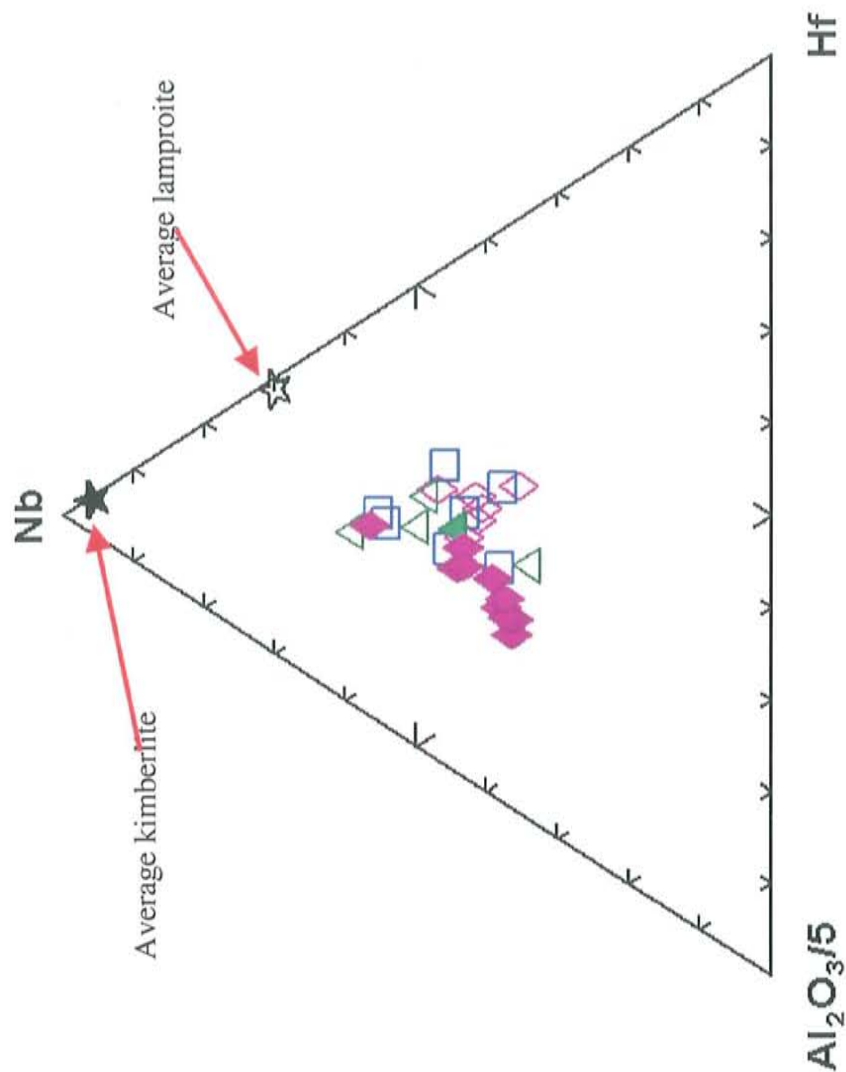
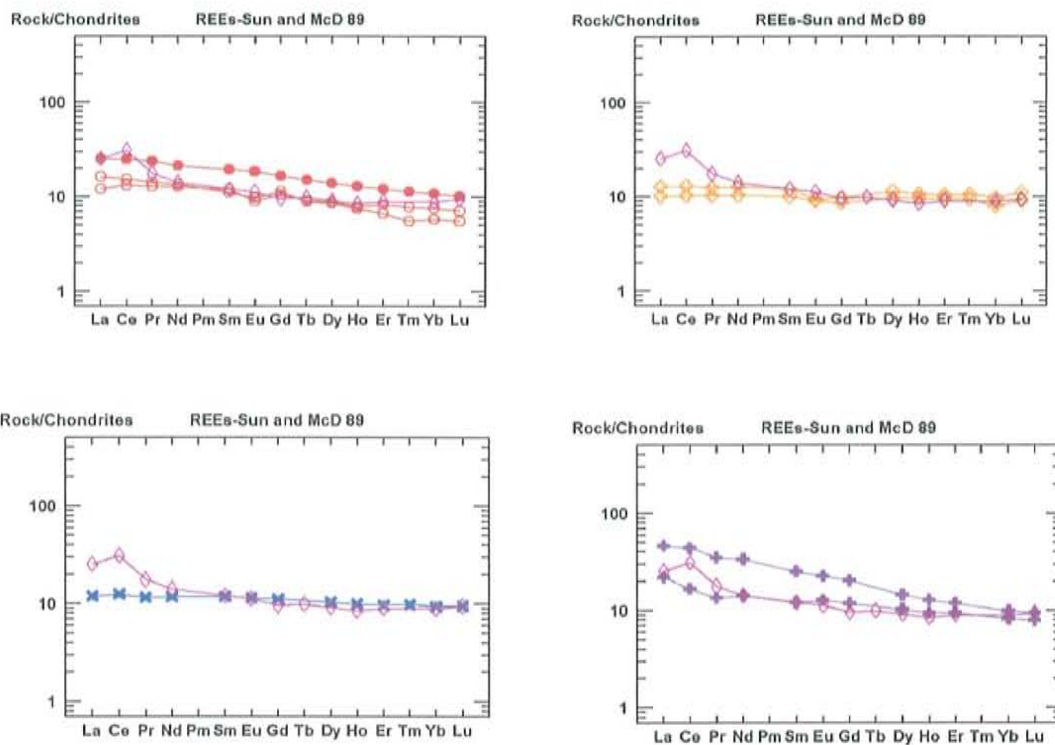


Figure 31. Ternary plot of immobile elements showing Akwatia rocks compared to Dachine diamondiferous komatiites, average kimberlites and lamproites. Open blue squares are actinolite schist, open pink diamonds are Akwatia diamondiferous rocks, open green triangles are high Mg medisediments (McKittrick, 1996), and filled pink diamonds are Dachine diamondiferous rocks. Data for Dachine rocks from (Capdevila, 2003). Data for average Kimberlite and lamproite from Mitchell in (Ross et al., 1989).





- Fragmental Komatiitic basalt from Murchison Terrane in Western Australia data from (Barley et al. 2000).
- Fragmental Komatiite from Murchison Terrane in Western Australia data from (Barley et al. 2000).
- ✕ Fragmental Komatiites from Steep Rock And Lumby Lake Western Superior Province Canada data from (Tomlinson et al. 1998).
- ✚ Gorgona Island komatiites and komatiitic basalts data from (Kerr et al. 1996).
- ✕ Munro komatiite data from (Hollings et al. 1999).
- ◇ Average Akwatia diamond bearing rocks.

Figure 32. Chondrite normalized REE plots of selected representative samples of worldwide komatiites and komatiitic basalts (mentioned in this work) compared to Akwatia diamondiferous rocks.

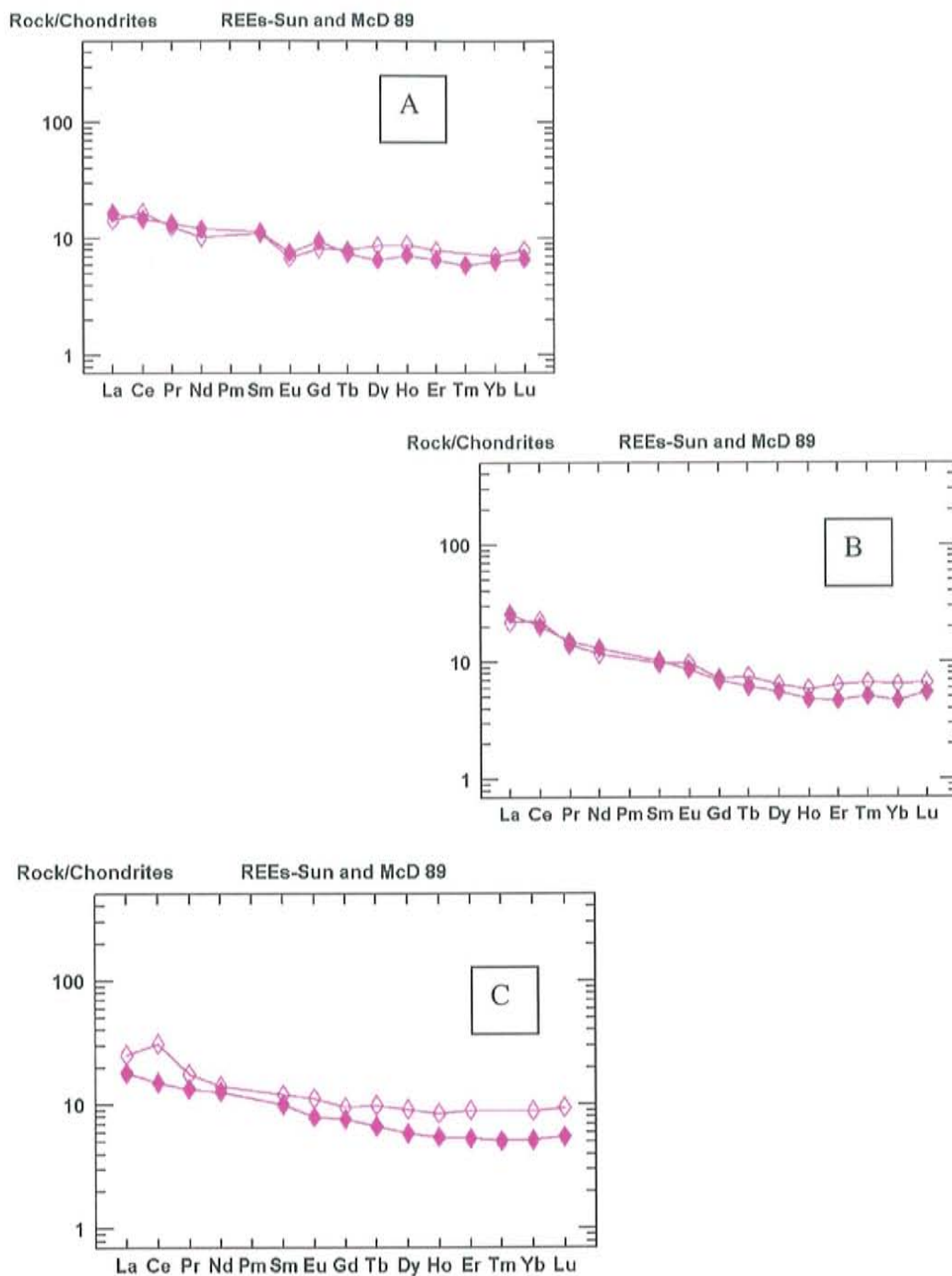
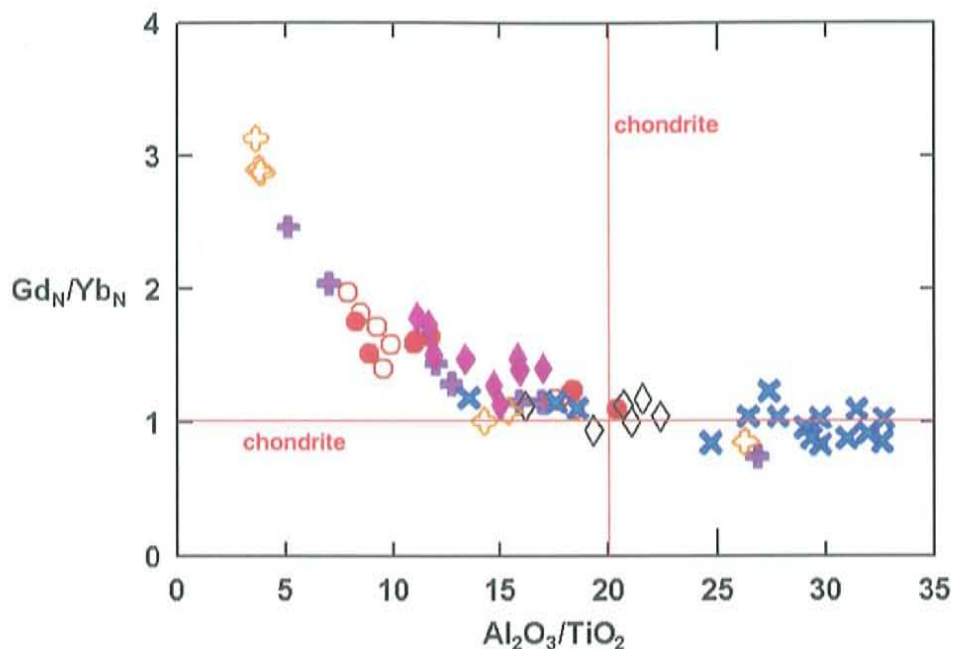


Figure 33. Diamondiferous rocks from Dachine and Akwatia.

A. Sample 1437 (filled diamonds) from Dachine, French Guiana and sample G-4 (open diamonds) from Akwatia Ghana.

B. Sample 2403 (filled diamonds) from Dachine, French Guiana and sample DM-2 (open diamonds) from Akwatia Ghana.

C. Average compositions (filled diamonds) from Dachine, French Guiana and sample average compositions (open diamonds) from Akwatia Ghana. Data for Dachine samples from (Capdevila 2003)



- Fragmental Komatiitic basalt from Murchison Terrane in Western Australia data from (Barley et al. 2000).
- Fragmental Komatiite from Murchison Terrane in Western Australia data from (Barley et al. 2000).
- + Fragmental Komatiites from Steep Rock And Lumby Lake Western Superior Province Canada data from (Tomlinson et al. 1998).
- ◆ Diamondiferous Komatiite from Dachine French Guiana data from (Capdevila 2003).
- + Gorgona Island komatiites and komatiitic basalts data from (Kerr et al. 1996).
- × Munro komatiites and komatiitic basalts data from (Hollings et al., 1999).
- ◇ Akwatia diamond bearing rocks.

Figure 34. Ratio plot  $\text{Al}_2\text{O}_3/\text{TiO}_2$  vs.  $\text{Gd}_\text{N}/\text{Yb}_\text{N}$  comparing komatiites. Red lines are chondritic ratios;  $\text{Gd}_\text{N}/\text{Yb}_\text{N}$  is normalized to primitive mantle (Sun and McDonough, 1989). The form of the diagram is from (Tomlinson et al., 1998).



## Komatiite Generation and Tectonic Setting

Komatiites are ultramafic lavas generated at great depth. There is still considerable debate as to the exact temperatures and tectonic setting of komatiite formation. A number of competing hypotheses exists in recent literature including plumes, hydrous plumes, plumes interacting with subduction zones and boninite-like melting all being advocated (Grove and Parman, 2004). It is possible that komatiites were generated by more than one process in the Archean and early Proterozoic, in the same way that basalts are produced in a range of tectonic settings today. Many komatiites and komatiitic basalts have geochemical characteristics similar to modern subduction-related magmas. These include variable enrichments in large ion lithophile and light rare earth elements along with depletions in high field strength elements, indicating input of trace element-enriched material into the komatiites. It is unclear whether it was added as a hydrous fluid into the komatiite source in a subduction zone (subduction model), or was introduced by the addition of granitic material as the komatiite traversed the crust (plume model) (Grove and Parman, 2004). Figure 35 depicts pressure/temperature/depth regimes required to produce komatiites in either hydrous or anhydrous. The light blue line is the diamond stability field. Clearly some komatiites produced in one or more of the regimes depicted could encounter diamonds on their way to the surface.

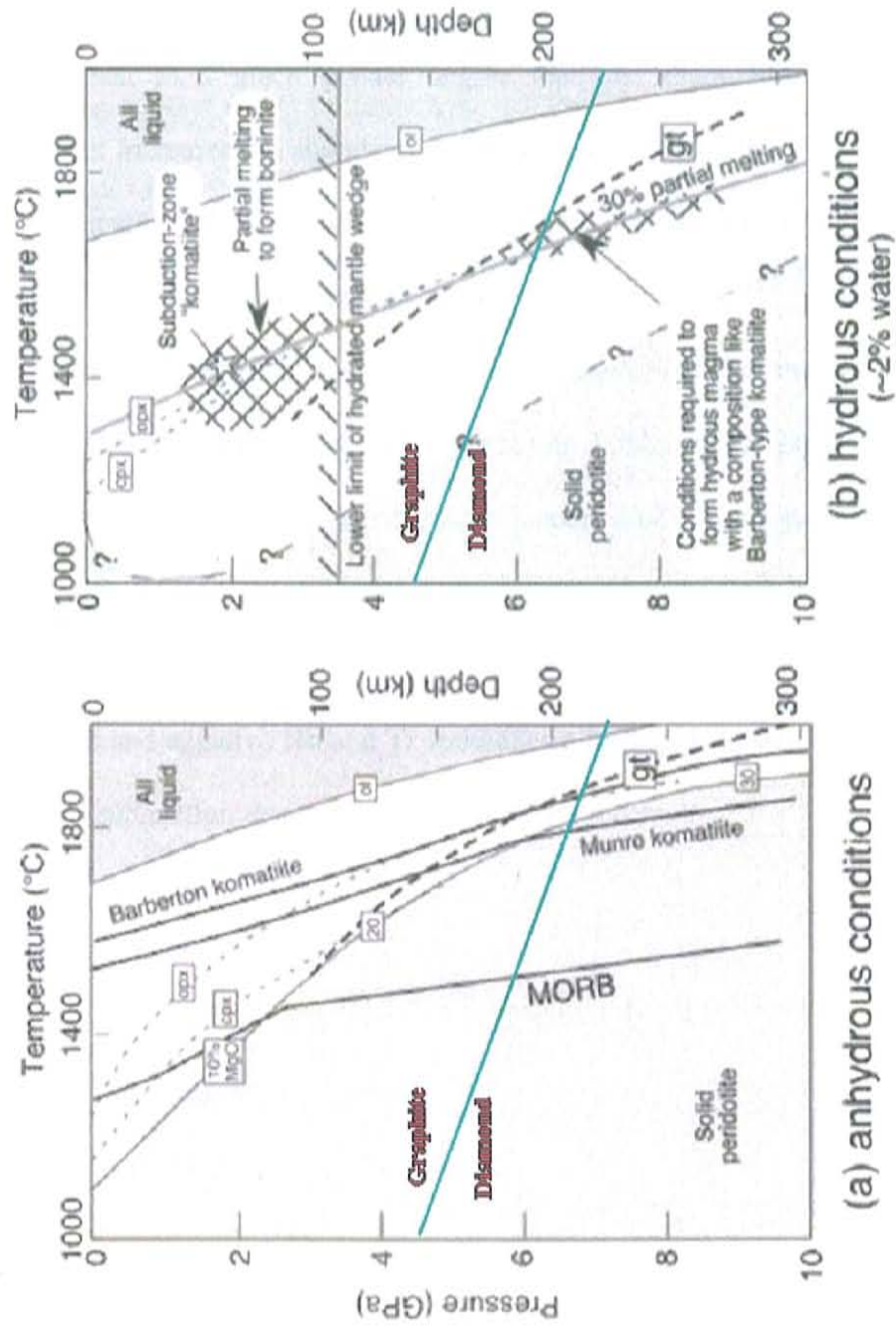


Figure 35. Pressure/temperature conditions required to form komatiites in (a) anhydrous conditions or in (b) hydrous conditions. The light blue line is the diamond/graphite stability field. Modified after (Arndt, 2003).

## Crustal Contamination

Both the diamond bearing rocks and the actinolite schist show enrichment in LREE, positive Th anomalies and negative Nb and Ti anomalies (figure 20), the actinolite schist to a much greater degree than the diamondiferous rocks. Crustal contamination increases the abundances of incompatible elements such as the LREE and Th with a smaller effect on Nb and Ti resulting in an enriched LREE signature and negative Nb and Ti anomalies (Jochum et al., 1991).

The bulk chemistry of the actinolite- tremolite schist is komatiitic (figure 18) but the REE signature is highly enriched resembling kimberlite or lamproite though it is virtually barren of diamonds. Furthermore isocon analysis suggests REE have been mobilized and are thus an unreliable indicator of protolith. Both mobile and immobile elements in the schists behave erratically (figure 20) and enrichment in LREE, positive Th anomalies and negative Nb and Ti anomalies all suggest crustal contamination or the addition of a subduction-derived hydrous fluid component.



## **Tectonic Setting**

Trace element analysis suggests that Akwatia rocks are derived from a subduction-island arc setting. On the discrimination diagram (Wood, 1980; Wood et al., 1979) all Akwatia rocks plot in the arc basalt field (figure 21). High field strength element bivariate plot  $Zr/Y$  vs.  $Nb/Y$  (Figure 36) strongly suggest a subduction-island arc provenance for Akwatia diamond-bearing rocks (Condie, 2005).

Other researchers agree that the Birimian Supergroup is derived from an island arc setting (Abouchami et al., 1990; Ama Salah et al., 1996; Davis et al., 1994a; Sylvester and Attah, 1992). (Sylvester and Attah, 1992) point to similarities in trace element chemistry between Birimian volcanic belts and Archean greenstone belts specifically  $La/Yb$  ratios  $< 4$ ,  $La/Ta$  ratios  $< 35$  and  $Hf/Ta$  ratios  $< 10$ . Furthermore they show that intermediate Birimian calc-alkaline units have high  $Ba/La$ ,  $Rb/La$ ,  $Tb/Yb$ ,  $Th/La$ ,  $Sr/Nd$  and low  $Ta/La$  ratios relative to NMORB. These geochemical characteristics, they state, are indicative of modern arc dacites derived by direct melting of the subducted slab. They suggest that this data shows a broad similarity between Archean island arc magmas and the intermediate Birimian calc-alkaline rocks of Ghana.

Abouchami et al., (1990) suggest that Birimian basalts are more recent equivalents of Archean greenstone belts, that is oceanic flood basalts similar to those that form oceanic plateaus and are later accreted to continents as allochthonous terrains. The komatiites of Gorgona Island are suggested to fit best with their proposed model of intraplate volcanism for the Birimian terrains of West Africa. (Davis et al., 1994b) point to striking similarities in regional geological patterns and relative internal age relationships between the Paleoproterozoic Ebunian orogen of Ghana and the Archean Kenoran orogen of the southern superior province in Canada. They propose that these relationships support an accretionary model for crustal growth (in Ghana) by subduction-collision processes. (McKittrick, 1996) also concluded the provenance of Akwatia metasediments was an island arc setting.

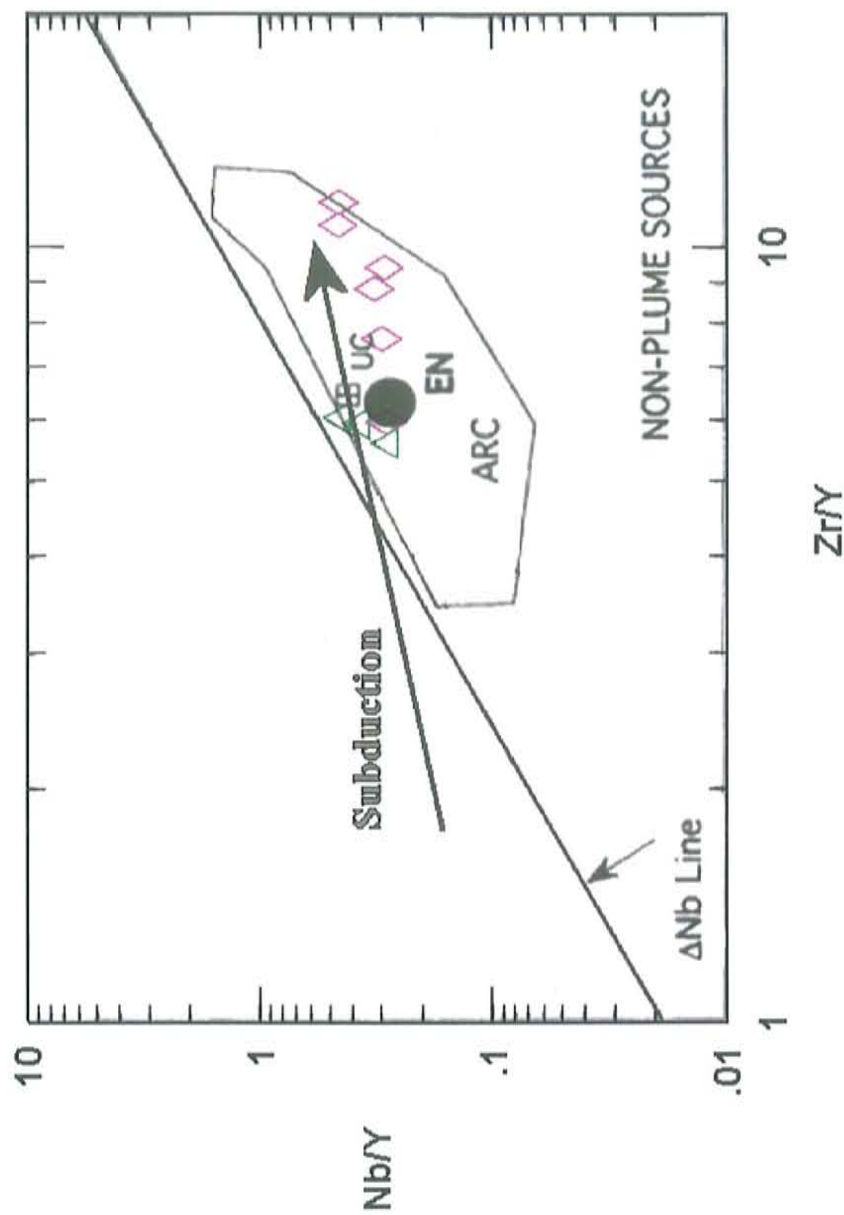


Figure 36. Showing Akwatia diamondiferous rocks (open pink diamonds) and high-Mg metasediments (green triangles) from (McKittrick, 1996) plotted on a diagram showing mantle compositional component and the field for arc-related basalts (ARC); EN, enriched component and UC, upper crust. Arrow indicates the effect of subduction. Modified after (Condie, 2005).



## **Emplacement of Akwatia Rocks**

Field evidence suggests brecciated, diamond-bearing rocks were emplaced rapidly in a sub-aqueous environment. The turbiditic nature of area rocks indicates sub-aqueous deposition and the very poorly sorted, matrix-supported (with clasts up 16cm.) nature of the diamond-bearing rock indicates rapid deposition (figure 5). (Gammon, 2003) notes CAST geologists also observe these features and that diamond bearing rocks commonly display normal graded bedding. (McKitrick, 1996) notes much of the metasediments in the area are a coarse-grained clastic turbidite.

The intercalation of the actinolite schists and the komattite breccia suggests the lithologies were deposited contemporaneously. Clasts of actinolite schists and other metasediments are observed within the breccia (figure 5). Geologists from CAST observed clasts of metasediments within the actinolite schist (Gammon, 2003). (McKitrick, 1996) observed a minimally weathered outcrop revealing a concordant, undulating contact between clast-rich breccia and turbiditic metasediments showing no evidence of heating or intrusion. Furthermore CAST geologists state that all Birimian rocks in the Akwatia area are of clastic origin. Tropical weathering and greenschist facies metamorphism have destroyed or obscured structural relationships making it impossible to establish a sequence or succession in the Akwatia area.

Field observations indicate the protoliths of the schists and metasediments were emplaced before metamorphism as clasts within the metasediments exhibit preferential orientation (figure 6) and are concordant with the local strike and schistosity of Birimian strata.

The actinolite schist and the fine-grained high-Mg metasediments may be the products of fine-grained, low-density turbidity current deposition or distal products of the erosion of ultramafic/ mafic and felsic sources.

### **Resorption**

The small size of Akwatia diamonds, apparent lack of micro-diamonds and the virtual lack of diamonds in the schist may be a result of resorption. The predominant form of Akwatia diamonds is the rounded dodecahedron (also called dodecahedriods or tetrahexahedriods) followed by the octahedron (Kaminsky, 1996). It has been firmly established that the rounded dodecahedron form is the result of resorption e.g. Robinson in (Ross et al., 1989). Further, many of the diamonds bear marks of natural oxidative dissolution in the form of etch channels or patterns, caverns and corrosion induced fabric on crystal surfaces (Kaminsky, 1996). The two factors governing resorption are the depth during magma ascent at which the diamond is liberated from an enclosing xenolith or xenocryst and the initial size of the diamond (figure 37). Resorption results in eliminating small diamonds while larger ones are reduced in size. Resorption features may also suggest transport in a highly reactive or very hot magma. The coarse brecciated nature of the diamondiferous rock suggests rapid explosive emplacement. This may result from a hydrated magma, or one charged with CO<sub>2</sub>.

In either case rapid decompression on ascent would cause the magma to be super-cooled preventing total resorption of the diamonds. The schist may represent a magma that ascended more slowly and thus most of the diamonds were completely resorbed. Furthermore slower ascent would provide more opportunity for the magma and the crust to interact, increasing contamination, and indeed the schists shows qualitative signs of greater crustal contamination than the diamondiferous rocks.



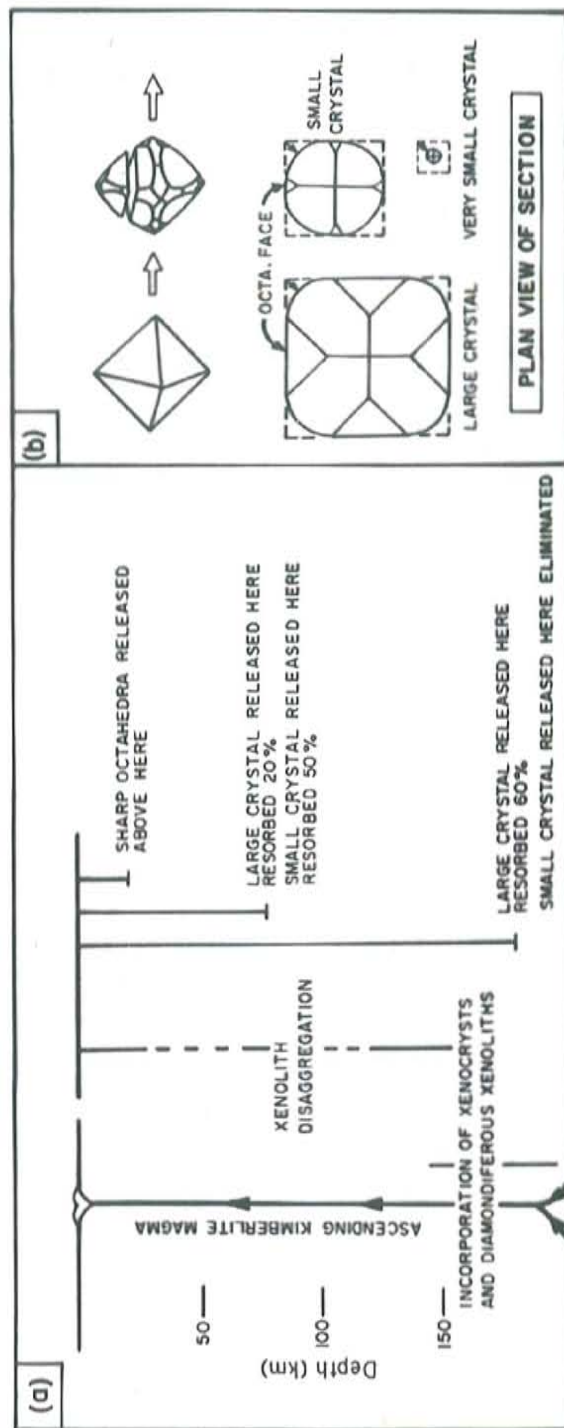


Figure 37. Diagrammatic representation of the factors responsible for producing the range of diamond crystal forms, from sharp octahedron to pure tetrahedron, in the kimberlites considered. (a) The amount of resorption, of initially large and small octahedra, as a function of the depth (diagrammatic only, actual depths are not known) at which exposure to kimberlite magma commences during emplacement. (b) The effect of original size, viewed in cube-plane section. Degree of modification of the original crystal is determined by the distance of retreat from octahedral coigns and edges. This distance will be similar, during unit time, irrespective of the original size of the crystal (see small arrows in the three cube-plane sections). Therefore, small crystals will be changed to tetrahedra (and might subsequently be eliminated) more rapidly than large crystals. Modified from Robinson in (Ross et al., 1989)

## Akwatia Compared To Dachine

Akwatia, Ghana, and Dachine, French Guiana, are located within greenstone belts of nearly identical ages and tectonic setting. Geochronological and paleomagnetic data for the West African craton and Guyana shield in S America, are concordant and suggest the existence of a single unit (Figure 38) grouping them during Archean and Lower Proterozoic times (Caen-Vachette, 1988; Gruau et al., 1985; Nomade et al., 2003; Onstott and Hargraves, 1981). Dachine is in the Inini greenstone belt, which is dominated by calc-alkaline andesite to rhyolite, and immature sedimentary rocks, all intruded by granitoids (Capdevila et al., 1999).

Diamond size and grade at Dachine are similar to Akwatia. Residual diamond grades overlying diamond-bearing rocks at Dachine French Guiana are similar to those at Akwatia. Bulk samples from this rock contain <1 to 77 diamonds per kg. the diamond population is dominated by micro-diamonds, the largest diamond found is ~ 4.6mm in diameter. Larger diamonds >1mm are abundant in the poorly sorted alluvium overlying diamondiferous rock with grades of 4 carats per cubic meter (Capdevila et al., 1999).

Diamond-bearing rocks at Dachine and Akwatia are very similar in texture and lithological association. Dachine diamondiferous volcanoclastic komatiites are associated with metagreywacks, talc-chlorite schists and contain clasts of country rock. Researchers at Dachine refer to the diamond-bearing rocks as "volcanoclastic" because, as a result of metamorphism, they are unable to tell whether the protolith is pyroclastic or sedimentary (Captevilla 2003).

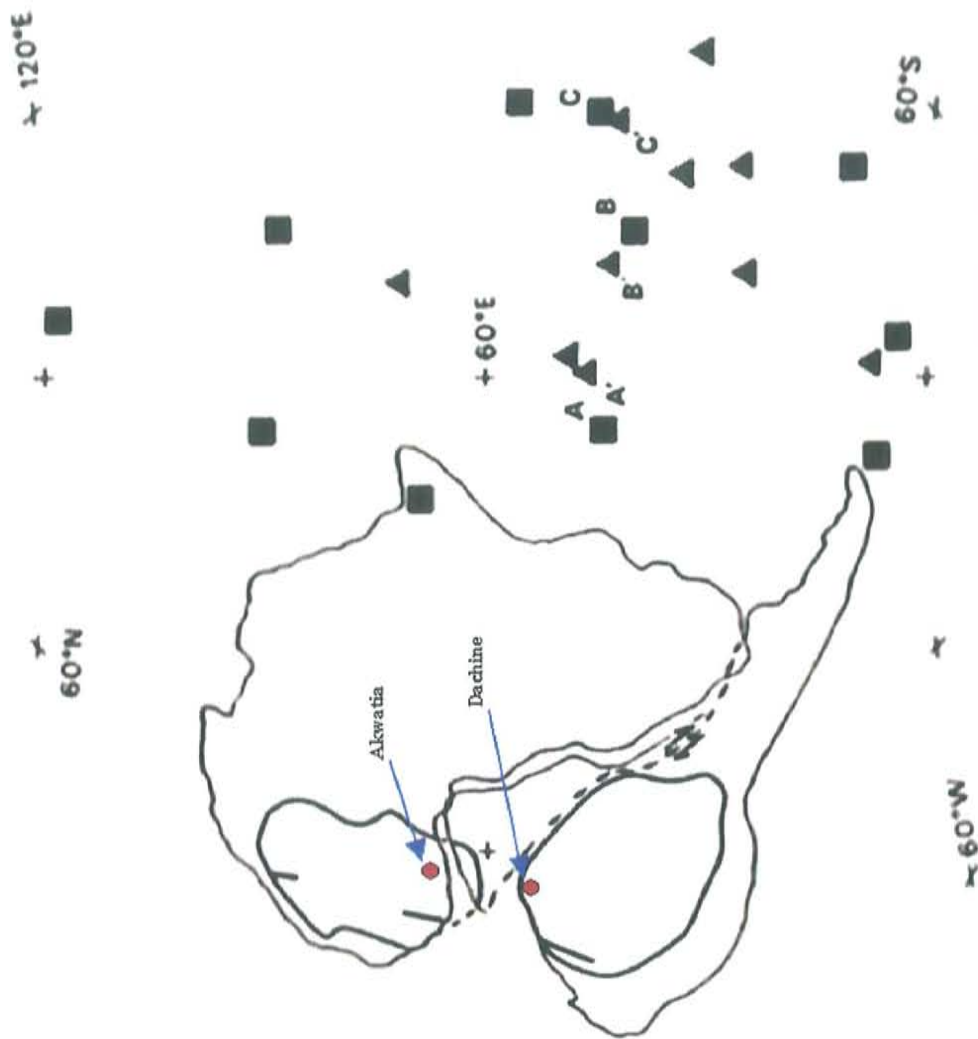


Figure 38. One proposed reconstruction for the period 2,100—1,500 Ma., which brings together the correlatable data points from each shield and also aligns the basement structures between the two shields. Transcurrent fault is shown with direction of displacement indicated by small arrows. Modified after (Onstott and Hargraves, 1981).



Traditional diamond indicator minerals do not accompany diamonds at Dachine or Akwatia. Diamond indicator minerals magnesian ilmenite, chrome diopside and perovskite are absent (Capdevila et al., 1999). Remainers of ilherzolitic and subcalcic harzburgitic type garnets are present at Dachine but these are only found in drill core by the caustic fusion method (Capdevilla p.c.). The caustic fusion method uses caustic chemicals and extreme heat to reduce rock samples down to 0.2% of their original volume leaving only the most resistant minerals. To date, this type of analysis has not been done with Akwatia diamond-bearing rocks. Titanium poor Mn rich spinels are present in Dachine. Spinel from Akwatia have not been analyzed. Finally, greenstone belts in Ghana and French Guiana are both significant sources of gold (Associates, 1997; Kesse, 1985).

The differences between Akwatia and Dachine are: Akwatia diamonds are wholly of peridotitic affinity. Dachine diamonds show evidence of eclogitic sources, having low carbon-isotope ratios and diamond morphologies dominated by cubo-octahedra (Capdevila et al., 1999). This may reflect differences in the lithosphere beneath Dachine and Akwatia. Perhaps the lithosphere beneath West Africa is a richer source of peridotitic diamonds than is the Guiana shield. In general Dachine diamondiferous rocks have higher chondrite-normalized  $\text{Al}_2\text{O}_3/\text{TiO}_2$  and Gd/Yb ratios (and fewer diamonds) than Akwatia diamondiferous rocks, though there is some overlap (figure 34). These near chondritic ratios may be the key to distinguishing potential diamond bearing komatiites from non- diamond bearing komatiites. Akwatia may represent a new and potentially significant diamond resource while Dachine may not. Results of reconnaissance by Golden Star Resources at Dachine are disappointing and further exploration has been put

on hold. In contrast Akwatia is large and economically significant diamond deposit with well over a hundred million carats of diamonds having been exported to date and a potentially vast unmined bedrock resource. Intensive trenching on Beduwara Hill by CAST Geologists delineates seventeen "bands" of source rock one of which contains in plan view has dimensions of 125,000 sq. ft. (~ 100 sq. meters) note – at the maximum they would have about 6 million carats (worth about \$ 200 million) of diamondiferous material with an average grade of .93 carats per cubic yard. This trenching was only done on Beduwara Hill. This research suggests that these source bands are common within the diamondiferous area. Figure 17 may show the location of these "bands" in the sub-surface. Ghana Consolidated Diamonds preferring to mine the higher-grade alluvial areas does not mine the bedrock or delineate it as a proven resource; rather they leave this to the small-scale miners. Figure 39 is, a map of anomalous diamond occurrences. Many of these occurrences correspond to island arcs or greenstone belts and thus Akwatia type deposits may be widespread.

## **A Speculative Model for the Emplacement of Akwatia Komatiites**

High temperature komatiitic lavas associated with a subduction zone are generated at a depth below the diamond stability field (Figure 35). On ascent the lava incorporated diamond-bearing xenoliths, upon reaching the hydrated lithosphere water and/or CO<sub>2</sub> are picked up causing the magma to rise rapidly, bringing the diamonds to the surface in an explosive eruption. Second, the continued subduction of the lithosphere cools and hydrates the mantle establishing a mature subduction zone. Subsequent lower-temperature hydrous magmas are emplaced less explosively (and thus subject to greater crustal contamination) on top of earlier, brecciated, diamond bearing lithologies. Third, the komatiitic crust is obducted onto continents and isoclinally folded during continent collision at the end of subduction. Finally, weathering dispersed diamonds into local streams and the Birim River. The broad occurrence of diamonds in Ghana may be the result of similar processes throughout the Birimian.



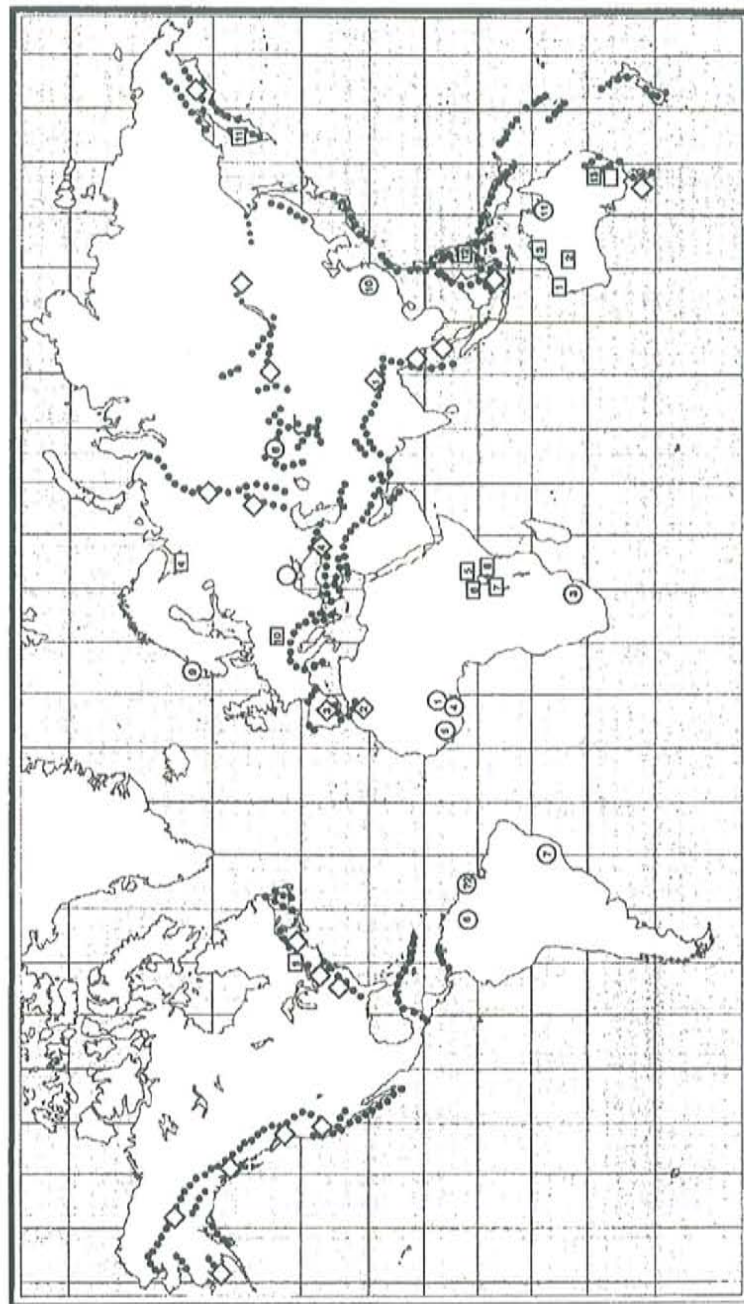


Fig 39. Worldwide localities of "anomalous" diamonds (black dots).

Diamonds associated with non kimberlite/lamproite volcanic rocks (box symbols): 1, Wandagee, Western Australia; 2, Bulljiah Pool, Western Australia; 3, Maude Creek, Western Australia; 4, Omega Peninsula, Russia; 5, north east Uganda; 6, south west Uganda; 7, Ngualla, Chunya District, Tanzania; 8, Losogoroi, Kenya and Lashaine, Tanzania; 9, Ile Bizard, Montreal; 10, Linhorka pipe, Bohemia; 11, Almazny volcano, Kamchatka; 12, Ruang volcano, Sulawesi; 13, Copeton, NSW, Australia. Diamonds, including graphitised diamonds, from peridotites or alluvial deposits from alpine/ophiolite type belts; (diamond-shaped symbols): 1, Tibet; 2, Beni Bousera; 3, Ronda; 4, Armenia. Peridotite belts after Coleman (1977). Diamonds from metamorphic terrain, excluding alpine peridotites (circles): 1, Burkina Faso; 2, French Guiana; 3, Witwatersrand; 4, Tarkwain; 5, Birimian; 6, Roraima; 7, Espinhaco; 8, Kazakhstan; 9, W. Norway; 10, Dabie Shan; 11, Coanjula. Localities for carbonado and meteoritic diamonds are not shown. Modified after (Nixon and Griffin, 1995).

## CONCLUSIONS

- **Akwatia is a primary diamond deposit.**

Diamond production, high diamond grades in un-mined bedrock and continuing production of diamonds distinguish Akwatia as a one of the world's largest diamond deposits. High quality diamonds with no evidence of sedimentary transport, the immature nature of the host rock and the lack of correlation between bedrock, diamond grade and topography make alluvial classification of the Akwatia diamond deposit unappealing.

- **The most likely protolith of the host rock is a syn-eruptive volcanoclastic mega-turbidite derived from a diamond-bearing Karasjok- type komatiite.**

The primary host rock at Akwatia resembles neither kimberlite nor lamproite either texturally or geochemically and traditional diamond indicator minerals are wholly absent. Rare earth element patterns of weathered diamond bearing rocks strongly resemble diamondiferous komatiites from Dachine, French Guiana and other Karasjok-type komatiites. Adjacent un-weathered or less-weathered rocks contain up to 21.1 wt. % magnesium. Akwatia Ghana and Dachine French Guiana are located within greenstone belts of nearly identical ages and tectonic settings.

- **The host rock is widely distributed in the diamond field.**

High diamond grades extend over an area of approximately 32 kilometers. Small-scale mining pits and trenches expose diamond-bearing rock throughout the 32-kilometer area.

- **Akwatia may be representative of a new and potentially significant type of diamond occurrence.**

Akwatia is a world-class diamond occurrence. Anomalous diamond occurrences are correlated with greenstone belts and ancient island arcs worldwide and represent a potentially vast diamond exploration target.



## REFERENCES

- Abouchami, W., Boher, M., Michard, A., and Albarede, F., 1990, A major 2.1 Ga event of mafic magmatism in West Africa: an early stage of crustal accretion: *Journal of Geophysical Research*, v. 95, p. 17,605-17,629.
- Ama Salah, I., Liegeois, J. P., and Pouclet, A., 1996, Evolution d'un arc insulaire oceanique birimien precoce au Liptako nigerien (Sirba): geologie, geochronologie et geochemie Evolution of an early Birrimian oceanic island arc of the Nigerian Liptako (Sirba): geology, geochronology and geochemistry: *Journal of African Earth Sciences*, v. 22, p. 235-254.
- Arndt, N., 2003, Komatiites, kimberlites, and boninites: *Journal of Geophysical Research B: Solid Earth*, v. 108, p. ECV 5-1 - 5-11.
- Associates, V. a., 1997, Canarc (CCM-TSE), Canarc Resource Corp., p. 9.
- Barley, M. E., Kerrich, R., Reudavy, I., and Xie, Q., 2000, Late Archaean Ti-rich, Al-depleted komatiites and komatiitic volcanoclastic rocks from the Murchison Terrane in Western Australia: *Australian Journal of Earth Sciences*, v. 47, p. 873-883.
- Boher, M., Arndt, N. T., Abouchami, W., Michard, A., and Albarede, F., 1992, Crustal growth in West Africa at 2.1 Ga: *Journal of Geophysical Research*, v. 97, p. 345-369.
- Caen-Vachette, M., 1988, Le craton ouest-africain et le bouclier guyanais: un seul craton au Proterozoique inferieur? (The West African craton and the Guyana shield: a single craton from the Lower Proterozoic Palaeomagnetism): *Journal of African Earth Sciences*, v. 7, p. 479-488.
- Capdevila, R., 2003, Diamonds, in Canales, D., ed.: Rennes, France, Ramon Capdevila.
- Capdevila, R., Arndt, N., Letendre, J., and Sauvage, J.-F., 1999, Diamonds in volcanoclastic komatiite from French Guiana: *Nature (London)*, v. 399, p. 456-458.
- Condie, K. C., 2005, High field strength element ratios in Archean basalts: a window to evolving sources of mantle plumes?: *Lithos*, v. 79, p. 491-504.
- Cullers, R. L., Barrett, T., Carlson, R., and Robinson, B., 1987, Rare-earth element and mineralogic changes in Holocene soil and stream sediment: a case study in the Wet Mountains, Colorado, USA: *Chemical Geology*, v. 63, p. 275-297.
- Davis, D. W., Hirdes, W., Schaltegger, U., and Nunoo, E. A., 1994a, U-Pb age constraints on deposition and provenance of Birimian and gold-bearing Tarkwaian sediments in Ghana, West Africa: *Precambrian Research*, v. 67, p. 89-107.
- Davis, D. W., Hirdes, W., Schaltegger, U., and Nunoo, E. A., 1994b, U---Pb age constraints on deposition and provenance of Birimian and gold-bearing

- Tarkwaian sediments in Ghana, West Africa: *Precambrian Research*, v. 67, p. 89-107.
- Fedo, C. M., Nesbitt, H. W., and Young, G. M., 1995, Unravelling the effects of potassium metasomatism in sedimentary rocks and paleosols, with implications for paleoweathering conditions and provenance: *Geology*, v. 23, p. 921-924.
- Feybesse, J. L., and Milesi, J. P., 1994, The Archaean/Proterozoic contact zone in West Africa: a mountain belt of decollement thrusting and folding on a continental margin related to 2.1 Ga convergence of Archaean cratons?: *Precambrian Research*, v. 69, p. 199-227.
- Fleet, A. J., 1984, Aqueous and sedimentary geochemistry of the rare earth elements (REE), in Henderson, P., ed., *Rare earth element geochemistry: Developments in Geochemistry 2*, Elsevier, p. 343-373.
- Gammon, J. F., 2003, The Geology of the 1/4 degree Field Sheets No. 57, Nsaba NW, and No. 93 Kibi SW: Accra, Ghana, Ghana Geological Survey Department, p. 106.
- Grant, J. A., 1986, The isocon diagram; a simple solution to Gresens' equation for metasomatic alteration: *Economic Geology and the Bulletin of the Society of Economic Geologists*, v. 81, p. 1976-1982.
- Grove, T. L., and Parman, S. W., 2004, Thermal evolution of the Earth as recorded by komatiites: *Earth and Planetary Science Letters*, v. 219, p. 173-187.
- Gruau, G., Martin, H., Leveque, B., Capdevila, R., and Marot, A., 1985, Rb--Sr and Sm--Nd geochronology of lower Proterozoic granite--greenstone terrains in French Guiana, South America: *Precambrian Research*, v. 30, p. 63-80.
- Hirdes, W., Davis, D. W., and Eisenlohr, B. N., 1992, Reassessment of Proterozoic granitoid ages in Ghana on the basis of U/Pb zircon and monazite dating: *Precambrian Research*, v. 56, p. 89-96.
- Hirdes, W., Konan, G., Davis, D. W., and Ludtke, G., 1996, Two generations of Birimian (Paleoproterozoic) volcanic belts in northeastern Cote d'Ivoire (West Africa): consequences for the 'Birimian controversy': *Precambrian Research*, v. 80, p. 173-191.
- Hollings, P., Wyman, D., Kerrich, R., Condie, K. C., and Abbott, D. H., 1999, Komatiite-basalt-rhyolite volcanic associations in northern Superior Province greenstone belts; significance of plume-arc interaction in the generation of the proto continental Superior Province, Elsevier, Amsterdam, International, p. 137-161.
- Janse, A. J. A., and Sheahan, P. A., 1995, Catalogue of world wide diamond and kimberlite occurrences: a selective and annotative approach: *Journal of Geochemical Exploration*, v. 53, p. 73-111.
- Jensen, L. S., 1976, A new cation plot for classifying subalkalic volcanic rocks.
- Jochum, K. P., Arndt, N. T., and Hofmann, A. W., 1991, Nb-Th-La in komatiites and basalts: constraints on komatiite petrogenesis and mantle evolution: *Earth & Planetary Science Letters*, v. 107, p. 272-289.
- Junner, N. R., 1943, The diamond deposits of the Gold Coast, with notes on other deposits in west Africa, and appendix, the crystal form of diamonds from the Gold Coast by F. A. Bannister.



- Kaminsky, F. V., Zakharchenko, O.D., Sablukova, L. I., 1996, Report On Studies Of Diamonds And Concentrate Samples From The Volta Diamond Concession, Ghana: Moscow-Vancouver, KM Diamond Exploration, p. 26.
- Kesse, G. O., 1985, The mineral and rock resources of Ghana, Rotterdam, A. A. Balkema, Netherlands, 610 p.
- Krauskopf, K. B., and Bird, D. K., 1995, Introduction to geochemistry Edition: 3, New York, McGraw-Hill, 647 p.
- Leube, A., Hirdes, W., Mauer, R., and Kesse, G. O., 1990, The early Proterozoic Birimian Supergroup of Ghana and some aspects of its associated gold mineralization: *Precambrian Research*, v. 46, p. 139-165.
- McKittrick, S., 1996, The Akwatia Diamondfield, Ghana, West Africa: Socorro, NM, New Mexico Tech, p. 19.
- McLennan, S. M., McCulloch, M. T., Taylor, S. R., and Maynard, J. B., 1989, Effects of sedimentary sorting on neodymium isotopes in deep-sea turbidites: *Nature*, v. 337, p. 547-549.
- McPhie, J., Doyle, M., and Allen, R., 1993, Volcanic textures; a guide to the interpretation of textures in volcanic rocks, Launceston, TAS, University of Tasmania, Centre for Ore Deposit and Exploration Studies, Australia, 196 p.
- Meyer, H. O. A., and Boyd, F. R., 1972, Composition and origin of crystalline inclusions in natural diamonds: *Geochimica et Cosmochimica Acta*, v. 36, p. 1255-1273.
- Nesbitt, H. W., and Young, G. M., 1982, Early Proterozoic climates and plate motions inferred from major element chemistry of lutites ( Lake Huron): *Nature*, v. 299, p. 715-717.
- Nixon, P. H., 1987, Mantle xenoliths, Mantle xenoliths, J.Wiley, p. 846.
- Nixon, P. H., and Griffin, W. L., 1995, The morphology and nature of primary diamondiferous occurrences, Elsevier, Amsterdam-New York, International, p. 41-71.
- Nomade, S., Chen, Y., Pouclet, A., Feraud, G., Theveniaut, H., Daouda, B. Y., Vidal, M., and Rigolet, C., 2003, The Guiana and the West African Shield Palaeoproterozoic grouping; new palaeomagnetic data for French Guiana and the Ivory Coast: *Geophysical Journal International*, v. 154, p. 677-694.
- Oberthur, T., Vetter, U., Davis, D. W., and Amanor, J. A., 1998, Age constraints on gold mineralization and Paleoproterozoic crustal evolution in the Ashanti belt of southern Ghana: *Precambrian Research*, v. 89, p. 129-143.
- Onstott, T. C., and Hargraves, R. B., 1981, Proterozoic transcurrent tectonics: paleomagnetic evidence from Venezuela and Africa: *Nature*, v. 289, p. 131-136.
- Palmer, C., Hamilton, M., and Ward, T., 2002, Understanding the Biogeochemistry of Cesium--An investigation of factors influencing cesium mobility, SubsurfaceTopics, INEEL.
- Rollinson, H. R., 1993, Using geochemical data; evaluation, presentation, interpretation, Harlow, Longman Scientific & Technical, United Kingdom, 352 p.
- Rose, A. W., Hawkes, H. E., and Webb, J. S., 1979, Geochemistry in mineral exploration Edition: 2: State College, PA, London, Acad. Press, United Kingdom, 635 p.
- Ross, J., editor, Jaques, A. L., Ferguson, J., Green, D. H., O'Reilly, S. Y., Danchin, R. V., and Janse, A. J. A., 1989, Kimberlites and related rocks, v. 2.



- Sun, S. S., and McDonough, W. F., 1989, Chemical and isotopic systematics of oceanic basalts: implications for mantle composition and processes, *in* Saunders, A. D., ed., *Magmatism in the ocean basins: Geological Society Special Publication*, 42, Blackwell Scientific, p. 313-345.
- Sylvester, P. J., and Atttoh, K., 1992, Lithostratigraphy and composition of 2.1 Ga greenstone belts of the West African Craton and their bearing on crustal evolution and the Archean-Proterozoic boundary: *Journal of Geology*, v. 100, p. 377-393.
- Taylor, P. N., Moorbath, S., Leube, A., and Hirdes, W., 1992, Early Proterozoic crustal evolution in the birimian of Ghana: constraints from geochronology and isotope geochemistry: *Precambrian Research*, v. 56, p. 97-111.
- Tomlinson, K. Y., Stevenson, R. K., Hughes, D. J., Hall, R. P., Thurston, P. C., and Henry, P., 1998, The Red Lake greenstone belt, Superior Province; evidence of plume-related magmatism at 3 Ga and evidence of an older enriched source: *Precambrian Research*, v. 89, p. 59-76.
- Voicu, G., and Bardoux, M., 2002, Geochemical behavior under tropical weathering of the Barama-Mazaruni greenstone belt at Omai gold mine, Guiana Shield: *Applied Geochemistry*, v. 17, p. 321-336.
- Ward, J. R., 1998, Physical and geochemical aspects of diamonds from the Tarkwa and Akwatia diamondfields of southern Ghana, West Africa: Unpub. M.S. thesis, New Mexico Institute of Mining and Technology.
- Wood, D. A., 1980, The application of a Th-Hf-Ta diagram to problems of tectonomagmatic classification and to establishing the nature of crustal contamination of basaltic lavas of the British Tertiary volcanic province: *Earth and Planetary Science Letters*, v. 50, p. 11-30.
- Wood, D. A., Joron, J.-L., and Treuil, M., 1979, A re-appraisal of the use of trace elements to classify and discriminate between magma series erupted in different tectonic settings: *Earth and Planetary Science Letters*, v. 45, p. 326-336.
- Wright, J. B., Hastings, D. A., Jones, W. B., and Williams, H. R., 1985, *Geology and Mineral Resources of West Africa*, *Geology and Mineral Resources of West Africa*, London (George Allen & Unwin), p. xiv + 188.

Appendix 1: Akwatia samples analyzed in this study.

| analyte | method  |      | Limit | g-1   | g-2   | g-3   | g-5   | g-9   | g-10  | g-11  | g-12  | DM2   |
|---------|---------|------|-------|-------|-------|-------|-------|-------|-------|-------|-------|-------|
| SiO2    | ICP-AES | wt.% | 0.01  | 60.30 | 46.60 | 61.30 | 42.00 | 62.40 | 43.30 | 43.10 | 62.20 | 63.49 |
| Al2O3   | ICP-AES | wt.% | 0.01  | 16.65 | 20.60 | 20.30 | 14.35 | 13.10 | 9.79  | 9.79  | 17.90 | 15.10 |
| Fe2O3   | ICP-AES | wt.% | 0.01  | 12.40 | 20.30 | 6.61  | 10.55 | 9.43  | 11.35 | 11.35 | 8.25  | 12.31 |
| CaO     | ICP-AES | wt.% | 0.01  | 0.00  | 0.00  | 0.00  | 1.98  | 0.00  | 3.63  | 3.63  | 0.09  | 0.00  |
| MgO     | ICP-AES | wt.% | 0.01  | 0.06  | 0.04  | 0.14  | 18.70 | 3.11  | 18.85 | 18.80 | 0.51  | 0.15  |
| Na2O    | ICP-AES | wt.% | 0.01  | 0.12  | 0.00  | 0.01  | 0.05  | 0.00  | 0.00  | 0.03  | 0.00  | 0.02  |
| K2O     | ICP-AES | wt.% | 0.01  | 0.05  | 0.03  | 0.33  | 0.05  | 0.44  | 0.08  | 0.08  | 1.75  | 0.00  |
| Cr2O3   | ICP-AES | wt.% | 0.01  | 0.27  | 0.28  | 0.03  | 0.33  | 0.14  | 0.36  | 0.36  | 0.06  | nd    |
| TiO2    | ICP-AES | wt.% | 0.01  | 0.68  | 0.92  | 1.05  | 0.47  | 0.81  | 0.58  | 0.61  | 0.85  | 0.73  |
| MnO     | ICP-AES | wt.% | 0.01  | 0.00  | 0.04  | 0.00  | 0.09  | 0.04  | 0.16  | 0.17  | 0.01  | 0.07  |
| P2O5    | ICP-AES | wt.% | 0.01  | 0.11  | 0.30  | 0.15  | 0.08  | 0.07  | 0.09  | 0.06  | 0.15  | 0.09  |
| SrO     | ICP-AES | wt.% | 0.01  | 0.00  | 0.00  | 0.00  | 0.00  | 0.00  | 0.01  | 0.00  | 0.00  | nd    |
| BaO     | ICP-AES | wt.% | 0.01  | 0.01  | 0.00  | 0.03  | 0.00  | 0.02  | 0.01  | 0.01  | 0.14  | nd    |
| LOI     | ICP-AES |      | 0.01  | 8.86  | 10.85 | 9.30  | 10.20 | 7.75  | 10.90 | 10.95 | 7.27  | 6.99  |
| Tm      | ICP-MS  | ppm  | 0.5   | 0.0   | 0.0   | 0.5   | 0.0   | 0.0   | 3.5   | 3.6   | 0.0   | 0.2   |
| U       | ICP-MS  | ppm  | 0.5   | 1.1   | 2.4   | 1.5   | 0.6   | 1.5   | 0.8   | 0.9   | 1.4   | 1.5   |
| V       | ICP-MS  | ppm  | 5     | 179   | 266   | 94    | 132   | 178   | 94    | 85    | 193   | 186   |
| W       | ICP-MS  | ppm  | 1     | 52    | 40    | 27    | 3     | 31    | 6     | 6     | 21    | 18    |
| Y       | ICP-MS  | ppm  | 0.5   | 16.4  | 17.0  | 27.9  | 22.3  | 8.6   | 286.0 | 294.0 | 16.6  | 9.0   |
| Yb      | ICP-MS  | ppm  | 0.1   | 1.6   | 2.3   | 2.9   | 1.9   | 1.4   | 18.1  | 18.4  | 1.9   | 1.1   |
| Zn      | ICP-MS  | ppm  | 5     | 36    | 108   | 41    | 146   | 108   | 144   | 143   | 46    | 45    |
| Zr      | ICP-MS  | ppm  | 0.5   | 91.0  | 159.5 | 165.5 | 62.9  | 91.6  | 68.5  | 69.7  | 126.0 | 102.7 |
| La      | ICP-MS  | ppm  | 0.5   | 34.5  | 7.4   | 8.8   | 64.9  | 6.6   | 332.0 | 354.0 | 7.8   | 5.2   |
| Lu      | ICP-MS  | ppm  | 0.1   | 0.3   | 0.4   | 0.4   | 0.3   | 0.2   | 2.6   | 2.7   | 0.3   | 0.2   |
| Nb      | ICP-MS  | ppm  | 1.0   | 5     | 5     | 8     | 3     | 4     | 3     | 4     | 5     | 4     |
| Nd      | ICP-MS  | ppm  | 0.5   | 17    | 11    | 8     | 50    | 8     | 299   | 314   | 8     | 5     |
| Ni      | ICP-MS  | ppm  | 5.0   | 530   | 743   | 58    | 1550  | 501   | 1535  | 1510  | 75    | 697   |

## Appendix 1, con't.

|    |        |     |      |      |      |       |       |       |       |       |      |      |
|----|--------|-----|------|------|------|-------|-------|-------|-------|-------|------|------|
| Pb | ICP-MS | ppm | 5.0  | 21   | 18   | 15    | 18    | 9     | 6     | 6     | 16   | 9    |
| Pr | ICP-MS | ppm | 0.1  | 5.3  | 2.5  | 2.2   | 14.8  | 2.0   | 77.7  | 83.2  | 2.1  | 1.3  |
| Rb | ICP-MS | ppm | 0.2  | 0.9  | 0.5  | 7.6   | 0.7   | 11.8  | 2.0   | 1.9   | 41.1 | nd   |
| Sm | ICP-MS | ppm | 0.1  | 3.2  | 3.3  | 2.3   | 7.7   | 1.8   | 51.6  | 55.4  | 1.9  | 1.5  |
| Sn | ICP-MS | ppm | 1.0  | 2.0  | 3.0  | 2.0   | 1.0   | 1.0   | 1.0   | 1.0   | 2.0  | 1.2  |
| Sr | ICP-MS | ppm | 0.1  | 16.7 | 2.6  | 4.3   | 42.1  | 3.4   | 48.6  | 48.7  | 21.3 | 3.0  |
| Ta | ICP-MS | ppm | 0.5  | 0.0  | 0.5  | 0.6   | 0.0   | 0.0   | 0.0   | 0.0   | 0.0  | 0.3  |
| Tb | ICP-MS | ppm | 0.1  | 0.5  | 0.6  | 0.7   | 0.8   | 0.3   | 8.0   | 8.2   | 0.4  | 0.3  |
| Th | ICP-MS | ppm | 0.1  | 3    | 5    | 4     | 2     | 3     | 2     | 2     | 4    | 3    |
|    |        |     |      |      |      |       |       |       |       | 1190. |      |      |
| Ba | ICP-MS | ppm | 0.5  | 47.7 | 9.7  | 212.0 | 32.8  | 185.0 | 113.0 | 123.5 | 0    | 15.9 |
| Ce | ICP-MS | ppm | 0.5  | 16.6 | 26.7 | 22.7  | 108.0 | 39.4  | 42.7  | 45.1  | 21.5 | 13.9 |
| Co | ICP-MS | ppm | 0.5  | 15.1 | 11.1 | 5.6   | 65.2  | 37.8  | 70.3  | 75.5  | 6.8  | 6.0  |
| Cr | ICP-MS | ppm | 10.0 | 1920 | 2050 | 230   | 2480  | 1020  | 2630  | 2700  | 430  | 492  |
| Cs | ICP-MS | ppm | 0.1  | 0.2  | 0.1  | 0.2   | 0.4   | 2.1   | 1.0   | 1.0   | 1.0  | nd   |
| Cu | ICP-MS | ppm | 5.0  | 42   | 38   | 32    | 44    | 2140  | 914   | 1765  | 78   | 53   |
| Dy | ICP-MS | ppm | 0.1  | 3.3  | 3.6  | 4.8   | 4.1   | 1.9   | 44.3  | 46.0  | 2.6  | 1.6  |
| Er | ICP-MS | ppm | 0.1  | 1.8  | 2.3  | 2.9   | 2.4   | 1.3   | 24.8  | 25.0  | 1.8  | 1.1  |
| Eu | ICP-MS | ppm | 0.1  | 1.0  | 1.0  | 1.0   | 1.6   | 0.6   | 13.6  | 14.5  | 0.7  | 0.6  |
| Ga | ICP-MS | ppm | 1.0  | 24   | 23   | 16    | 12    | 17    | 13    | 14    | 21   | 15   |
| Gd | ICP-MS | ppm | 0.1  | 3.4  | 2.9  | 3.3   | 7.1   | 1.9   | 53.1  | 54.9  | 2.3  | 1.5  |
| Hf | ICP-MS | ppm | 1.0  | 3    | 5    | 5     | 2     | 3     | 2     | 2     | 3    | 3    |
| Ho | ICP-MS | ppm | 0.1  | 0.6  | 0.7  | 1.0   | 0.8   | 0.4   | 9.1   | 9.4   | 0.6  | 0.3  |



Appendix 2: Akwatia samples analyzed by McKittrick

| analyte | method | pre<br>c. % | 93-33 | 93-20 | 93-19 | 93-16 | ha-2  | BH-170 | BH-197 | BH-226 | BH-243  | Bh1-168 | Bh2-97 |
|---------|--------|-------------|-------|-------|-------|-------|-------|--------|--------|--------|---------|---------|--------|
| SiO2    | XRF    | wt. %       | 44.71 | 57.36 | 44.69 | 54.82 | 49.99 | 60.25  | 52.96  | 39.89  | 62.21   | 58.24   | 62.78  |
| TiO2    | XRF    | wt. %       | 0.48  | 0.52  | 0.46  | 0.45  | 0.5   | 0.5    | 0.41   | 0.4    | 0.53    | 0.6     | 0.54   |
| Al2O3   | XRF    | wt. %       | 10.47 | 7.73  | 11.88 | 8.05  | 9.6   | 8.85   | 9.54   | 8.36   | 15.8    | 16.1    | 16.81  |
| Fe2O3   | XRF    | wt. %       | 9.25  | 7.63  | 10.03 | 8.76  | 8.77  | 7.01   | 7.92   | 8.5    | 8.03    | 6.68    | 6.42   |
| MnO     | XRF    | wt. %       | 0.15  | 0.21  | 0.16  | 0.09  | 0.13  | 0.09   | 0.14   | 0.22   | 0.09    | 0.1     | 0.11   |
| MgO     | XRF    | wt. %       | 20.01 | 16    | 20.29 | 20.64 | 18.35 | 15.37  | 20.7   | 21.2   | 10.81   | 5.91    | 6.32   |
| CaO     | XRF    | wt. %       | 6.1   | 5.04  | 4.9   | 0.12  | 5.97  | 3.81   | 7.63   | 9.23   | 2.76    | 4.31    | 5.16   |
| Na2O    | XRF    | wt. %       | 0.11  | 0.09  | 0.09  | 0.05  | 0.2   | 0      | 0      | 0      | 1.05    | 2.84    | 2.95   |
| K2O     | XRF    | wt. %       | 0.01  | 0.02  | 0.01  | 0.03  | 0.02  | 1.81   | 0.13   | 0.11   | 2.65    | 2.52    | 2.14   |
| P2O5    | XRF    | wt. %       | 0.14  | 0.13  | 0.07  | 0.11  | 0.14  | 0.23   | 0.2    | 0.24   | 0.29    | 0.24    | 0.2    |
| LOI     |        | wt. %       | 7.13  | 6.28  | 8.33  | 6.46  | 6.15  | 4.21   | 5.55   | 12.25  | 5.28    | 7.63    | 7.24   |
| Total   |        |             | 98.56 | 101.0 | 100.9 | 99.58 | 99.82 | 102.1  | 105.18 | 100.4  | 109.5   | 105.17  | 110.67 |
| La      | INAA   | 2 ppm       | 626.5 | 296.6 | 105.6 | 70.8  | 173.3 | 9.6    | 8.11   | 7.71   | 12.65   | 14.56   | 14.34  |
| Ce      | INAA   | 3 ppm       | 5     | 514   | 158   | 5     | 281.4 | 21.5   | 17.9   | 16     | 27.2    | 31.2    | 30.4   |
| Nd      | INAA   | 8 ppm       | 614.5 | 262   | 49.3  | 73.3  | 163   | 10.3   | 8.5    | 7.5    | 12.6    | 14      | 11.8   |
| Sm      | INAA   | 2 ppm       | 92.85 | 47.8  | 9.18  | 16.59 | 35.8  | 2.69   | 2.19   | 2.18   | 2.31    | 3.08    | 3.09   |
| Eu      | INAA   | 1.5 ppm     | 21.53 | 11.44 | 1.91  | 3.88  | 8.07  | 0.88   | 0.69   | 0.61   | 0.46    | 0.85    | 0.86   |
| Tb      | INAA   | 3 ppm       | 10.29 | 7.05  | 0.94  | 1.85  | 3.95  | 0.42   | 0.31   | 0.28   | 0.19    | 0.36    | 0.41   |
| Yb      | INAA   | 4 ppm       | 15.36 | 14.62 | 1.71  | 2.31  | 6.59  | 1.36   | 1.08   | 1.04   | 0.71    | 1.12    | 1.17   |
| Lu      | INAA   | 4 ppm       | 1.87  | 1.82  | 0.27  | 0.28  | 0.78  | 0.21   | 0.16   | 0.15   | 0.15    | 0.15    | 0.18   |
| Ba      | INAA   | 5 ppm       | 3     | 237   | 147   | 280   | 132.3 | 676    | 61     | 30     | 1314    |         | 1025   |
| Sr      | XRF    | 1 ppm       | 36.92 | 4     | 160   | 35.4  | 54.9  | 30     | 208    | 358    | 261     | 323     | 412    |
| Rb      | XRF    | 1 ppm       | 1.65  | 4     | 3     | 3.5   | 0.3   | 57.1   | 7      | 4      | 83      | 69.7    | 64     |
| Zr      | XRF    | 1 ppm       | 74.81 | 82.28 | 63.87 | 60.27 | 66.7  | 71.63  | 57.33  | 58.38  | 79.28   | 95.07   | 97.07  |
| Hf      | INAA   | 5 ppm       | 2.18  | 2.34  | 1.84  | 1.98  | 1.79  | 2.07   | 1.73   | 1.4    | 2.27    | 2.88    | 2.93   |
| Nb      | XRF    | 2 ppm       | 5.3   | 3.3   | 3.52  | 2.17  | 4.4   | 3.57   | 3.56   | 4.38   | 2.76    | 4.28    | 3.24   |
| Ta      | INAA   | 5 ppm       | 0.26  | 0.36  | 0.15  | 0.24  | 0.29  | 0.34   | 0.21   | 0.16   | 0.21    | 0.39    | 0.36   |
| U       | INAA   | 5 ppm       | 3.01  | 2.38  | 0.7   | 0.58  | 0.8   | 4.43   | 4.18   | 3.62   | 4.96    | 4.48    | 4.74   |
| Th      | INAA   | 5 ppm       | 4.3   | 3.79  | 6.09  | 4.12  | 1.47  | 5.35   | 4.98   | 4.33   | 2.47    | 3.38    | 5.72   |
| Cr      | INAA   | 5 ppm       | 1669  | 1010  | 816   | 5     | 1706  | 1107   | 1978.3 | 2071.2 | 1569.49 | 493.51  | 522.61 |
| Ni      | XRF    | 5 ppm       | 5     | 816   | 1443  | 1136  | 1015  | 449.5  | 926.3  | 955.13 | 416.72  | 183.4   | 184.42 |
| Cu      | XRF    | 5 ppm       | 11.49 | 18.79 | 32.39 | 9.65  | 3.3   | 7.24   | 0.95   | 16.07  | 31.98   | 22.97   | 11.07  |
| Pb      | XRF    | 4 ppm       | 16.42 | 12.1  | 27.18 | 14.5  | 4.6   | 17.29  | 45.99  | 36.63  | 15.2    | 20.08   | 6.11   |
| Zn      | XRF    | 3 ppm       | 131.3 | 91.5  | 101.5 | 93.65 | 96    | 50.8   | 59.23  | 63.94  | 73.63   | 69.47   | 57.03  |
| Ga      | XRF    | 3 ppm       | 38.39 | 33.64 | 38.95 | 35.08 | 11.4  | 65.04  | 1.13   | 65.83  | 10.67   | 66.43   | 67.16  |
| Sc      | INAA   | 1 ppm       | 25.7  | 22.1  | 20.6  | 31.7  | 23    | 17.2   | 19.12  | 17.87  | 26.38   | 17.46   | 17.53  |
| Y       | XRF    | 1 ppm       | 1     | 96.53 | 126.2 | 32.75 | 86.5  | 12.85  | 9.7    | 9.72   | 3.49    | 4.62    | 11.08  |
| V       | XRF    | 5 ppm       | 126.5 | 96.53 | 126.2 | 6     | 129.6 | 147.8  | 124.64 | 135.44 | 220.4   | 169     | 167.98 |
| Cs      | INAA   | 4 ppm       | 0.3   | 0.18  | 0.2   | 0.08  | 0.03  | 6.52   | 0.9    | 0.65   | 7.96    | 2.7     | 3.69   |

Data suspect +/-2

Appendix 3: Samples from Dachine French Guiana from Capdevila (2003)

| analyte                        | limit % | q9802396 | q9802398 | q9802401 | q9802403 | q9802388 | q9802389 | q980 2394 | q9706 267 | 101435 | 101437 |
|--------------------------------|---------|----------|----------|----------|----------|----------|----------|-----------|-----------|--------|--------|
| SiO <sub>2</sub>               | 0.8     | 47.25    | 44.69    | 46.75    | 42.49    | 45.49    | 45.34    | 43.19     | 48.22     | 46.26  | 43.94  |
| TiO <sub>2</sub>               | 0.09    | 0.32     | 0.36     | 0.31     | 0.41     | 0.36     | 0.48     | 0.46      | 0.62      | 0.55   | 0.55   |
| Al <sub>2</sub> O <sub>3</sub> | 0.3     | 5.09     | 4.82     | 5.26     | 6.48     | 5.74     | 7.20     | 6.77      | 7.24      | 6.14   | 6.54   |
| Fe <sub>2</sub> O <sub>3</sub> | 0.1     | 9.32     | 9.12     | 9.18     | 8.87     | 9.65     | 10.35    | 9.60      | 11.24     | 11.20  | 11.29  |
| MnO                            | 0.03    | 0.13     | 0.13     | 0.13     | 0.15     | 0.14     | 0.15     | 0.15      | 0.10      | 0.15   | 0.21   |
| MgO                            | 0.4     | 23.00    | 22.83    | 23.19    | 18.22    | 22.06    | 21.51    | 20.12     | 19.31     | 22.60  | 24.32  |
| CaO                            | 0.5     | 6.55     | 7.12     | 6.18     | 7.54     | 6.03     | 6.46     | 7.66      | 3.18      | 7.85   | 6.74   |
| Na <sub>2</sub> O              | 0.08    | 0.11     | 0.02     | 0.09     | 0.09     | 0.62     | 0.18     | 0.82      | 1.91      | 0.06   | 0.28   |
| K <sub>2</sub> O               | 0.05    | 0.03     | 0.22     | 0.09     | 0.08     | 0.05     | 0.35     | 0.21      | 0.03      | 0.03   | 0.03   |
| P <sub>2</sub> O <sub>5</sub>  | 0.2     | 0.28     | 0.27     | 0.29     | 0.27     | 0.24     | 0.32     | 0.32      | 0.22      | 0.19   | 0.17   |
| L.O.I.                         |         | 7.86     | 10.35    | 8.47     | 15.33    | 9.57     | 7.59     | 10.63     | 7.04      | 5.30   | 5.75   |
| Total                          |         | 99.94    | 99.93    | 99.94    | 99.93    | 99.95    | 99.93    | 99.93     | 99.11     | 100.33 | 99.82  |
| CO <sub>2</sub>                |         | 2.76     | 5.38     | 3.30     | 10.67    | 4.23     | 0.04     | 5.65      | 2.90      | 0.04   | 0.50   |
| LOI-CO <sub>2</sub>            |         | 5.10     | 4.97     | 5.17     | 4.66     | 5.34     | 7.55     | 4.98      | 4.14      | 5.26   | 5.25   |
| limit ppm                      |         |          |          |          |          |          |          |           |           |        |        |
| As                             | 0.23    | 1.00     | 1.36     | 2.84     | 2.97     | 4.24     | 1.68     | 4.00      | 58.95     | 2.28   | 95.74  |
| Ba                             | 5       | 6        | 231      | 19       | 115      | 58       | 16       | 36        | 11        | 49     | 238    |
| Be                             | 0.9     | 0.6      | 0.4      | 0.0      | 0.6      | 0.1      | 0.1      | 0.1       | 0.7       | 0.5    | 1.2    |
| Bi                             | 0.05    | 0.06     | 0.05     | 0.01     | 0.00     | 0.04     | 0.04     | 0.02      | 0.05      | 0.13   | 0.45   |
| Cd                             | 0.15    | 2.8      | 1.6      | 2.0      | 2.7      | 1.5      | 1.7      | 2.5       | 0.2       | 0.2    | 0.2    |
| Ce                             | 0.05    | 5.83     | 5.98     | 6.10     | 12.32    | 6.30     | 6.71     | 7.06      | 16.78     | 16.24  | 9.01   |
| Co                             | 0.3     | 74.8     | 72.8     | 69.1     | 59.2     | 72.8     | 73.5     | 68.1      | 79.3      | 64.2   | 88.1   |
| Cr                             | 5       | 2330     | 1726     | 2171     | 1569     | 2254     | 2302     | 2010      | 1753      | 2094   | 1878   |
| Cs                             | 0.1     | 0.3      | 0.4      | 0.5      | 0.5      | 0.6      | 2.4      | 0.5       | 0.4       | 0.1    | 0.1    |
| Cu                             | 5       | 69       | 90       | 63       | 68       | 65       | 95       | 80        | 75        | 71     | 59     |
| Dy                             | 0.03    | 1.00     | 1.28     | 1.08     | 1.41     | 1.16     | 1.49     | 1.59      | 1.94      | 2.30   | 1.67   |
| Er                             | 0.02    | 0.58     | 0.70     | 0.64     | 0.77     | 0.68     | 0.92     | 0.89      | 1.19      | 1.30   | 1.09   |
| Eu                             | 0.02    | 0.28     | 0.42     | 0.35     | 0.50     | 0.42     | 0.48     | 0.43      | 0.65      | 0.66   | 0.44   |
| Ga                             | 0.13    | 6.4      | 6.5      | 6.3      | 7.9      | 7.7      | 8.5      | 8.2       | 10.4      | 8.2    | 8.6    |
| Gd                             | 0.07    | 0.99     | 1.21     | 1.12     | 1.41     | 1.21     | 1.45     | 1.43      | 2.30      | 2.63   | 1.97   |
| Ge                             | 0.08    | 1.42     | 0.95     | 0.92     | 0.98     | 1.56     | 1.24     | 1.21      | 1.19      | 1.78   | 1.61   |
| Hf                             | 0.04    | 0.43     | 0.63     | 0.50     | 0.82     | 0.59     | 0.69     | 0.74      | 1.30      | 0.95   | 0.88   |
| Ho                             | 0.01    | 0.19     | 0.24     | 0.22     | 0.27     | 0.27     | 0.34     | 0.32      | 0.41      | 0.45   | 0.41   |
| In                             | 0.09    | 0.08     | 0.05     | 0.04     | 0.04     | 0.08     | 0.07     | 0.09      | 0.09      | 0.05   | 0.05   |
| La                             | 0.05    | 2.46     | 2.32     | 2.59     | 6.10     | 2.63     | 3.40     | 3.14      | 7.45      | 8.73   | 3.92   |
| Lu                             | 0.01    | 0.11     | 0.11     | 0.10     | 0.14     | 0.13     | 0.16     | 0.15      | 0.18      | 0.20   | 0.17   |
| Mo                             | 0.15    | 0.2      | 0.3      | 0.2      | 0.2      | 0.1      | 0.2      | 0.2       | 0.4       | 0.2    | 0.5    |
| Nb                             | 0.05    | 0.83     | 1.26     | 0.88     | 1.36     | 1.06     | 1.25     | 1.25      | 3.57      | 1.66   | 1.67   |
| Nd                             | 0.15    | 3.9      | 4.4      | 4.2      | 6.1      | 4.3      | 4.7      | 4.9       | 9.9       | 11.2   | 5.7    |
| Ni                             | 8       | 851      | 932      | 828      | 609      | 831      | 921      | 758       | 767       | 853    | 1023   |
| Pb                             | 0.60    | 3.6      | 4.8      | 2.1      | 5.0      | 2.8      | 1.5      | 3.8       | 1.6       | 2.0    | 0.5    |
| Pr                             | 0.02    | 0.82     | 0.89     | 0.79     | 1.42     | 0.88     | 1.03     | 1.05      | 2.13      | 2.42   | 1.28   |
| Rb                             | 0.8     | 2.3      | 7.3      | 5.1      | 4.0      | 3.2      | 15.4     | 5.9       | 0.8       | 0.3    | 0.3    |
| Sb                             | 0.1     | 0.6      | 0.5      | 0.8      | 0.8      | 0.9      | 0.8      | 0.5       | 0.3       | 0.2    | 0.7    |

|    |      |      |      |      |      |      |       |      |       |       |       |
|----|------|------|------|------|------|------|-------|------|-------|-------|-------|
| Sm | 0.06 | 1.08 | 1.14 | 1.18 | 1.56 | 1.05 | 1.36  | 1.40 | 2.22  | 2.51  | 1.75  |
| Sn | 0.3  | 0.4  | 0.7  | 0.7  | 0.7  | 0.6  | 0.5   | 0.7  | 1.7   | 0.3   | 1.0   |
| Sr | 4    | 156  | 375  | 125  | 423  | 241  | 81    | 425  | 185   | 41    | 112   |
| Ta | 0.01 | 0.06 | 0.08 | 0.06 | 0.10 | 0.08 | 0.08  | 0.10 | 0.24  | 0.12  | 0.14  |
| Tb | 0.01 | 0.15 | 0.19 | 0.18 | 0.23 | 0.19 | 0.23  | 0.22 | 0.35  | 0.44  | 0.28  |
| Th | 0.05 | 0.29 | 0.28 | 0.24 | 0.57 | 0.01 | 0.30  | 0.38 | 0.66  | 0.41  | 0.34  |
| Tm | 0.01 | 0.09 | 0.10 | 0.09 | 0.13 | 0.12 | 0.14  | 0.15 | 0.16  | 0.17  | 0.15  |
| U  | 0.05 | 0.16 | 0.16 | 0.14 | 0.23 | 0.14 | 0.12  | 0.19 | 0.25  | 0.15  | 0.17  |
| V  | 1.5  | 125  | 128  | 137  | 145  | 140  | 171   | 160  | 195   | 160   | 159   |
| W  | 0.1  | 0.3  | 0.3  | 0.3  | 2.8  | 0.2  | 0.1   | 1.8  | 0.7   | 0.2   | 0.5   |
| Y  | 0.05 | 6.26 | 7.29 | 7.10 | 8.20 | 7.80 | 10.73 | 9.79 | 12.09 | 14.90 | 10.85 |
| Yb | 0.03 | 0.59 | 0.68 | 0.66 | 0.79 | 0.72 | 1.06  | 0.93 | 1.10  | 1.22  | 1.08  |
| Zn | 4    | 82   | 71   | 72   | 78   | 83   | 90    | 81   | 86    | 84    | 87    |
| Zr | 0.5  | 16.8 | 22.1 | 19.6 | 31.0 | 23.3 | 27.0  | 28.2 | 50.2  | 33.1  | 33.4  |



**Sample #: G-2**

**Diamond bearing: Yes**

Location: (latitude/ longitude West of Greenwich)

05° 01' 17" N

000° 47' 23" W

(Ghana National map units used in this work)

x = 974.5 y = 473.8

Approximate depth of sample: 10 meters

Description: Breccia with clasts up to 1 cm. Extremely weathered and ferruginised to variegated clays. (Colors from "Munsell" color chart for soils). Brick red (2.5YR4/4), light brown (10YR6/8), white (2.5Y8/3) yellow (10YR8/6) and gray (2.5Y7/6 and 2.5Y3/1) in color. White patches may be relic feldspar phenocrysts.

Grey patches are clasts of phyllite. (See photos #'s      ).

Diamond bearing confirmed by observing processing from start to finish resulting in observable diamonds.

**Sample #: G-3**

**Diamond bearing: Yes**

Location: (latitude/ longitude West of Greenwich)

06° 01' 17" N

000° 47' 49" W

(Ghana National map units used in this work)

x = 968.9 y = 473.8

Approximate depth of sample: 3 meters

Description: Breccia with clasts up to 2 cm. Extremely weathered and ferruginised to variegated clays. (Colors from "Munsell" color chart for soils. Yellow (2.5Y7/8) brown (10 YR3/2) white (2.5Y8/1), and gray (2.5Y7/6 and 2.5Y3/1) in color. Grey patches are clasts of phyllite.

Diamond bearing confirmed by historical investigations by CAST geologists and observing processing from start to finish resulting in observable diamonds.

**Sample #: G-4**

**Diamond bearing: Yes**

Location: (latitude/ longitude West of Greenwich)

05° 59' 59" N

000° 48' 46" W

(Ghana National map units used in this work)

x = 974.5 y = 483.2

Approximate depth of sample: 1.5 meters

Description: Breccia with clasts up to 2mm. Extremely weathered and ferruginised. Looks like weathered basalt from other parts of Ghana. White phyllo silicates obvious. (Colors from "Munsell" color chart for soils. Brownish reds (7.5YR5/6), white (7.5YR3/4), (2.5Y8/1) and silver gray (10YR8/1) in color. Silver gray is phyllo silicate.

Diamond bearing confirmed by observing processing from start to finish resulting in observable diamonds.



**Sample #: G-9**

**Diamond bearing: Yes**

Location: (latitude/ longitude West of Greenwich)

05<sup>0</sup> 57' 23" N

000<sup>0</sup> 48' 54" W

(Ghana National map units used in this work)

x = 967.1 y = 466.6

Approximate depth of sample: 6 meters.

Description: Breccia with clasts to 1cm. extremely weathered and ferruginised. Looks like weathered basalt from other parts of Ghana. White phyllo silicates visible. (Colors from "Munsell" color chart for soils.) Brick red (2.5YR3/6), light brown (10YR5/8), brown gray (10 YR6/3) and whitish (10YR8/2) in color. Diamond bearing confirmed by (Kaminsky et al.1996).

**Sample #: G-12 (same as G-3 except depth)**

**Diamond bearing: Yes**

Location: (latitude/ longitude West of Greenwich)

06° 01' 17" N

000° 47' 49" W

(Ghana National map units used in this work)

x = 974.5 y = 490.5

Approximate depth of sample: 15 meters

Description: Breccia with clasts up to 2 cm. extremely weathered and ferruginised.

(Colors from "Munsell" color chart for soils.) Yellow (2.5Y7/8) brown (10 YR3/2) white (2.5Y8/1), and gray (2.5Y7/6 and 2.5Y3/1) in color. Grey patches are clasts of phyllite.

Diamond bearing confirmed by historical investigations by CAST geologists and observing processing from start to finish resulting in observable diamonds.

**Sample #: DM-2**

**Diamond bearing: Yes**

Location: (latitude/ longitude West of Greenwich)

06<sup>0</sup> 01' 32" N

000<sup>0</sup> 47' 03" W

(Ghana National map units used in this work)

x = 977.9 y = 492.5

Approximate depth of sample: 8 meters

Description: Breccia with clasts up to 3cm extremely weathered and ferruginised. (Colors from "Munsell" color chart for soils.) Browns (7.5YR7/3), (7.5YR7/4), (7.5YR4/6), flecks of gray black (5Y5/1) 1 cm patches of granoblastic quartz (2.5Y7/1).

Diamond bearing confirmed by visible diamond in sample.



**Sample #: G-5**

**Diamond bearing: No**

Location: (latitude/ longitude West of Greenwich)

05<sup>0</sup> 58' 53" N

000<sup>0</sup> 47' 55" W

(Ghana National map units used in this work)

x = 973.23 y = 476.23

Approximate depth of sample: 2 meters

Description: Actinolite, tremolite chlorite, talc, schist moderately weathered slightly ferruginised. Some phyllo silicates visible, dense, powdery. (Colors from "Munsell" color chart for soils.) Gray green (5GY7/1) brown (7.5YR5/6) pinkish white flecks (7.5YR8/3).

**Sample #: G-10, 11 (duplicates)**

**Diamond bearing: No**

Location: (latitude/ longitude West of Greenwich)

05° 57' 23" N

000° 48' 54" W

(Ghana National map units used in this work)

x = 967.1 y = 466.6

Approximate depth of sample: 6 meters.

Description: Actinolite, tremolite chlorite, talc, schist moderately weathered slightly ferruginised. Hard and dense least weathered sample reported here. Some phyllo silicates visible. (Colors from "Munsell" color chart for soils.) Gray green (5GY7/1) brown (7.5YR5/6), white flecks (5Y8/2) graphite-like flecks (5Y3/1).

**Sample #: G-1**

**Diamond bearing: No**

Location: (latitude/ longitude West of Greenwich)

06° 01' 17" N

000° 47' 49" W

(Ghana National map units used in this work)

x = 974.5 y = 490.5

Approximate depth of sample: 1 meter.

Description: Weathered phyllite? Extremely weathered and ferruginised. (Colors from "Munsell" color chart for soils.) Tan (10YR7/4) 1mm brick red spots(10R3/6).

**Field site: Beduwara Hill.**

Location: (latitude/ longitude West of Greenwich)

06° 01' 17" N

000° 47' 49" W

(Ghana National map units used in this work)

x = 974.5 y = 490.5

**Samples: G-1, G-3 and 12.**

This is the site of systematic sampling by CAST geologists. A large exploration trench dug by CAST geologists dominates the area, with numerous smaller trenches dug by small-scale miners. The total exposed area is 1.5 km long by .5 km wide. The general strike of the ore body, bedding and schistosity is 201 degrees the dip is vertical.

Trenching reaches 15 meters below present surface and at least 1-4 meters of overburden has been removed over the exposed area.

All exposed lithologies at this sight are severely weathered and ferruginised. Observable lithologies include; actinolite-tremolite-chlorite-talc schist, phyllite (fine grained pelitic schist), various fine to medium grained meta-sediments and the diamondiferous breccia. The diamondiferous breccia exhibits clasts up to 18 cm. at this location. Small-scale miners routinely walk the area and gather diamonds exposed by rain. Trenching by hand and light machinery continues. Discontinuous trenching by small-scale miners results in an anastomosing pattern of trenches reflecting the structural relationship between the diamondiferous breccia and the adjacent, barren lithologies.



**Field site: Diamond in matrix.**

Location: (latitude/ longitude West of Greenwich)

06° 01' 32" N

000° 47' 03" W

(Ghana National map units used in this work)

x = 977.9 y = 492.5

***Samples: Dm-2.***

This is the site of sample DM-2 containing a diamond in matrix. Small-scale miners are digging trenches the largest being 300 meters long by 10 meters wide by 10 meters deep. Exposing a diamondiferous body of unknown dimensions. The strike of the body is 210 degrees and dip of schistosity is vertical. All exposed lithologies at this sight are severely weathered and ferruginised. Observable lithologies include; actinolite-tremolite-chlorite-talc schist, phyllite (fine grained pelitic schist), quartz veins and the diamondiferous breccia. The diamondiferous material is a breccia with clasts of at least 18 cm. Poor exposure and slumping obscure the relationship between the diamondiferous material and adjacent barren material though their trenches are sub-parallel form an anastomosing pattern.

**Field site: Sandy Creek.**

Location: (latitude/ longitude West of Greenwich)

05° 59' 59" N

000° 48' 46" W

(Ghana National map units used in this work)

x = 974.5 y = 483.2

***Samples: G-4.***

Approximately 1 square kilometer of over burden has been stripped from this area. Most of the surface is covered in hard laterite with numerous pits and trenches dug by small-scale miners. The trench in diamondiferous material sampled is adjacent and parallel to a sheared quartz vein striking 260 degrees with a dip of 85 degrees following a diamondiferous body with the same strike and dip. The depth of the trench is 3 meters below the present surface. All exposed lithologies at this site are severely weathered and ferruginised. Observable lithologies include; actinolite-tremolite-chlorite-talc schist, phyllite (fine grained pelitic schist), quartz veins and the diamondiferous breccia. The diamondiferous rock displays a brecciated texture though clasts are smaller in the sample gathered here (2mm) than at the other sites. The small-scale diamond workings here are comparatively shallow, and are sub-parallel though less so than other sites. Quartz veining is more numerous here than other sites. Little structure is visible as the pits and trenches tend to be smaller at this site.

**Field site: KMD trench.**

Location: (latitude/ longitude West of Greenwich)

05° 57' 23" N

000° 48' 54" W

(Ghana National map units used in this work)

x = 967.1 y = 466.6

**Samples: G-9, G-10 and G-11.**

This is the site of an exploration trench dug by KMD (Kaminsky, 1996). The trench is approximately 6 meters deep and 2 meters wide. Observable lithologies include; actinolite-tremolite-chlorite-talc schist and the diamondiferous breccia. Diamond bearing rock is in sharp contact with the actinolite schist. The diamond bearing rock at this sight is severely weathered and ferruginised but the actinolite schist is the least weathered of the other sites visited. The site has been recently exploited for the diamond bearing material. Random trenching and pitting has disturbed the area obscuring structural relationships. The diamondiferous breccia sample from this site displays small clasts (1cm), though the more recently exposed lithologies are highly brecciated with clasts up to 15 cm.



**Field site: Kokotitin.**

Location: (latitude/ longitude West of Greenwich)

05° 01' 17" N

000° 47' 23" W

(Ghana National map units used in this work)

x = 974.5 y = 473.8

***Samples: G-2.***

This is the site of the deepest trench dug by small-scale miners approximately 35 meters deep by 20 meters wide. Approximately 1 square km of overburden has been striped off here much of the area is covered with hard laterite. Observable lithologies include; phyllite (fine grained pelitic schist) and the diamondiferous breccia. Diamond bearing rock is in sharp contact with the phyllite. Diamondiferous breccia displays clasts up to 18 cm. The general strike of the ore body is 210 degrees and vertical dip. Diamonds up to 1.5 carats have been reported from this location.

**Field site: Slime dam road**

Location: (latitude/ longitude West of Greenwich)

05° 58' 53" N

000° 47' 55" W

(Ghana National map units used in this work)

x = 973.23 y = 476.23

***Samples: G-5***

Approximately ½ km of overburden has been stripped from this area. Observable lithologies include; phyllite (fine grained pelitic schist) and the actinolite schist. A road cut at the site exposes a vertical contact between the actinolite schist and the diamond bearing rock. The narrow (.35 meters) "dike-like" structure strikes approximately 250 degrees with a vertical dip.

Appendix 6: Statistical reports generated by "Surfer" for image maps.

Data Filter Report

Source Data File Name: e:\maya\Desktop\awatia nov 1\all1.xlslast.xls  
 X Column: A  
 Y Column: B  
 Z Column: C

Data Counts

Number of Active Data: 7673  
 Number of Original Data: 12639  
 Number of Excluded Data: 0  
 Number of Deleted Duplicates: 4966  
 Number of Retained Duplicates: 2979  
 Number of Artificial Data: 0

Filter Rules

Duplicate Points to Keep: First  
 X Duplicate Tolerance: 0  
 Y Duplicate Tolerance: 0  
 Exclusion Filter String: Not In Use

Duplicate Data

| X       | Y        | Z    | ID  | Status |
|---------|----------|------|-----|--------|
| 961.381 | 473      | 0.9  | 71  |        |
|         | Retained |      |     |        |
| 961.381 | 473      | 0.9  | 72  |        |
|         | Deleted  |      |     |        |
| 961.692 | 473.795  | 0.77 | 116 |        |
|         | Retained |      |     |        |
| 961.692 | 473.795  | 0.77 | 117 |        |
|         | Deleted  |      |     |        |
| 962     | 471      | 0.54 | 151 |        |
|         | Retained |      |     |        |
| 962     | 471      | 0.73 | 153 |        |
|         | Deleted  |      |     |        |
| 962.804 | 470      | 1    | 258 |        |
|         | Retained |      |     |        |
| 962.804 | 470      | 1.06 | 259 |        |
|         | Deleted  |      |     |        |
| 963     | 470      | 0.2  | 284 |        |
|         | Retained |      |     |        |
| 963     | 470      | 0.2  | 285 |        |
|         | Deleted  |      |     |        |



|     |          |      |     |
|-----|----------|------|-----|
| 965 | 470      | 0.09 | 714 |
|     | Retained |      |     |
| 965 | 470      | 0.14 | 730 |
|     | Deleted  |      |     |
| 965 | 470      | 1.27 | 824 |
|     | Deleted  |      |     |
| 965 | 470.197  | 0.03 | 677 |
|     | Retained |      |     |
| 965 | 470.197  | 1.25 | 821 |
|     | Deleted  |      |     |
| 965 | 470.197  | 1.25 | 822 |
|     | Deleted  |      |     |
| 965 | 470.4    | 0.02 | 670 |
|     | Retained |      |     |
| 965 | 470.4    | 0.32 | 782 |
|     | Deleted  |      |     |
| 965 | 470.4    | 0.32 | 783 |
|     | Deleted  |      |     |
| 965 | 470.607  | 0.06 | 702 |
|     | Retained |      |     |
| 965 | 470.607  | 0.06 | 703 |
|     | Deleted  |      |     |
| 965 | 470.607  | 0.84 | 815 |
|     | Deleted  |      |     |
| 965 | 470.79   | 0.21 | 760 |
|     | Retained |      |     |
| 965 | 470.79   | 0.41 | 798 |
|     | Deleted  |      |     |
| 965 | 475      | 0.03 | 678 |
|     | Retained |      |     |
| 965 | 475      | 0.03 | 679 |
|     | Deleted  |      |     |
| 965 | 475      | 0.03 | 680 |
|     | Deleted  |      |     |
| 965 | 475      | 0.08 | 710 |
|     | Deleted  |      |     |
| 965 | 475.609  | 0    | 631 |
|     | Retained |      |     |
| 965 | 475.609  | 0    | 632 |
|     | Deleted  |      |     |
| 965 | 475.609  | 0.35 | 791 |
|     | Deleted  |      |     |
| 965 | 475.609  | 0.35 | 792 |
|     | Deleted  |      |     |
| 965 | 475.609  | 1.54 | 827 |
|     | Deleted  |      |     |
| 965 | 475.609  | 1.54 | 828 |
|     | Deleted  |      |     |
| 965 | 476      | 0.04 | 684 |
|     | Retained |      |     |
| 965 | 476      | 0.04 | 685 |
|     | Deleted  |      |     |
| 965 | 476      | 0.32 | 784 |
|     | Deleted  |      |     |
| 965 | 476      | 0.32 | 785 |

|     |                     |      |     |
|-----|---------------------|------|-----|
|     | Deleted             |      |     |
| 965 | 476.204<br>Retained | 0.08 | 711 |
| 965 | 476.204<br>Deleted  | 0.08 | 712 |
| 965 | 476.204<br>Deleted  | 2.08 | 835 |
| 965 | 476.204<br>Deleted  | 2.08 | 836 |
| 965 | 476.402<br>Retained | 0.04 | 686 |
| 965 | 476.402<br>Deleted  | 0.04 | 687 |
| 965 | 476.402<br>Deleted  | 0.09 | 715 |
| 965 | 476.402<br>Deleted  | 0.09 | 716 |
| 965 | 476.498<br>Retained | 0    | 633 |
| 965 | 476.498<br>Deleted  | 0    | 634 |
| 965 | 476.498<br>Deleted  | 0.01 | 659 |
| 965 | 476.498<br>Deleted  | 0.01 | 660 |
| 965 | 476.609<br>Retained | 0.2  | 753 |
| 965 | 476.609<br>Deleted  | 0.2  | 754 |
| 965 | 476.609<br>Deleted  | 0.46 | 801 |
| 965 | 476.609<br>Deleted  | 0.46 | 802 |
| 965 | 477<br>Retained     | 0.01 | 661 |
| 965 | 477<br>Deleted      | 0.01 | 662 |
| 965 | 477<br>Deleted      | 0.14 | 731 |
| 965 | 477<br>Deleted      | 0.14 | 732 |
| 965 | 477.204<br>Retained | 0    | 635 |
| 965 | 477.204<br>Deleted  | 0    | 636 |
| 965 | 477.204<br>Deleted  | 0.05 | 691 |
| 965 | 477.204<br>Deleted  | 0.05 | 692 |
| 965 | 477.204<br>Deleted  | 0.34 | 789 |
| 965 | 477.204<br>Deleted  | 0.34 | 790 |
| 965 | 477.406<br>Retained | 0    | 637 |
| 965 | 477.406             | 0    | 638 |

|     |                               |      |     |
|-----|-------------------------------|------|-----|
| 965 | Deleted<br>477.406            | 0.17 | 742 |
| 965 | Deleted<br>477.406<br>Deleted | 0.17 | 743 |
| 965 | 477.612<br>Retained           | 0.19 | 749 |
| 965 | 477.612<br>Deleted            | 0.19 | 750 |
| 965 | 477.812<br>Retained           | 0.07 | 708 |
| 965 | 477.812<br>Deleted            | 0.07 | 709 |
| 965 | 478<br>Retained               | 0.01 | 663 |
| 965 | 478<br>Deleted                | 0.01 | 664 |
| 965 | 478<br>Deleted                | 1.7  | 831 |
| 965 | 478<br>Deleted                | 1.7  | 832 |
| 965 | 478.197<br>Retained           | 0.01 | 665 |
| 965 | 478.197<br>Deleted            | 0.01 | 666 |
| 965 | 478.197<br>Deleted            | 0.18 | 745 |
| 965 | 478.197<br>Deleted            | 0.18 | 746 |
| 965 | 478.402<br>Retained           | 0    | 639 |
| 965 | 478.402<br>Deleted            | 0    | 640 |
| 965 | 478.402<br>Deleted            | 0.95 | 818 |
| 965 | 478.402<br>Deleted            | 0.95 | 819 |
| 965 | 478.604<br>Retained           | 0.32 | 786 |
| 965 | 478.604<br>Deleted            | 0.32 | 787 |
| 965 | 478.604<br>Deleted            | 0.32 | 788 |
| 965 | 478.803<br>Retained           | 0.03 | 681 |
| 965 | 478.803<br>Deleted            | 0.03 | 682 |
| 965 | 478.803<br>Deleted            | 0.15 | 735 |
| 965 | 478.803<br>Deleted            | 0.15 | 736 |
| 965 | 479<br>Retained               | 0    | 641 |
| 965 | 479<br>Deleted                | 0    | 642 |



|          |                     |      |     |
|----------|---------------------|------|-----|
| 965      | 479<br>Deleted      | 0.05 | 693 |
| 965      | 479<br>Deleted      | 0.05 | 694 |
| 965      | 479.199<br>Retained | 0.02 | 671 |
| 965      | 479.199<br>Deleted  | 0.02 | 672 |
| 965      | 479.199<br>Deleted  | 1.3  | 825 |
| 965      | 479.199<br>Deleted  | 1.3  | 826 |
| 965      | 479.404<br>Retained | 0.38 | 795 |
| More ... |                     |      |     |

---

#### Data Statistics Report

##### Data Counts

|                                |       |
|--------------------------------|-------|
| Number of Active Data:         | 7673  |
| Number of Original Data:       | 12639 |
| Number of Excluded Data:       | 0     |
| Number of Deleted Duplicates:  | 4966  |
| Number of Retained Duplicates: | 2979  |
| Number of Artificial Data:     | 0     |

##### X Variable Statistics

|                       |         |
|-----------------------|---------|
| X Range:              | 20.718  |
| X Midrange:           | 969.641 |
| X Minimum:            | 959.282 |
| X 25%-tile:           | 967     |
| X Median:             | 970.6   |
| X 75%-tile:           | 973.809 |
| X Maximum:            | 980     |
| X Average:            | 970.551 |
| X Standard Deviation: | 4.39572 |
| X Variance:           | 19.3224 |

##### Y Variable Statistics

|             |         |
|-------------|---------|
| Y Range:    | 34.821  |
| Y Midrange: | 482.589 |
| Y Minimum:  | 465.179 |
| Y 25%-tile: | 473     |
| Y Median:   | 485.796 |
| Y 75%-tile: | 492.802 |
| Y Maximum:  | 500     |
| Y Average:  | 483.611 |

Y Standard Deviation: 10.5569  
Y Variance: 111.449

#### Z Variable Statistics

Z Range: 12.8  
Z Midrange: 6.4  
  
Z Minimum: 0  
Z 25%-tile: 0.03  
Z Median: 0.13  
Z 75%-tile: 0.39  
Z Maximum: 12.8  
  
Z Average: 0.342238  
Z Standard Deviation: 0.603841  
Z Variance: 0.364624  
  
Z Coef. of Variation: 1.76439  
Z Coef. of Skewness: 4.91776

#### Inter-Variable Correlation

|    | X | Y        | Z           |
|----|---|----------|-------------|
| X: | 1 | 0.361533 | -0.0347975  |
| Y: |   | 1        | -0.00419199 |
| Z: |   |          | 1           |

#### Inter-Variable Covariance

|    | X       | Y       | Z          |
|----|---------|---------|------------|
| X: | 19.3224 | 16.777  | -0.0923636 |
| Y: |         | 111.449 | -0.0267227 |
| Z: |         |         | 0.364624   |

#### Gridding Report

##### Search Rules

Use All Data: true

##### Gridding Rules

Gridding Method: Natural Neighbor  
Anisotropy Ratio: 1  
Anisotropy Angle: 0

##### Grid Summary

|                          |   |
|--------------------------|---|
| Grid File Name:          | e:\maya\Desktop\awatia nov 1\bedrock grade for thesis.grd |
| Minimum X:               | 959.282   |
| Maximum X:               | 980   |
| Minimum Y:               | 465.179   |
| Maximum Y:               | 500   |
| Minimum Z:               | 0   |
| Maximum Z:               | 6.84612   |
| Number of Rows:          | 200   |
| Number of Columns:       | 120   |
| Number of Filled Nodes:  | 17919   |
| Number of Blanked Nodes: | 6081  |
| Total Number of Nodes:   | 24000   |



## Statistical report for "Surfer" B1 horizon image map

### Data Filter Report

Source Data File Name: e:\maya\Desktop\awatia nov 1\all1.xlslast.xls  
 X Column: A  
 Y Column: B  
 Z Column: C

### Data Counts

Number of Active Data: 6616  
 Number of Original Data: 10680  
 Number of Excluded Data: 0  
 Number of Deleted Duplicates: 4064  
 Number of Retained Duplicates: 2612  
 Number of Artificial Data: 0

### Filter Rules

Duplicate Points to Keep: First  
 X Duplicate Tolerance: 0  
 Y Duplicate Tolerance: 0  
 Exclusion Filter String: Not In Use

### Duplicate Data

| X       | Y        | Z    | ID  | Status |
|---------|----------|------|-----|--------|
| 962.804 | 470      | 0.05 | 180 |        |
|         | Retained |      |     |        |
| 962.804 | 470      | 0.05 | 181 |        |
|         | Deleted  |      |     |        |
| 965     | 470      | 0.53 | 659 |        |
|         | Retained |      |     |        |
| 965     | 470      | 2.26 | 756 |        |
|         | Deleted  |      |     |        |
| 965     | 470      | 4.59 | 766 |        |
|         | Deleted  |      |     |        |
| 965     | 470.197  | 0.96 | 687 |        |
|         | Retained |      |     |        |
| 965     | 470.197  | 0.96 | 688 |        |
|         | Deleted  |      |     |        |
| 965     | 470.197  | 2.83 | 762 |        |
|         | Deleted  |      |     |        |
| 965     | 470.4    | 0.51 | 657 |        |
|         | Retained |      |     |        |
| 965     | 470.4    | 0.51 | 658 |        |
|         | Deleted  |      |     |        |

|     |                     |       |     |
|-----|---------------------|-------|-----|
| 965 | 470.607<br>Retained | 1.68  | 739 |
| 965 | 470.607<br>Deleted  | 1.68  | 740 |
| 965 | 470.607<br>Deleted  | 2.08  | 747 |
| 965 | 475<br>Retained     | 0.12  | 603 |
| 965 | 475<br>Deleted      | 0.12  | 604 |
| 965 | 475<br>Deleted      | 0.12  | 605 |
| 965 | 475<br>Deleted      | 0.18  | 608 |
| 965 | 475.609<br>Retained | 0.03  | 586 |
| 965 | 475.609<br>Deleted  | 0.03  | 587 |
| 965 | 475.609<br>Deleted  | 0.41  | 640 |
| 965 | 475.609<br>Deleted  | 0.41  | 641 |
| 965 | 475.609<br>Deleted  | 1.451 | 734 |
| 965 | 475.609<br>Deleted  | 1.451 | 735 |
| 965 | 476<br>Retained     | 0.33  | 628 |
| 965 | 476<br>Deleted      | 0.33  | 629 |
| 965 | 476<br>Deleted      | 2.18  | 752 |
| 965 | 476<br>Deleted      | 2.18  | 753 |
| 965 | 476.204<br>Retained | 0.54  | 664 |
| 965 | 476.204<br>Deleted  | 0.54  | 665 |
| 965 | 476.204<br>Deleted  | 3.46  | 764 |
| 965 | 476.204<br>Deleted  | 3.46  | 765 |
| 965 | 476.402<br>Retained | 1.18  | 714 |
| 965 | 476.402<br>Deleted  | 1.18  | 715 |
| 965 | 476.498<br>Retained | 0.21  | 612 |
| 965 | 476.498<br>Deleted  | 0.21  | 613 |
| 965 | 476.498<br>Deleted  | 1     | 698 |
| 965 | 476.498<br>Deleted  | 1     | 699 |
| 965 | 476.609             | 0.3   | 619 |

|     |                     |      |     |
|-----|---------------------|------|-----|
| 965 | Retained<br>476.609 | 0.3  | 620 |
|     | Deleted             |      |     |
| 965 | 476.609             | 0.31 | 624 |
|     | Deleted             |      |     |
| 965 | 476.609             | 0.31 | 625 |
|     | Deleted             |      |     |
| 965 | 477                 | 0.12 | 606 |
|     | Retained            |      |     |
| 965 | 477                 | 0.12 | 607 |
|     | Deleted             |      |     |
| 965 | 477                 | 0.23 | 614 |
|     | Deleted             |      |     |
| 965 | 477                 | 0.23 | 615 |
|     | Deleted             |      |     |
| 965 | 477.204             | 0.4  | 637 |
|     | Retained            |      |     |
| 965 | 477.204             | 0.4  | 638 |
|     | Deleted             |      |     |
| 965 | 477.204             | 0.42 | 643 |
|     | Deleted             |      |     |
| 965 | 477.204             | 0.42 | 644 |
|     | Deleted             |      |     |
| 965 | 477.204             | 1.11 | 706 |
|     | Deleted             |      |     |
| 965 | 477.204             | 1.11 | 707 |
|     | Deleted             |      |     |
| 965 | 477.406             | 0.44 | 646 |
|     | Retained            |      |     |
| 965 | 477.406             | 0.44 | 647 |
|     | Deleted             |      |     |
| 965 | 477.612             | 0.01 | 580 |
|     | Retained            |      |     |
| 965 | 477.612             | 0.01 | 581 |
|     | Deleted             |      |     |
| 965 | 477.612             | 0.3  | 621 |
|     | Deleted             |      |     |
| 965 | 477.612             | 0.3  | 622 |
|     | Deleted             |      |     |
| 965 | 477.812             | 0.01 | 582 |
|     | Retained            |      |     |
| 965 | 477.812             | 0.01 | 583 |
|     | Deleted             |      |     |
| 965 | 477.812             | 0.73 | 677 |
|     | Deleted             |      |     |
| 965 | 477.812             | 0.73 | 678 |
|     | Deleted             |      |     |
| 965 | 478                 | 0.48 | 653 |
|     | Retained            |      |     |
| 965 | 478                 | 0.48 | 654 |
|     | Deleted             |      |     |
| 965 | 478                 | 2.59 | 760 |
|     | Deleted             |      |     |
| 965 | 478                 | 2.59 | 761 |
|     | Deleted             |      |     |
| 965 | 478.197             | 0.67 | 671 |



|     |                                |      |     |
|-----|--------------------------------|------|-----|
| 965 | Retained<br>478.197<br>Deleted | 0.67 | 672 |
| 965 | 478.402<br>Retained            | 0.96 | 689 |
| 965 | 478.402<br>Deleted             | 0.96 | 690 |
| 965 | 478.402<br>Deleted             | 1.19 | 718 |
| 965 | 478.402<br>Deleted             | 1.19 | 719 |
| 965 | 478.604<br>Retained            | 0.05 | 590 |
| 965 | 478.604<br>Deleted             | 0.05 | 591 |
| 965 | 478.803<br>Retained            | 0.45 | 649 |
| 965 | 478.803<br>Deleted             | 0.45 | 650 |
| 965 | 478.803<br>Deleted             | 2.22 | 754 |
| 965 | 478.803<br>Deleted             | 2.22 | 755 |
| 965 | 479<br>Retained                | 1.37 | 731 |
| 965 | 479<br>Deleted                 | 1.37 | 732 |
| 965 | 479.199<br>Retained            | 0.24 | 616 |
| 965 | 479.199<br>Deleted             | 0.24 | 617 |
| 965 | 479.404<br>Retained            | 0.19 | 609 |
| 965 | 479.404<br>Deleted             | 0.19 | 610 |
| 965 | 479.608<br>Retained            | 0.05 | 592 |
| 965 | 479.608<br>Deleted             | 0.05 | 593 |
| 965 | 482.2<br>Retained              | 0.05 | 594 |
| 965 | 482.2<br>Deleted               | 0.05 | 595 |
| 965 | 482.42<br>Retained             | 0.85 | 682 |
| 965 | 482.42<br>Deleted              | 0.85 | 683 |
| 965 | 482.6<br>Retained              | 1.22 | 720 |
| 965 | 482.6<br>Deleted               | 1.22 | 721 |
| 965 | 482.8                          | 1.05 | 701 |

|          |                              |      |     |
|----------|------------------------------|------|-----|
| 965      | Retained<br>482.8<br>Deleted | 1.05 | 702 |
| 965      | 483<br>Retained              | 0.67 | 673 |
| 965      | 483<br>Deleted               | 0.67 | 674 |
| 965      | 483.2<br>Retained            | 1.32 | 728 |
| 965      | 483.2<br>Deleted             | 1.32 | 729 |
| 965      | 483.4<br>Retained            | 2.27 | 757 |
| 965      | 483.4<br>Deleted             | 2.27 | 758 |
| 965      | 485<br>Retained              | 1.06 | 703 |
| More ... |                              |      |     |

---

#### Data Statistics Report

##### Data Counts

|                                |       |
|--------------------------------|-------|
| Number of Active Data:         | 6616  |
| Number of Original Data:       | 10680 |
| Number of Excluded Data:       | 0     |
| Number of Deleted Duplicates:  | 4064  |
| Number of Retained Duplicates: | 2612  |
| Number of Artificial Data:     | 0     |

##### X Variable Statistics

|                       |         |
|-----------------------|---------|
| X Range:              | 20.718  |
| X Midrange:           | 969.641 |
| X Minimum:            | 959.282 |
| X 25%-tile:           | 966.812 |
| X Median:             | 970.409 |
| X 75%-tile:           | 973.789 |
| X Maximum:            | 980     |
| X Average:            | 970.473 |
| X Standard Deviation: | 4.40543 |
| X Variance:           | 19.4078 |

##### Y Variable Statistics

|             |         |
|-------------|---------|
| Y Range:    | 34.821  |
| Y Midrange: | 482.589 |
| Y Minimum:  | 465.179 |
| Y 25%-tile: | 472.799 |

Y Median: 485  
Y 75%-tile: 492.591  
Y Maximum: 500  
  
Y Average: 483.244  
Y Standard Deviation: 10.5206  
Y Variance: 110.684

#### Z Variable Statistics

Z Range: 14.69  
Z Midrange: 7.345  
  
Z Minimum: 0  
Z 25%-tile: 0.19  
Z Median: 0.49  
Z 75%-tile: 1.08  
Z Maximum: 14.69  
  
Z Average: 0.880818  
Z Standard Deviation: 1.2334  
Z Variance: 1.52127  
  
Z Coef. of Variation: 1.40029  
Z Coef. of Skewness: 3.86138

#### Inter-Variable Correlation

|    | X | Y        | Z         |
|----|---|----------|-----------|
| X: | 1 | 0.375765 | 0.0804977 |
| Y: |   | 1        | 0.0681776 |
| Z: |   |          | 1         |

#### Inter-Variable Covariance

|    | X       | Y       | Z        |
|----|---------|---------|----------|
| X: | 19.4078 | 17.4159 | 0.437396 |
| Y: |         | 110.684 | 0.884683 |
| Z: |         |         | 1.52127  |

#### Gridding Report

##### Search Rules

Use All Data: true

##### Gridding Rules

Gridding Method: Natural Neighbor  
Anisotropy Ratio: 1  
Anisotropy Angle: 0



### Grid Summary

|                          |  |
|--------------------------|--|
| Grid File Name:          | e:\maya\Desktop\awatia nov 1\b 1 horizen.grd |
| Minimum X:               | 959.282                                      |
| Maximum X:               | 980  |
| Minimum Y:               | 465.179                                      |
| Maximum Y:               | 500  |
| Minimum Z:               | 0  |
| Maximum Z:               | 10.2614                                      |
| Number of Rows:          | 200  |
| Number of Columns:       | 120  |
| Number of Filled Nodes:  | 17695  |
| Number of Blanked Nodes: | 6305   |
| Total Number of Nodes:   | 24000  |

# Statistical report for "Surfer" topsoil image map

## Data Filter Report

Source Data File Name: e:\maya\Desktop\awatia nov 1\all1.xlslast.xls  
 X Column: A  
 Y Column: B  
 Z Column: C

## Data Counts

Number of Active Data: 7187  
 Number of Original Data: 12251  
 Number of Excluded Data: 0  
 Number of Deleted Duplicates: 5064  
 Number of Retained Duplicates: 3045  
 Number of Artificial Data: 0

## Filter Rules

Duplicate Points to Keep: First  
 X Duplicate Tolerance: 0  
 Y Duplicate Tolerance: 0  
 Exclusion Filter String: Not In Use

## Duplicate Data

| X   | Y        | Z    | ID   | Status |
|-----|----------|------|------|--------|
| 965 | 470      | 0.1  | 3352 |        |
|     | Retained |      |      |        |
| 965 | 470      | 0.29 | 6450 |        |
|     | Deleted  |      |      |        |
| 965 | 470      | 0.52 | 8532 |        |
|     | Deleted  |      |      |        |
| 965 | 470.197  | 0.1  | 3359 |        |
|     | Retained |      |      |        |
| 965 | 470.197  | 0.22 | 5461 |        |
|     | Deleted  |      |      |        |
| 965 | 470.197  | 0.22 | 5462 |        |
|     | Deleted  |      |      |        |
| 965 | 470.4    | 0.45 | 8020 |        |
|     | Retained |      |      |        |
| 965 | 470.4    | 0.45 | 8021 |        |
|     | Deleted  |      |      |        |
| 965 | 470.4    | 0.64 | 9215 |        |
|     | Deleted  |      |      |        |
| 965 | 470.607  | 0.16 | 4456 |        |
|     | Retained |      |      |        |

|     |                     |      |       |
|-----|---------------------|------|-------|
| 965 | 470.607<br>Deleted  | 0.49 | 8303  |
| 965 | 470.607<br>Deleted  | 0.49 | 8304  |
| 965 | 470.79<br>Retained  | 0.32 | 6787  |
| 965 | 470.79<br>Deleted   | 0.41 | 7677  |
| 965 | 475<br>Retained     | 0.08 | 2898  |
| 965 | 475<br>Deleted      | 0.08 | 2899  |
| 965 | 475<br>Deleted      | 0.08 | 2900  |
| 965 | 475<br>Deleted      | 0.08 | 2901  |
| 965 | 475.609<br>Retained | 0.03 | 1535  |
| 965 | 475.609<br>Deleted  | 0.03 | 1536  |
| 965 | 475.609<br>Deleted  | 0.46 | 8086  |
| 965 | 475.609<br>Deleted  | 0.46 | 8087  |
| 965 | 475.609<br>Deleted  | 1.17 | 10988 |
| 965 | 475.609<br>Deleted  | 1.17 | 10989 |
| 965 | 476<br>Retained     | 0.12 | 3809  |
| 965 | 476<br>Deleted      | 0.12 | 3810  |
| 965 | 476<br>Deleted      | 0.2  | 5180  |
| 965 | 476<br>Deleted      | 0.2  | 5181  |
| 965 | 476.204<br>Retained | 0.12 | 3811  |
| 965 | 476.204<br>Deleted  | 0.12 | 3812  |
| 965 | 476.204<br>Deleted  | 0.46 | 8088  |
| 965 | 476.204<br>Deleted  | 0.46 | 8089  |
| 965 | 476.402<br>Retained | 0.03 | 1543  |
| 965 | 476.402<br>Deleted  | 0.03 | 1544  |
| 965 | 476.402<br>Deleted  | 0.03 | 1545  |
| 965 | 476.402<br>Deleted  | 0.03 | 1546  |
| 965 | 476.498<br>Retained | 0.15 | 4324  |
| 965 | 476.498<br>Deleted  | 0.15 | 4325  |

|     |                     |      |      |
|-----|---------------------|------|------|
| 965 | 476.498<br>Deleted  | 0.2  | 5183 |
| 965 | 476.498<br>Deleted  | 0.2  | 5184 |
| 965 | 476.609<br>Retained | 0    | 169  |
| 965 | 476.609<br>Deleted  | 0    | 170  |
| 965 | 476.609<br>Deleted  | 0.05 | 2107 |
| 965 | 476.609<br>Deleted  | 0.05 | 2108 |
| 965 | 477<br>Retained     | 0.12 | 3815 |
| 965 | 477<br>Deleted      | 0.12 | 3816 |
| 965 | 477<br>Deleted      | 0.23 | 5656 |
| 965 | 477<br>Deleted      | 0.23 | 5657 |
| 965 | 477.204<br>Retained | 0.4  | 7600 |
| 965 | 477.204<br>Deleted  | 0.4  | 7601 |
| 965 | 477.204<br>Deleted  | 0.42 | 7820 |
| 965 | 477.204<br>Deleted  | 0.42 | 7821 |
| 965 | 477.406<br>Retained | 0.43 | 7899 |
| 965 | 477.406<br>Deleted  | 0.43 | 7900 |
| 965 | 477.406<br>Deleted  | 0.51 | 8495 |
| 965 | 477.406<br>Deleted  | 0.51 | 8496 |
| 965 | 477.612<br>Retained | 0.3  | 6579 |
| 965 | 477.612<br>Deleted  | 0.3  | 6580 |
| 965 | 477.812<br>Retained | 0.26 | 6078 |
| 965 | 477.812<br>Deleted  | 0.26 | 6079 |
| 965 | 478<br>Retained     | 0.05 | 2127 |
| 965 | 478<br>Deleted      | 0.05 | 2128 |
| 965 | 478<br>Deleted      | 0.05 | 2129 |
| 965 | 478<br>Deleted      | 0.05 | 2130 |
| 965 | 478.197<br>Retained | 0.01 | 873  |
| 965 | 478.197             | 0.01 | 874  |



|     |                                |      |       |
|-----|--------------------------------|------|-------|
| 965 | Deleted<br>478.197             | 0.79 | 9894  |
| 965 | Deleted<br>478.197<br>Deleted  | 0.79 | 9895  |
| 965 | 478.402                        | 0.07 | 2680  |
| 965 | Retained<br>478.402            | 0.07 | 2681  |
| 965 | Deleted<br>478.402             | 0.23 | 5666  |
| 965 | Deleted<br>478.402<br>Deleted  | 0.23 | 5667  |
| 965 | 478.604                        | 0.92 | 10413 |
| 965 | Retained<br>478.604            | 0.92 | 10414 |
| 965 | Deleted<br>478.604<br>Deleted  | 0.92 | 10415 |
| 965 | 478.803                        | 0.01 | 885   |
| 965 | Retained<br>478.803            | 0.01 | 886   |
| 965 | Deleted<br>478.803             | 0.48 | 8260  |
| 965 | Deleted<br>478.803<br>Deleted  | 0.48 | 8261  |
| 965 | 479                            | 0.06 | 2438  |
| 965 | Retained<br>479                | 0.06 | 2439  |
| 965 | Deleted<br>479                 | 0.57 | 8861  |
| 965 | Deleted<br>479<br>Deleted      | 0.57 | 8862  |
| 965 | 479.199                        | 1.57 | 11579 |
| 965 | Retained<br>479.199<br>Deleted | 1.57 | 11580 |
| 965 | 479.404                        | 1.75 | 11698 |
| 965 | Retained<br>479.404<br>Deleted | 1.75 | 11699 |
| 965 | 479.608                        | 1.19 | 11026 |
| 965 | Retained<br>479.608<br>Deleted | 1.19 | 11027 |
| 965 | 482.42                         | 0.31 | 6713  |
| 965 | Retained<br>482.42<br>Deleted  | 0.31 | 6714  |
| 965 | 482.6                          | 0.03 | 1591  |
| 965 | Retained<br>482.6              | 0.03 | 1592  |

|          |          |      |      |
|----------|----------|------|------|
|          | Deleted  |      |      |
| 965      | 482.8    | 0.12 | 3837 |
|          | Retained |      |      |
| 965      | 482.8    | 0.12 | 3838 |
|          | Deleted  |      |      |
| 965      | 483      | 0.13 | 3981 |
|          | Retained |      |      |
| 965      | 483      | 0.13 | 3982 |
|          | Deleted  |      |      |
| 965      | 483.2    | 0.07 | 2703 |
|          | Retained |      |      |
| 965      | 483.2    | 0.07 | 2704 |
|          | Deleted  |      |      |
| 965      | 483.4    | 0.22 | 5517 |
|          | Retained |      |      |
| More ... |          |      |      |

---

#### Data Statistics Report

---

#### Data Counts

|                                |       |
|--------------------------------|-------|
| Number of Active Data:         | 7187  |
| Number of Original Data:       | 12251 |
| Number of Excluded Data:       | 0     |
| Number of Deleted Duplicates:  | 5064  |
| Number of Retained Duplicates: | 3045  |
| Number of Artificial Data:     | 0     |

#### X Variable Statistics

|                       |         |
|-----------------------|---------|
| X Range:              | 20.718  |
| X Midrange:           | 969.641 |
| X Minimum:            | 959.282 |
| X 25%-tile:           | 967.789 |
| X Median:             | 971     |
| X 75%-tile:           | 974     |
| X Maximum:            | 980     |
| X Average:            | 971.007 |
| X Standard Deviation: | 4.09507 |
| X Variance:           | 16.7696 |

#### Y Variable Statistics

|             |         |
|-------------|---------|
| Y Range:    | 34.802  |
| Y Midrange: | 482.599 |
| Y Minimum:  | 465.198 |
| Y 25%-tile: | 474     |
| Y Median:   | 486.808 |
| Y 75%-tile: | 493.101 |

Y Maximum: 500  
Y Average: 484.492  
Y Standard Deviation: 10.267  
Y Variance: 105.412

#### Z Variable Statistics

Z Range: 10.58  
Z Midrange: 5.29  
  
Z Minimum: 0  
Z 25%-tile: 0.06  
Z Median: 0.19  
Z 75%-tile: 0.48  
Z Maximum: 10.58  
  
Z Average: 0.389608  
Z Standard Deviation: 0.579401  
Z Variance: 0.335705  
  
Z Coef. of Variation: 1.48714  
Z Coef. of Skewness: 4.25038

#### Inter-Variable Correlation

|    | X | Y        | Z         |
|----|---|----------|-----------|
| X: | 1 | 0.286869 | 0.0146437 |
| Y: |   | 1        | 0.147055  |
| Z: |   |          | 1         |

#### Inter-Variable Covariance

|    | X       | Y       | Z         |
|----|---------|---------|-----------|
| X: | 16.7696 | 12.0612 | 0.0347449 |
| Y: |         | 105.412 | 0.874792  |
| Z: |         |         | 0.335705  |

#### Gridding Report

##### Search Rules

Use All Data: true

##### Gridding Rules

Gridding Method: Natural Neighbor  
Anisotropy Ratio: 1  
Anisotropy Angle: 0

#### Grid Summary

|                          |   |
|--------------------------|---|
| Grid File Name:          | e:\maya\Desktop\awatia nov 1\top soll grade.grd |
| Minimum X:               | 959.282   |
| Maximum X:               | 980   |
| Minimum Y:               | 465.198   |
| Maximum Y:               | 500   |
| Minimum Z:               | 0   |
| Maximum Z:               | 9.30239   |
| Number of Rows:          | 200   |
| Number of Columns:       | 120   |
| Number of Filled Nodes:  | 17725   |
| Number of Blanked Nodes: | 6275  |
| Total Number of Nodes:   | 24000   |



#### Appendix 7: Results of magnetometer survey

The results of this survey are inconclusive for the following: Proton precession magnetometers have low resolution at the equator due to the low angle of the earth's magnetic field although all procedures were followed to minimize this effect. Anomalies are clustered around areas with possible anthropogenic interference (unknown amounts of metal, cables, old pipes lay covered or buried). The source rock/rocks have low magnetic susceptibility because they contain little or no magnetic minerals such as magnetite or pyrrhotite. The area is covered in low dense jungle so surveys had to be conducted as traverses along existing roads rather than as grids.

Total magnetic variation is less than 600 gammas. Diurnal variations during individual surveys were between 0-55 gammas. The largest anomalies were at most 4 data points indicating a shallow source most likely buried metal. Regional variations though small (~100 gammas) may reflect the underlying lithology. Negative results confirm unsuccessful attempts by CAST geologists to delineate diamond bearing rock using magnetics (Gammon, 2003).

Map units are decimal degrees.

